

# Computing the Geometric Intersection Number of Curves

VINCENT DESPRÉ, École Normale Supérieure de Lyon

FRANCIS LAZARUS\*, CNRS, Grenoble

The geometric intersection number of a curve on a surface is the minimal number of self-intersections of any homotopic curve, i.e. of any curve obtained by continuous deformation. Given a curve  $c$  represented by a closed walk of length at most  $\ell$  on a combinatorial surface of complexity  $n$  we describe simple algorithms to (1) compute the geometric intersection number of  $c$  in  $O(n + \ell^2)$  time, (2) construct a curve homotopic to  $c$  that realizes this geometric intersection number in  $O(n + \ell^4)$  time, (3) decide if the geometric intersection number of  $c$  is zero, i.e. if  $c$  is homotopic to a simple curve, in  $O(n + \ell \log^2 \ell)$  time. The algorithms for (2) and (3) are restricted to orientable surfaces, but the algorithm for (1) is also valid on non-orientable surfaces.

To our knowledge, no exact complexity analysis had yet appeared on those problems. An optimistic analysis of the complexity of the published algorithms for problems (1) and (3) gives at best a  $O(n + g^2 \ell^2)$  time complexity on a genus  $g$  surface without boundary. No polynomial time algorithm was known for problem (2) for surfaces without boundary. Interestingly, our solution to problem (3) provides a quasi-linear algorithm to a problem raised by Poincaré more than a century ago. Finally, we note that our algorithm for problem (1) extends to computing the geometric intersection number of two curves of length at most  $\ell$  in  $O(n + \ell^2)$  time.

CCS Concepts: • **Mathematics of computing** → **Combinatorial algorithms; Graphs and surfaces; Geometric topology**;

\*The corresponding author

This work was supported by the LabEx PERSYVAL-Lab ANR-11-LABX-0025-01.

Permission to make digital or hard copies of all or part of this work for personal or classroom use is granted without fee provided that copies are not made or distributed for profit or commercial advantage and that copies bear this notice and the full citation on the first page. Copyrights for components of this work owned by others than ACM must be honored. Abstracting with credit is permitted. To copy otherwise, or republish, to post on servers or to redistribute to lists, requires prior specific permission and/or a fee. Request permissions from [permissions@acm.org](mailto:permissions@acm.org).

© 2017 Association for Computing Machinery.

Manuscript submitted to ACM

Manuscript submitted to ACM

45 Additional Key Words and Phrases: Computational topology, curves on surfaces, combinatorial  
 46 geodesic, intersection number  
 47

48 **ACM Reference format:**

49 Vincent Despré and Francis Lazarus. 2017. Computing the Geometric Intersection Number of Curves.  
 50 *J. ACM* ?, ?, Article ? (May 2017), 63 pages.

51 <https://doi.org/0000001.0000001>  
 52  
 53

54  
 55 CONTENTS

56	Abstract	1
57	Contents	2
58	1 Introduction	3
59	2 Historical notes	5
60	3 Our strategy for counting intersections	8
61	4 Combinatorial framework	10
62	4.1 Combinatorial curves on surfaces	11
63	4.2 Systems of quads	14
64	4.3 Geodesics	17
65	5 Counting intersections combinatorially	19
66	5.1 Thick double-paths	20
67	5.2 Proof of Theorem 1: the primitive case	23
68	5.3 Non-primitive curves	23
69	5.4 End of proof of Theorem 1	25
70	6 Computing intersection numbers on oriented surfaces	27
71	6.1 Crossing double-paths	29
72	6.2 Proof of Theorem 1 in the orientable case	31
73	7 Computing a minimal immersion	34
74	7.1 Bigons and monogons	34
75	7.2 Proof of Theorem 2	36
76	8 Detecting simple curves	37
77	8.1 Some preparatory lemmas for Theorem 3	37
78	8.2 The unzip algorithm	41
79	9 Concluding remarks	50
80	References	51
81	A Proof of the direct implication of Proposition 29	54
82	B Proof of Lemma 30	56
83	C End of proof of Lemma 16	59
84	Manuscript submitted to ACM	

## 1 INTRODUCTION

Let  $S$  be a surface. Two closed curves  $\alpha, \beta : \mathbb{R}/\mathbb{Z} \rightarrow S$  are **freely homotopic**, written  $\alpha \sim \beta$ , if there exists a continuous map  $h : [0, 1] \times \mathbb{R}/\mathbb{Z}$  such that  $h(0, t) = \alpha(t)$  and  $h(1, t) = \beta(t)$  for all  $t \in \mathbb{R}/\mathbb{Z}$ . Assuming the curves in generic position, their number of intersections is

$$|\alpha \cap \beta| = |\{(t, t') \mid t, t' \in \mathbb{R}/\mathbb{Z} \text{ and } \alpha(t) = \beta(t')\}|.$$

Their **geometric intersection number** only depends on their free homotopy classes and is defined as

$$i(\alpha, \beta) = \min_{\alpha' \sim \alpha, \beta' \sim \beta} |\alpha' \cap \beta'|$$

Likewise, the number of self-intersections of  $\alpha$  is given by

$$\frac{1}{2} |\{(t, t') \mid t \neq t' \in \mathbb{R}/\mathbb{Z} \text{ and } \alpha(t) = \alpha(t')\}|,$$

and its minimum over all the curves freely homotopic to  $\alpha$  is its **geometric self-intersection number**  $i(\alpha)$ . Note the one half factor that comes from the identification of  $(t, t')$  with  $(t', t)$ .

The geometric intersection number is an important parameter that allows to stratify the set of homotopy classes of curves on a surface. The surface is usually endowed with a hyperbolic metric, implying that each homotopy class is identified by its unique geodesic representative. Extending a former result by Mirzakhani [Mirzakhani 2008], Sapir [Mirzakhani 2016; Sapir 2015] has recently provided upper and lower bounds for the number of closed geodesics with bounded length and bounded geometric intersection number. Chas and Lalley [Chas and Lalley 2012] also proved that the distribution of the geometric intersection number with respect to the word length approaches the Gaussian distribution as the length grows to infinity. Other more experimental results were obtained with the help of a computer to show the existence of length-equivalent homotopy classes with distinct geometric intersection numbers [Chas 2014]. Hence, for both theoretical and practical reasons various aspects of the computation of geometric intersection numbers have been studied in the past including the algorithmic ones. Nonetheless, all the previous approaches rely on rather complex mathematical arguments and to our knowledge no exact complexity analysis has yet appeared. In this paper, we make our own the words of Dehn who noted that the metric on words (on some basis of the fundamental group of the surface) can advantageously replace the hyperbolic metric [De La Harpe 2010]. We propose a combinatorial framework that leads to simple algorithms of low complexity to compute the geometric intersection number of curves or to test if this number is zero. Our approach is based on the computation of

133 canonical forms as recently introduced in the purpose of testing whether two curves are  
 134 homotopic [Erickson and Whittelsey 2013; Lazarus and Rivaud 2012]. Canonical forms  
 135 are instances of combinatorial geodesics who share nice properties with the geodesics of a  
 136 hyperbolic surface. On such surfaces each homotopy class contains a unique geodesic that  
 137 moreover minimizes the number of self-intersections. Although a combinatorial geodesic is  
 138 generally not unique in its homotopy class, it must stay at distance one from its canonical  
 139 representative and a careful analysis of its structure leads to the first result of the paper.  
 140  
 141

142 **THEOREM 1.** *Given two curves represented by closed walks of length at most  $\ell$  on a*  
 143 *combinatorial surface of complexity  $n$  we can compute the geometric intersection number of*  
 144 *each curve or of the two curves in  $O(n + \ell^2)$  time.*  
 145

146 As usual the complexity of a combinatorial surface stands for its total number of vertices,  
 147 edges and faces. A key point in our algorithm is the ability to compute the primitive root  
 148 of a canonical curve  $c$  in linear time. This is a curve  $r$  that is not homotopic to a proper  
 149 power of any other curve and such that  $c \sim r^k$  for some integer  $k$ . We next provide an  
 150 algorithm to compute an actual curve immersion – its combinatorial description is part  
 151 of our combinatorial framework – that minimizes the number of self-intersections in its  
 152 homotopy class. While the combinatorial surface in Theorem 1 may be non-orientable, the  
 153 next two results only apply to orientable surfaces.  
 154  
 155

156 **THEOREM 2.** *Given a curve  $c$  represented by a closed walk of length  $\ell$  on an orientable*  
 157 *combinatorial surface of complexity  $n$  we can compute a combinatorial immersion with  $i(c)$*   
 158 *crossings in  $O(n + \ell^4)$  time.*  
 159

160 We also propose a nearly optimal algorithm that answers an old problem studied by  
 161 Poincaré [Poincaré 1904, §4]: decide if the geometric intersection number of a curve is null,  
 162 that is if the curve is homotopic to a simple curve.  
 163  
 164

165 **THEOREM 3.** *Given a curve represented by a closed walk of length  $\ell$  on an orientable*  
 166 *combinatorial surface of complexity  $n$  we can decide if the curve is homotopic to a simple*  
 167 *curve in  $O(n + \ell \log^2 \ell)$  time. In the affirmative we can construct an embedding of  $c$  in the*  
 168 *same amount of time.*  
 169

170 We emphasize that our results represent significant progress with respect to the state  
 171 of the art. No precise analysis appeared in the previously proposed algorithms [Birman  
 172 and Series 1984; Chillingworth 1969, 1972; Cohen and Lustig 1987; de Graaf and Schrijver  
 173 1997; Gonçalves et al. 2005; Lustig 1987; Paterson 2002] concerning Theorems 1 or 3. An  
 174 optimistic analysis of what seems the most efficient approach [Lustig 1987, Th. 3.7], although  
 175 Manuscript submitted to ACM  
 176

177 particularly complex, gives at best a quadratic time complexity for computing the geometric  
178 intersection number on an orientable genus  $g$  surface without boundary, assuming that the  
179 curves are primitive and expressed as words in a canonical basis of the fundamental group.  
180 Schaefer et al. [Schaefer et al. 2008] propose an efficient computation of the geometric  
181 intersection number of curves represented by normal coordinates in a triangulated surface.  
182 However, their approach is limited to *simple* input curves. Apart from a recent algorithm  
183 by Aretinnes [Aretinnes 2015], which is restricted to surfaces with *nonempty* boundary, we  
184 know of no polynomial time algorithm for Theorem 2. Finally, Theorem 3 states the first  
185 quasi-linear algorithm for detecting homotopy classes of simple curves since the problem  
186 was raised by Poincaré more than a century ago [Poincaré 1904, §4].  
187

188  
189 In the next section we review some of the previous relevant works. Section 3 presents  
190 our general simple strategy to compute the geometric intersection number. We introduce  
191 our combinatorial framework in Section 4. The proof of Theorem 1 is given in Section 5  
192 where the case of primitive and non-primitive curves are treated separately. In Section 6 we  
193 provide another proof of Theorem 1 restricted to orientable surfaces. The computation of a  
194 minimally crossing immersion is presented in Section 7 with the proof of Theorem 2. We  
195 finally propose a simple algorithm to detect and embed curves homotopic to simple curves  
196 (Theorem 3) in Section 8.  
197  
198  
199

## 200 2 HISTORICAL NOTES

201  
202 In the fifth supplement to its *Analysis situs* Poincaré [Poincaré 1904, §4] describes a method  
203 to decide whether a given closed curve  $\gamma$  on a surface can be continuously deformed to a  
204 simple curve. For this, he considers the surface as the quotient  $\mathbb{D}/\Gamma$  of the Poincaré disk  
205  $\mathbb{D}$  by a (Fuchsian) group  $\Gamma$  of hyperbolic transformations. The endpoints of a lift of  $\gamma$  in  
206 the Poincaré disk are related by a hyperbolic transformation whose axis is a hyperbolic  
207 line  $L$  representing the unique geodesic homotopic to  $\gamma$ . He concludes that  $\gamma$  is homotopic  
208 to a simple curve if and only if all the transforms of  $L$  by  $\Gamma$  are pairwise disjoint or equal.  
209 This method was turned into an algorithm by Reinhart [Reinhart 1962] who worked out  
210 the explicit computations in the Poincaré disk using the usual representation of hyperbolic  
211 transformations by two-by-two matrices. The entries of the matrices being algebraic the  
212 computation could indeed be performed accurately on a computer. The ability to recognize  
213 curves that are **primitive**, i.e. whose homotopy class cannot be expressed as a proper power  
214 of another class, happens to be crucial in this algorithm though computationally expensive.  
215  
216

217 Birman and Series [Birman and Series 1984] subsequently proposed an algorithm for the  
218 case of surfaces with nonempty boundary that avoids manipulating algebraic numbers. While  
219

221 their arguments appeal to a hyperbolic structure, their algorithm is purely combinatorial.  
222 Intuitively, a surface with boundary deform retracts onto a fat graph (in fact a fat bouquet  
223 of circles) whose universal covering space embeds as a fat tree in the Poincaré disk. The  
224 successive lifts of a curve  $\gamma$  trace a bi-infinite path in this tree. The limit points of this path  
225 belongs to the circle  $\partial\mathbb{D}$  at infinity and coincide with the ideal endpoints of the axis of the  
226 hyperbolic transformation corresponding to any of the lifts of the curve in the path. The  
227 question as to whether two lifts give rise to intersecting axes can thus be reduced to test if  
228 the corresponding bi-infinite paths have separating limit points on  $\partial\mathbb{D}$ . As for Reinhart,  
229 Birman and Series assume that the homotopy class of  $\gamma$  is given by a word  $W$  on some  
230 given set of generators of the fundamental group of the surface. In turn, the above test on  
231 bi-infinite paths boils down to consider the cyclic permutations of  $W$  and  $W^{-1}$  in a cyclic  
232 lexicographic order and to check if this ordering is well-parenthesized with respect to some  
233 pairing of the words.  
234

235  
236 Cohen and Lustig [Cohen and Lustig 1987] further observed that the approach of Birman  
237 and Series could be extended to count the geometric intersection number of one or two  
238 curves. In a second paper Lustig [Lustig 1987] tackles the case where the curves are taken  
239 on a surface without boundary. Like Poincaré he considers a closed surface with negative  
240 Euler characteristic as the quotient of the Poincaré disk by a group of transformations  
241 isomorphic to the fundamental group of the surface. The main contribution of the paper is  
242 to define a canonical representative for every free homotopy class  $\alpha$  given as a word in some  
243 fixed system of loops generating the fundamental group. Lustig first notes that there is no  
244 obvious way of choosing a canonical form among the words representing  $\alpha$ . In particular,  
245 the shortest words are far from unique. He rather represents (a lift of)  $\alpha$  by a path in the  
246 union  $G \cup N \cup H$  of three tessellations of  $\mathbb{D}$ , where the edges of  $G$  are all the lifts of the  
247 generating loops,  $N$  is the dual tessellation, and the edges of  $H$  joins the vertices of  $G$   
248 with the vertices of  $N$ . (Although the graphs of  $G$ ,  $N$  and  $H$  are embedded their union  
249 is not as every edge of  $G$  crosses its dual edge in  $N$ .) Lustig gives a purely combinatorial  
250 characterization of canonical paths and argues that the method in his first paper [Cohen  
251 and Lustig 1987] can be applied to the canonical representative of  $\alpha$ . Overall the two papers  
252 adds up to 60 pages with essential arguments from hyperbolic geometry and the complexity  
253 of the whole procedure remains to be done.  
254

255  
256 Other approaches were developed without assuming any hyperbolic structure. Based on the  
257 notion of winding number, Chillingworth [Chillingworth 1969, 1972] provides an algorithm  
258 to test whether a curve is homotopic (this time with fixed basepoint) to a simple curve on  
259 a surface with nonempty boundary. He also proposed an algorithm for determining when a  
260  
261  
262  
263

265 given set of *simple* closed curves can be made disjoint by (free) homotopy [Chillingworth  
266 1971]. While the winding number relies on a differentiable structure, Zieschang [Zieschang  
267 1965, 1969] used the connection between the automorphisms of a topological surface and  
268 the automorphisms of its fundamental group in order to detect the homotopy classes of  
269 simple closed curves. We also mention some works by Schaefer et al. [Schaefer et al. 2008]  
270 to compute the geometric intersection number of two *simple* curves given by their normal  
271 coordinates in a triangulated surface. Their algorithm is based on repeated applications of  
272 Dehn twists and is claimed to have polynomial time complexity.  
273  
274

275 A related work by Hass and Scott [Hass and Scott 1985] is concerned with curves which  
276 have excess intersection, i.e. that can be homotoped so as to reduce their number of  
277 intersections. Hass and Scott introduce various types of monogons and bigons that can  
278 be either embedded, singular or weak. A *singular monogon* of a curve  $\gamma : \mathbb{R}/\mathbb{Z} \rightarrow S$  is a  
279 contractible subpath of  $\gamma$  whose endpoints define a self-intersection of  $\gamma$ . A *bigon* of  $\gamma$  is  
280 defined by two self-intersections joined by two homotopic subpaths (with fixed endpoints)  
281  $\gamma|_{\sigma}$  and  $\gamma|_{\sigma'}$  with  $\sigma, \sigma' \subset \mathbb{R}/\mathbb{Z}$ . The bigon is said *singular* if the defining segments  $\sigma, \sigma'$  are  
282 disjoint and *weak* otherwise. Hass and Scott prove that a curve with excess self-intersection  
283 on an orientable surface must have a singular monogon or a singular bigon. Their result  
284 directly suggests an algorithm to compute the geometric intersection number of a curve:  
285 iteratively remove monogons or untie bigons until there is no more. The final configuration  
286 must have the minimal number of self-intersections. Designing an efficient procedure to  
287 find monogons and bigons remains the crux of this approach. Recently, Arettines [Arettines  
288 2015] has proposed an algorithm based on this approach to compute a minimal configuration  
289 of a single curve on a surface with *nonempty* boundary. Note that the method cannot be  
290 extended to compute the geometric intersection number of a curve on a non-orientable  
291 surface since Hass and Scott give a counter-example of a curve with excess self-intersections  
292 and no singular monogon or bigon. The method can neither be extended to compute the  
293 geometric intersection number of two curves on an orientable surface. Indeed, Hass and Scott  
294 give two counter-examples to the fact that two curves with excess intersections should have  
295 a singular bigon. (A singular bigon between two curves is a pair of homotopic subpaths, one  
296 of each curve.) One of their counter-examples contains a curve with excess self-intersections  
297 and the other one contains a non-primitive curve. Our counter-example, Figure 1, shows  
298 that even assuming each curve to be primitive and in minimal configuration, we may have  
299 excess intersections without singular bigons. Nonetheless, it was proved [de Graaf and  
300 Schrijver 1997; Hass and Scott 1994; Paterson 2002] that starting from any configuration of  
301 curves one may reach a configuration with a minimal number of intersections by applying a  
302  
303  
304  
305  
306  
307  
308

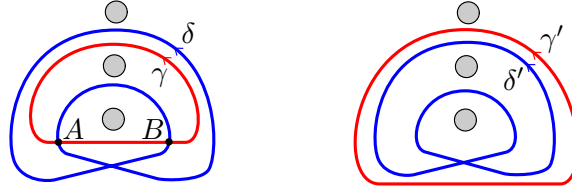


Fig. 1. The plain circles represent non-contractible curves. The two curves  $\gamma$  and  $\delta$  on the left have homotopic disjoint curves  $\gamma'$  and  $\delta'$ . The curves  $\gamma$  and  $\delta$  thus have excess intersection although there is no singular bigon between the two. If  $A = \gamma(0) = \delta(0)$  and  $B = \gamma(u) = \delta(v)$  we nonetheless have  $\delta|_{[0,v]} \sim \gamma|_{[0,1+u]}$  where  $\gamma|_{[0,1+u]}$  is the concatenation of  $\gamma$  with  $\gamma|_{[0,u]}$ . In particular,  $\gamma|_{[0,1+u]}$  wraps more than once around  $\gamma$ .

finite sequence of elementary moves involving monogons, bigons and trigons similar to the Reidemeister moves in knot theory. A surprising consequence was obtained by Neumann-Coto [Neumann-Coto 2001]. Define a *cut and paste* on a family of curves by cutting the curves at some of their intersection points and glueing the resulting arcs in a different order. Neumann-Coto proves that any set of primitive curves can be brought to a homotopic set with minimal (self-)intersections by a set of cut and paste operations. Note that each intersection of two curve pieces can be re-arranged in three different manners, including the original one, by a cut and paste. Hence, if the curves have  $I$  (self-)intersections we may find a minimal configuration out of the  $3^I$  possible re-configurations!

We also mention the algebraic approach of Gonçalves et al. [Gonçalves et al. 2005] based on previous works by Turaev [Turaev 1979] who introduced intersection forms over the integral group ring of the fundamental group of the surface. This approach is based on the transformation of each curve into a certain algebraic sum of homotopy classes. A simple analysis of the time complexity for the computation of this sum leads to  $O(\ell^5)$  operations for a curve with  $\ell$  self-intersections. See [Cohen and Lustig 1987; Gonçalves et al. 2005] for more historical notes.

### 3 OUR STRATEGY FOR COUNTING INTERSECTIONS

Following Poincaré's original approach we represent a surface  $S$  with negative Euler characteristic as the hyperbolic quotient surface  $\mathbb{D}/\Gamma$  where  $\Gamma$  is a discrete group of hyperbolic motions of the Poincaré disk  $\mathbb{D}$ . We denote by  $p : \mathbb{D} \rightarrow \mathbb{D}/\Gamma = S$  the universal covering map. Any closed curve  $\alpha : \mathbb{R}/\mathbb{Z} \rightarrow S$  gives rise to its infinite power  $\alpha^\infty : \mathbb{R} \rightarrow \mathbb{R}/\mathbb{Z} \rightarrow S$  that wraps around  $\alpha$  infinitely many times. A **lift** of  $\alpha$  is any curve  $\tilde{\alpha} : \mathbb{R} \rightarrow \mathbb{D}$  such that  $p \circ \tilde{\alpha} = \alpha^\infty$  where the parameter of  $\tilde{\alpha}$  is defined up to an integer translation (we thus identify the curves  $t \mapsto \tilde{\alpha}(t+k)$ ,  $k \in \mathbb{Z}$ ). Note that  $p^{-1}(\alpha)$  is the union of all the images



353  $\Gamma \cdot \tilde{\alpha}$  of  $\tilde{\alpha}$  by the motions in  $\Gamma$ . The curve  $\tilde{\alpha}$  has two limit points on the boundary of  $\mathbb{D}$   
 354 which can be joined by a unique hyperbolic line  $L$ . The projection  $p(L)$  covers infinitely  
 355 many times around the unique geodesic homotopic to  $\alpha$ . In particular, the set of pairs of  
 356 limit points of all lifts of  $\alpha$  only depends on the homotopy class of  $\alpha$ .  
 357

358 No two motions of  $\Gamma$  have a limit point in common unless they are powers of the same  
 359 motion. This can be used to show that when  $\alpha$  is primitive, its lifts are uniquely identified  
 360 by their limit points [Farb and Margalit 2012]. Let  $\alpha$  and  $\beta$  be two primitive curves. We fix  
 361 a lift  $\tilde{\alpha}$  of  $\alpha$  and denote by  $\tau \in \Gamma$  the hyperbolic motion sending  $\tilde{\alpha}(0)$  to  $\tilde{\alpha}(1)$ . Let  $\Gamma \cdot \tilde{\beta}$  be  
 362 the set of lifts of  $\beta$ . We consider the subset of lifts  
 363

$$364 \quad B = \{\tilde{\beta}' \in \Gamma \cdot \tilde{\beta} \mid \text{the limit points of } \tilde{\beta}' \text{ and } \tilde{\alpha} \text{ alternate along } \partial\mathbb{D}\},$$

366 and we denote by  $B/\tau$  the set of equivalence classes of lifts generated by the relations  
 367  $\tilde{\beta}' \approx \tau(\tilde{\beta}')$ .  
 368

369 LEMMA 4 ([REINHART 1962]).  $i(\alpha, \beta) = |B/\tau|$ .  
 370

371 PROOF. Put  $I(\alpha, \beta) = \{(t, t') \mid t, t' \in \mathbb{R}/\mathbb{Z} \text{ and } \alpha(t) = \beta(t') \text{ and if } \alpha = \beta : t \neq t'\}$ . Define  
 372 a map  $\varphi : I(\alpha, \beta) \rightarrow (\Gamma \cdot \tilde{\beta})/\tau$  as follows. Given  $(u \bmod 1, v \bmod 1) \in I(\alpha, \beta)$  there is, by the  
 373 unique lifting property of coverings, a unique lift  $\tilde{\beta}'$  of  $\beta$  that satisfies  $\tilde{\beta}'(v) = \tilde{\alpha}(u)$ . We set  
 374  $\varphi(u \bmod 1, v \bmod 1)$  to the class of this lift. Note that changing  $u$  to  $u + k$ ,  $k \in \mathbb{Z}$ , leads to  
 375 the lift  $\tau^k(\tilde{\beta}')$ , so that  $\varphi$  is well-defined. We have  $B/\tau \subset \varphi(I(\alpha, \beta))$ . Indeed, if  $\tilde{\beta}' \in B$  then  
 376  $\tilde{\beta}'$  and  $\tilde{\alpha}$  must intersect at some point  $\tilde{\beta}'(v) = \tilde{\alpha}(u)$ . It follows that  $\varphi(u \bmod 1, v \bmod 1)$  is  
 377 the class of  $\tilde{\beta}'$ . As an immediate consequence,  
 378  
 379

$$380 \quad |I(\alpha, \beta)| \geq |B/\tau|$$

382 When  $\alpha$  and  $\beta$  are geodesics all their lifts are hyperbolic lines and  $\varphi$  is a bijection onto its  
 383 image  $B/\tau$ . We conclude that  $|I(\alpha, \beta)|$  is minimized among all homotopic curves, so that  
 384  $i(\alpha, \beta) = |B/\tau|$ .  $\square$   
 385

386 When  $\alpha$  and  $\beta$  are hyperbolic geodesics, their lifts being hyperbolic lines have alternating  
 387 limit points exactly when they have a non-empty intersection and they have a unique  
 388 intersection point in that case. This point projects to a crossing of  $\alpha$  and  $\beta$  that actually  
 389 identifies the corresponding element of  $B/\tau$ . When  $\alpha$  and  $\beta$  are not geodesic the situation  
 390 is more ambiguous and their lifts may have multiple intersection points. Those intersection  
 391 points project to crossings of  $\alpha$  and  $\beta$ , so that the elements of  $B/\tau$  are now identified with  
 392 subsets of crossing points (with odd cardinality) rather than single crossing points. The  
 393 induced partition is generated by the following relation: two crossings are equivalent if they  
 394  
 395  
 396

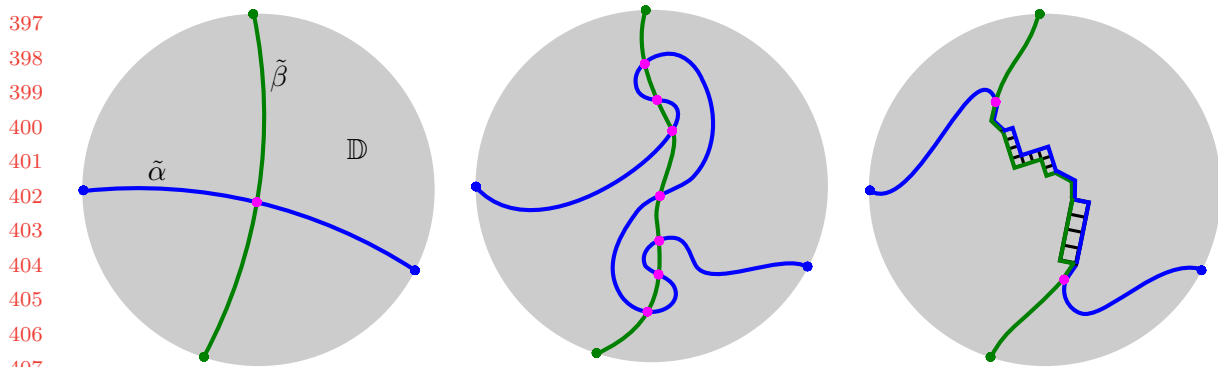


Fig. 2. Left, two intersecting hyperbolic lines. Middle, two lifts of non-geodesic curves may intersect several times. Right, lifts of combinatorial geodesics.

are connected by a pair of homotopic subpaths of  $\alpha$  and  $\beta$ , namely one of the two subpaths of  $\alpha$  and one of the two subpaths of  $\beta$  cut by the two crossings. Indeed, if the two crossings are projections of intersections of two lifts, then the paths between those intersections in each lift project to homotopic paths. Conversely, homotopic paths lift to paths with common endpoints that can be seen as subpaths of two intersecting lifts. In order to compute the above partition, we thus essentially need an efficient procedure for testing if two paths are homotopic. This homotopy test can indeed be performed in linear time according to Theorem 9. Since a combinatorial curve of length  $\ell$  may have  $O(\ell^2)$  crossings, we directly obtain an algorithm with time complexity  $O(\ell^5)$  to compute the above partition.

In practice, we shall work in a combinatorial framework as described in the next section. When dealing with combinatorial geodesics, the situation is more constrained and somehow intermediate between the ideal hyperbolic case and the most general situation. See Figure 2. This allows us to directly identify  $B/\tau$  with certain pairs of homotopic subpaths of  $\alpha$  and  $\beta$ . See Proposition 27.

#### 4 COMBINATORIAL FRAMEWORK

In order to study the computational aspects of the intersection number we need to specify the encoding of curves on surfaces. A common representation of the homotopy class of a curve on a surface consists of a word in some set of generators of the fundamental group of the surface. Typically, when the fundamental group is given by a combinatorial presentation with a single relation, one can build a two dimensional complex that is homeomorphic to the surface and such that the word for the curve corresponds to a homotopic closed path in this complex. We shall use a more general notion of combinatorial surfaces where curves a

441 represented by closed walks. We introduce below this combinatorial framework and show  
442 that it faithfully represents its continuous analogue. In order to mimic at best hyperbolic  
443 geometry we further restrict our framework to system of quads which are combinatorial  
444 surfaces composed only of quadrilaterals. We finally study the structure of geodesics in such  
445 systems.  
446

#### 448 4.1 Combinatorial curves on surfaces

449 *Combinatorial surfaces.* As usual in computational topology, we model a surface by  
450 a cellular embedding of a graph  $G$  in a compact topological surface  $S$ . Such a cellular  
451 embedding can be encoded by a **combinatorial surface** composed of the graph  $G$  itself  
452 together with a rotation system [Mohar and Thomassen 2001] that records for every vertex  
453 of the graph the **direct** cyclic order of the incident arcs. When  $S$  is orientable, this order can  
454 be chosen consistently for all vertices. We call this order clockwise. Nonorientable surfaces  
455 can be encoded by providing an additional signature with every edge that indicates if the  
456 direct orientations at its endpoints are consistent or not. The edge is said **half-twisted**  
457 when the orientations are inconsistent. The **facial walks** are obtained from the rotation  
458 system by the face traversal procedure as described in [Mohar and Thomassen 2001, p.93].  
459 In order to handle surfaces with boundaries we allow every face of  $G$  in  $S$  to be either  
460 an open disk or an annulus (open on one side). In other words  $G$  is a cellular embedding  
461 in the closure of  $S$  obtained by attaching a disk to every boundary of  $S$ . We record this  
462 information by storing a boolean for every facial walk of  $G$  indicating whether the associated  
463 face is perforated or not. All the considered graphs may have loop and multiple edges. A  
464 directed edge will be called an **arc** and each edge corresponds to two opposite arcs. We  
465 denote by  $a^{-1}$  the arc opposite to an arc  $a$ . Every combinatorial surface  $\Sigma$  can be reduced  
466 by first contracting the edges of a spanning tree and then deleting edges incident to distinct  
467 non-perforated faces. The resulting **reduced surface** has a single vertex. A reduced surface  
468 without boundary has a single face, but in general a reduced surface may have several faces.  
469 The combinatorial surface  $\Sigma$  and its reduced version encode different cellular embeddings  
470 on a same topological surface.  
471

472 *Combinatorial curves.* Consider a combinatorial surface with its graph  $G$ . A combinatorial  
473 curve (or path)  $c$  is a walk in  $G$ , i.e. an alternating sequence of vertices and arcs, starting  
474 and ending with a vertex, such that each vertex in the sequence is the target vertex of the  
475 previous arc and the source vertex of the next arc. We generally omit the vertices in the  
476 sequence. A combinatorial curve is closed when additionally the first and last vertex are  
477 equal. When no confusion is possible we shall drop the adjective combinatorial. A closed  
478

485 curve is **2-sided** if its number of half-twisted arcs is even. It is otherwise **1-sided**. The  
 486 **length** of  $c$  is its total number of arc occurrences, which we denote by  $|c|$ . If  $c$  is closed,  
 487 we write  $c(i)$ ,  $i \in \mathbb{Z}/|c|\mathbb{Z}$ , for the vertex of index  $i$  of  $c$  and  $c[i, i + 1]$  for the arc joining  $c(i)$   
 488 to  $c(i + 1)$ . For convenience we set  $c[i + 1, i] = c[i, i + 1]^{-1}$  to allow the traversal of  $c$  in  
 489 reverse direction. In order to differentiate the arcs with their occurrences we denote by  
 490  $[i, i \pm 1]_c$  the corresponding occurrence of the arc  $c[i, i \pm 1]$  in  $c^{\pm 1}$ , where  $c^{-1}$  is obtained by  
 491 traversing  $c^1 := c$  in the opposite direction. More generally, for any non-negative integer  $\ell$   
 492 and any sign  $\varepsilon \in \{-1, 1\}$ , The sequence of indices

$$(i, i + \varepsilon, i + 2\varepsilon, \dots, i + \varepsilon\ell)$$

496 is called an **index path** of  $c$  of length  $\ell$ . The index path can be **forward** ( $\varepsilon = 1$ ) or  
 497 **backward** ( $\varepsilon = -1$ ) and can be longer than  $c$  so that an index may appear more than  
 498 once in the sequence. We denote this path by  $[i \xrightarrow{\varepsilon\ell}]_c$ . Its **image path** is given by the arc  
 499 sequence

$$c[i \xrightarrow{\varepsilon\ell}] := (c[i, i + \varepsilon], c[i + \varepsilon, i + 2\varepsilon], \dots, c[\varepsilon(\ell - 1), \varepsilon\ell]).$$

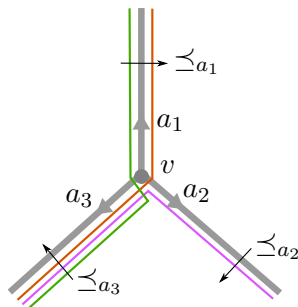
503 The image path of a length zero index path is just a vertex. There is an evident notion  
 504 of inclusion between index paths: a forward index path  $[i \xrightarrow{\ell}]_c$  is included in a forward  
 505 index path  $[j \xrightarrow{k}]_c$  if there exists a natural number  $s$  such that  $s + \ell \leq k$  and  $i = j + s$ .  
 506 This inclusion relationship extends to both forward and backward paths, replacing each  
 507 backward index path  $[i \xrightarrow{-\ell}]_c$  by  $[i - \ell \xrightarrow{\ell}]_c$  to perform the comparison.

509 A **spur** of  $c$  is a subsequence of the form  $(a, a^{-1})$  where  $a$  is an arc. A closed curve is  
 510 **contractible** if it is homotopic to a trivial curve (i.e., a curve reduced to a single vertex).  
 511 We will implicitly assume that a homotopy has fixed endpoints when applied to paths and  
 512 is free when applied to closed curves. If  $\alpha, \beta$  are two closed paths, we shall sometimes write  
 513  $\alpha \overset{*}{\sim} \beta$  to denote homotopy with fixed basepoint as opposed to  $\alpha \sim \beta$  for the free homotopy  
 514 relation.  
 515  
 516  
 517

518 *Combinatorial immersions.* A combinatorial curve may be seen as a continuous curve  
 519 in general position snapped to the graph of the combinatorial surface. When doing so  
 520 several parts of the continuous curve may be mapped to the same edge. In order not to lose  
 521 information, one needs to record their ordering. Following the notion of a combinatorial set  
 522 of loops as in [Colin de Verdière and Lazarus 2005], we define a **combinatorial immersion**  
 523 of a set  $\mathcal{C}$  of combinatorial curves as the data for each arc  $a$  in  $G$  of a left-to-right order  
 524  $\preceq_a$  over all the occurrences of  $a$  or  $a^{-1}$  in the curves of  $\mathcal{C}$ . The only requirement is that  
 525 opposite arcs should be associated with inverse orders if the corresponding edge is untwisted  
 526  
 527

529 and with the same order if the edge is half-twisted. Let  $A_v$  be the set of occurrences of  $a$   
 530 or  $a^{-1}$  in the curves of  $\mathcal{C}$  where  $a$  runs over all arcs of  $G$  with origin  $v$ . A combinatorial  
 531 immersion induces for each vertex  $v$  of  $G$  a circular order  $\preceq_v$  over  $A_v$ ; if  $a_1, \dots, a_k$  is the  
 532 direct cyclic order of the arcs of  $G$  with origin  $v$ , then  $\preceq_v$  is the cyclic concatenation of the  
 533 orders  $\preceq_{a_1}, \dots, \preceq_{a_k}$ . See Figure 3. An immersion of  $\mathcal{C}$  restricts to an immersion of each of

534  
535  
536  
537  
538  
539  
540  
541  
542  
543  
544



545 Fig. 3. The circular order  $\preceq_v$  is the concatenation of the orders  $\preceq_{a_1}, \preceq_{a_2}, \preceq_{a_3}$ .

546  
547  
548  
549  
550  
551

its curves. Conversely, given an immersion of each curve in  $\mathcal{C}$  we can build an immersion (in  
 549 general many) of their union by merging for each arc  $a$  the left-to-right orders  $\preceq_a$  of each  
 550 curve immersion.

552  
553  
554  
555  
556  
557  
558  
559

*Combinatorial crossings.* Given an immersion  $\mathcal{I}$  of two combinatorial closed curves  $c$   
 553 and  $d$  we define a **double point** of  $(c, d)$  as a pair of indices  $(i, j) \in \mathbb{Z}/|c|\mathbb{Z} \times \mathbb{Z}/|d|\mathbb{Z}$  such  
 554 that  $c(i) = d(j)$ . Likewise, a double point of  $c$  is a pair  $(i, j) \in \mathbb{Z}/|c|\mathbb{Z} \times \mathbb{Z}/|c|\mathbb{Z}$  with  $i \neq j$   
 555 and  $c(i) = c(j)$ . The double point  $(i, j)$  is a **crossing** in  $\mathcal{I}$  if the pairs of arc occurrences  
 556  $([i-1, i]_c, [i, i+1]_c)$  and  $([j-1, j]_d, [j, j+1]_d)$  are linked in the  $\preceq_{c(i)}$ -order, i.e. if they  
 557 appear in the cyclic order  
 558

$$559 \dots [i, i-1]_c \dots [j, j-1]_d \dots [i, i+1]_c \dots [j, j+1]_d \dots,$$

560  
561  
562  
563  
564  
565  
566

with respect to  $\preceq_{c(i)}$  or the opposite order. An analogous definition holds for a self-crossing  
 562 of a single curve, taking  $c = d$  in the above definition. Note that the notion of (self-)crossing  
 563 is independent of the traversal directions of  $c$  and  $d$ . The number of crossings of  $c$  and  $d$   
 564 and of self-crossings of  $c$  in  $\mathcal{I}$  is denoted respectively by  $i_{\mathcal{I}}(c, d)$  and  $i_{\mathcal{I}}(c)$ .

567  
568  
569  
570  
571  
572

We define the **combinatorial self-crossing number** of  $c$ , denoted by  $i(c)$ , as the  
 567 minimum of  $i_{\mathcal{I}}(c')$  over all the combinatorial immersions  $\mathcal{I}$  of any combinatorial curve  $c'$   
 568 freely homotopic to  $c$ . The **combinatorial crossing number** of two combinatorial curves  
 569  $c$  and  $d$  is defined the same way taking into account crossings between  $c$  and  $d$  only.

573 LEMMA 5. *The combinatorial (self-)crossing number coincides with the geometric (self-*  
 574 *)intersection number, i.e. for every combinatorial closed curves  $c$  and  $d$ :*

$$575 \quad i(c) = i(\rho(c)) \quad \text{and} \quad i(c, d) = i(\rho(c), \rho(d)).$$

577 *where  $\rho$  is any cellular embedding of  $G$ .*

579 PROOF. Every combinatorial immersion  $\mathcal{I}$  of  $c$  can be realized by a continuous curve  
 580  $\gamma \sim \rho(c)$  with the same number of self-intersections as the number of self-crossings of  $\mathcal{I}$ .  
 581 To construct  $\gamma$  we consider small disjoint disks centered at the images of the vertices of  
 582  $G$  in  $S$ . We connect those vertex disks by disjoint strips corresponding to the edges of  
 583  $G$ . For every arc  $a$  of  $G$  we draw inside the corresponding edge strip parallel curve pieces  
 584 labelled by the occurrences of  $a$  or  $a^{-1}$  in  $c$  in the left-to-right order  $\preceq_a$ . The endpoints of  
 585 those curve pieces appear on the boundary of the vertex disks in the circular vertex orders  
 586 induced by  $\mathcal{I}$ . It remains to connect those endpoints by straight line segments inside each  
 587 disk (via a parametrization over a Euclidean disk) according to the labels of their incident  
 588 curve pieces. The resulting curve  $\gamma$  can be homotoped to  $\rho(c)$  and its self-intersections  
 589 may only appear inside the vertex disks. Clearly, an intersection of two segments of  $\gamma$  in a  
 590 disk corresponds to linked pairs of arc occurrences, i.e. to a combinatorial crossing, and  
 591 vice-versa. It follows that  $i(c) \geq i(\rho(c))$ . To prove the reverse inequality we show that for  
 592 any continuous curve  $\gamma$  in generic position there exists a combinatorial immersion of a  
 593 curve  $c'$  such that  $\rho(c') \sim \gamma$  and the number of self-crossings of  $c'$  is at most the number  
 594 of self-intersections of  $\gamma$ . By an isotopy we can enforce the self-intersections of  $\gamma$  to lie  
 595 inside the vertex disks. After removing the vertex disks from  $S$ , we are left with a set of  
 596 disjoint and simple pieces of  $\gamma$  that can be isotoped inside the edge strips and vertex disks  
 597 without introducing any new intersections. If a piece of curve in a strip has its endpoints  
 598 on the same end of the strip we can further isotope the piece inside the incident vertex  
 599 disk. This way all the curve pieces join the two ends of their strip and can be ordered from  
 600 left-to-right inside each strip (assuming a preferred direction of the strip). Replacing each  
 601 curve piece by an arc occurrence we thus define a combinatorial immersion of a curve  $c'$   
 602 with the required properties. The same constructions apply to an immersion of two curves  
 603 showing that  $i(c, d) = i(\rho(c), \rho(d))$ . □

610

## 611 4.2 Systems of quads

612

613 *Reduction to a system of quads.* Let  $\Sigma$  be a combinatorial surface with negative Euler  
 614 characteristic. We first describe the construction of a system of quads for a surface without  
 615 boundary, i.e., when  $\Sigma$  has no perforated faces. Following Lazarus and Rivaud [[Lazarus](#)  
 616 Manuscript submitted to ACM

617 and Rivaud 2012] we start putting  $\Sigma$  into a standard form called a **system of quads** by  
 618 Erickson and Whittlesey [Erickson and Whittlesey 2013]. After reducing  $\Sigma$  to a surface  
 619  $\Sigma'$  with a single vertex  $v$  and a single face  $f$  this system of quads is obtained by adding a  
 620 vertex  $w$  at the center of  $f$ , adding edges between  $w$  and all occurrences of  $v$  in the facial  
 621 walk of  $f$ , and finally deleting the edges of  $\Sigma'$ . The graph of the resulting system of quads,  
 622 called the **radial graph** [Lazarus and Rivaud 2012], is bipartite. It contains two vertices,  
 623 namely  $v$  and  $w$ , and  $4g$  edges, where  $g$  is the genus of  $\Sigma$ . All its faces are quadrilaterals. A  
 624 similar construction applies when  $\Sigma$  has perforated faces. In this case, the reduced surface  
 625  $\Sigma'$  may have several non-perforated faces and we essentially perform the same sequence  
 626 of operations to each such face. However, when deleting edges of  $\Sigma'$  incident to both a  
 627 perforated and a non-perforated face, we merge the two faces to obtain a larger perforated  
 628 face. In the end, the non-perforated faces are quadrilaterals and every vertex is incident to  
 629 a perforated face. In order to get a bipartite graph, we eventually subdivide the loop edges  
 630 by introducing a vertex in the middle.  
 631  
 632  
 633

634 Note that the system of quads can be deduced from  $\Sigma$  by a sequence of edge contractions,  
 635 deletions, insertions and subdivisions. Every cycle  $c$  of  $\Sigma$  can thus be modified accordingly  
 636 to give a cycle  $\varphi(c)$  in the system of quads. Clearly, there exist cellular embeddings  $\rho, \rho'$   
 637 of the graphs of  $\Sigma$  and of the system of quads in a same topological surface such that  
 638  $\rho(c) \sim \rho'(\varphi(c))$ .  
 639

640  
 641 LEMMA 6 ([DEY AND GUHA 1999; LAZARUS AND RIVAUD 2012]). *Let  $n$  be the number*  
 642 *of edges of the combinatorial surface  $\Sigma$ . The above construction of a system of quads can be*  
 643 *performed in  $O(n)$  time so that for every closed curve  $c$  of length  $\ell$  in  $\Sigma$ , we can compute*  
 644 *in  $O(\ell)$  time a curve  $c'$  of length at most  $2\ell$  in the system of quads such that  $c' \sim \varphi(c)$ .*  
 645

646 For the rest of the paper we shall assume that **all surfaces have negative Euler**  
 647 **characteristic**.  
 648

649  
 650 *Diagrams.* A **disk diagram** over the combinatorial surface  $\Sigma$  is a combinatorial sphere  
 651  $\Delta$  with one perforated face together with a labelling of the arcs of  $\Delta$  by the arcs of  $\Sigma$  such  
 652 that  
 653

- 654 (1) opposite arcs receive opposite labels,
- 655 (2) the facial walk of each non-perforated face of  $\Delta$  is labelled by the facial walk of  
 656 some non-perforated face of  $\Sigma$ .

657 The diagram is **reduced** when no edge of  $\Delta$  is incident to two non-perforated faces labelled  
 658 by the same facial walk (with opposite orientations) of  $\Sigma$ . An **annular diagram** is defined  
 659

661 similarly by a combinatorial sphere with two distinct perforated faces. A vertex of a diagram  
 662 that is not incident to any perforated face is said **interior**.  
 663

664 LEMMA 7 (VAN KAMPEN, SEE [ERICKSON AND WHITTELEY 2013, SEC. 2.4]). *A cycle*  
 665 *of  $\Sigma$  is contractible if and only if it is the label of the facial walk of the perforated face of a*  
 666 *reduced disk diagram over  $\Sigma$ . Two cycles are freely homotopic if and only if the facial walks*  
 667 *of the two perforated faces of a reduced annular diagram over  $\Sigma$  are labelled by these two*  
 668 *cycles respectively.*  
 669

670 Note that two non-perforated faces that are adjacent and consistently oriented in a reduced  
 671 diagram are labelled by adjacent faces that are consistently oriented in  $\Sigma$ . Moreover, the  
 672 degree of an interior vertex of the diagram is a multiple of the degree of the corresponding  
 673 vertex in  $\Sigma$ . In the sequel, **all the considered diagrams will be supposed reduced**.  
 674  
 675

676 *Spurs, brackets and canonical curves.* Thanks to Lemma 6 we may assume that our  
 677 combinatorial surface  $\Sigma$  is a system of quads. Moreover, the construction of this system of  
 678 quads with the assumption on the Euler characteristic implies that **all interior vertices**  
 679 **have degree at least 6**. Let  $(a_1, a_2)$  be a pair of arcs sharing their origin vertex  $v$  and  
 680 such that the face corners between  $a_1$  and  $a_2$  in the direct cyclic order around  $v$  belong to  
 681 non-perforated faces. Following the terminology of Erickson and Whittlesey [Erickson and  
 682 Whittlesey 2013], we define the **turn** of  $(a_1, a_2)$  as the number of those face corners. Hence,  
 683 if  $v$  is an interior vertex of degree  $d$  in  $\Sigma$ , the turn of  $(a_1, a_2)$  is an integer modulo  $d$  that is  
 684 zero when  $a_1 = a_2$ . If  $v$  is a boundary vertex and one of the faces between  $a_1$  and  $a_2$  (in the  
 685 direct order) is perforated, while none of the faces between  $a_2$  and  $a_1$  is perforated, then  
 686 the turn of  $(a_1, a_2)$  is minus the number of face corners between  $a_2$  and  $a_1$ . The turn is  
 687 undefined when one of the faces between  $a_1$  and  $a_2$  and one of the faces between  $a_2$  and  $a_1$   
 688 are perforated. When  $\Sigma$  is oriented, the **turn sequence** of a subpath  $(a_i, a_{i+1}, \dots, a_{i+j-1})$   
 689 of a closed curve of length  $\ell$  is the sequence of  $j + 1$  turns of  $(a_{i+k}^{-1}, a_{i+k+1})$  for  $-1 \leq k < j$ ,  
 690 where indices are taken modulo  $\ell$ . The subpath may have length  $\ell$ , thus leading to a  
 691 sequence of  $\ell + 1$  turns. On a non-necessarily oriented surface the sign of the turn of  
 692  $(a_{i+k}^{-1}, a_{i+k+1})$  should be changed according to the parity of the number of half-twisted  
 693 arcs among  $(a_i, a_{i+1}, \dots, a_{i+k})$ . This amounts to untwist the path  $(a_i, a_{i+1}, \dots, a_{i+k})$  before  
 694 computing the turn sequence. Note that the turn of  $(a_{i+k}^{-1}, a_{i+k+1})$  is zero precisely when  
 695  $(a_{i+k}, a_{i+k+1})$  is a spur. A **bracket** is any subpath whose turn sequence has the form  $12^*1$   
 696 or  $\bar{1}\bar{2}^*\bar{1}$  where  $t^*$  stands for a possibly empty sequence of turns  $t$  and  $\bar{x}$  stands for  $-x$ . It  
 697 follows from Lemma 7 and a simple combinatorial Gauss-Bonnet theorem [Gersten and  
 698 Short 1990] that  
 699

700  
 701  
 702  
 703  
 704 Manuscript submitted to ACM



705 THEOREM 8 ([ERICKSON AND WHITTELEY 2013; GERSTEN AND SHORT 1990]). A  
 706 nontrivial contractible closed curve on a system of quads must have either a spur or four  
 707 brackets. Moreover, if the curve is the label of the boundary walk (i.e., of the facial walk of  
 708 the perforated face) of a disk diagram with at least one interior vertex, then the curve must  
 709 have either a spur or five brackets.  
 710

711 Lazarus and Rivaud [Lazarus and Rivaud 2012] have introduced a canonical form for  
 712 every nontrivial free homotopy class of closed curves in an oriented system of quads. In  
 713 particular, two curves are freely homotopic if and only if their canonical forms are equal  
 714 (up to a circular shift of their vertex indices). It was further characterized by Erickson and  
 715 Whittlesey [Erickson and Whittlesey 2013] in terms of turns and brackets.  
 716  
 717

718 THEOREM 9 ([ERICKSON AND WHITTELEY 2013; LAZARUS AND RIVAUD 2012]). The  
 719 canonical form of a combinatorial closed curve of length  $\ell$  on an oriented system of quads  
 720 can be computed in  $O(\ell)$  time. It is the unique homotopic curve that contains no spurs or  
 721 brackets and whose turning sequence contains no  $-1$ 's and contains at least one turn that is  
 722 not  $-2$ .  
 723  
 724

### 725 4.3 Geodesics

726 A **combinatorial geodesic** of length  $\ell$  is a curve that contains no spurs or brackets of  
 727 length  $\ell - 2$  or less. Given a curve on a system of quads, orientable or not, we can compute  
 728 a homotopic geodesic by iteratively removing spurs and brackets as much as possible. This  
 729 can be done efficiently using the same techniques as in [Erickson and Whittlesey 2013].  
 730  
 731

732 THEOREM 10. Given a combinatorial closed curve of length  $\ell$  on a system of quads, a  
 733 homotopic geodesic can be computed in  $O(\ell)$  time.  
 734

735 On an oriented surface, the canonical form is an instance of combinatorial geodesic. The  
 736 canonical form is the rightmost homotopic geodesic. The definitions of a geodesic and of a  
 737 canonical form extend trivially to paths. In particular, the canonical form of a path is its  
 738 unique rightmost homotopic geodesic and is characterized as for closed curves.  
 739

740 THEOREM 11. On an oriented surface, the canonical form of a combinatorial path is  
 741 the unique homotopic path that contains no spurs or brackets and whose turning sequence  
 742 contains no  $-1$ 's.  
 743

744 Although we cannot claim in general the uniqueness of geodesics in a homotopy class,  
 745 homotopic geodesics are almost equal and have the same length. Specifically, define a **(quad)**  
 746 **staircase** as a planar sequence of quads obtained by stitching an alternating sequence of  
 747  
 748

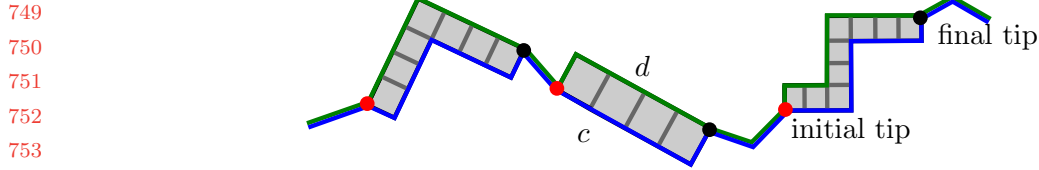


Fig. 4. A disk diagram for two homotopic paths  $c$  and  $d$  composed of paths and staircases.

rows and columns of quads to get the shape of a staircase. Assuming that the staircase goes up from left to right, we define the **initial tip** of a quad staircase as the lower left vertex of the first quad in the sequence. The **final tip** is defined as the upper right vertex of the last quad. See Figure 4. A **closed staircase** is obtained by identifying the two vertical arcs incident to the initial and final tips of a staircase.

**THEOREM 12.** *Let  $c, d$  be two nontrivial homotopic combinatorial geodesics. If  $c, d$  are closed curves, then they label the two boundary cycles of an annular diagram composed of a single closed staircase or of an alternating sequence of paths (possibly reduced to a vertex) and quad staircases connected through their tips. Likewise, if  $c, d$  are paths, then the closed curve  $c \cdot d^{-1}$  labels the boundary of a disk diagram composed of an alternating sequence of paths (possibly reduced to a vertex) and quad staircases connected through their tips.*

**PROOF.** We only detail the proof when  $c, d$  are paths. See Figure 4. The similar case of closed curves is covered in [Erickson and Whittelsey 2013]. By Lemma 7,  $c \cdot d^{-1}$  is the label of the facial walk of the perforated face of a disk diagram  $\Delta$ . This diagram has a cactus-like structure composed of 2-cells subdivided into quads and connected by trees. A vertex  $v$  such that  $\Delta \setminus v$  is not connected is called a *cut vertex*. We also consider as cut vertices the endpoints of  $c$  in  $\Delta$ . A 2-cell of  $\Delta$  must have more than one cut vertex on its boundary. Otherwise, this boundary is entirely labelled by a subpath of either  $c$  or  $d$  and Theorem 8 implies the existence of four brackets, one of which (in fact two) must avoid the cut vertex, hence be contained in the interior of this subpath. This would contradict that  $c$  and  $d$  are geodesic. Moreover, because  $c$  and  $d$  have no spur,  $\Delta$  cannot have more than two degree one vertices, namely the common endpoints of  $c$  and  $d$ . It follows that  $\Delta$  is an alternating sequence of paths and 2-cells. In particular, each 2-cell has exactly two cut vertices. No 2-cell in this sequence has an interior vertex. For otherwise, by the second part of Theorem 8, the boundary of this 2-cell would contain five brackets one of which would be contained in the interior of either  $c$  or  $d$  and this would again contradict that  $c$  and  $d$  are geodesic. It follows that the dual of a 2-cell, viewed as an assembling of quads, is a tree.

793 We finally remark that this tree must be a path with a staircase shape. Indeed, any other  
 794 shape would imply the existence of a bracket in either  $c$  or  $d$ .  $\square$   
 795

796 **COROLLARY 13.** *With the hypothesis of Theorem 12,  $c$  and  $d$  have equal length which is*  
 797 *minimal among homotopic curves.*  
 798

799 A geodesic curve of length  $\ell$  is **exceptional** if it has a bracket of length  $\ell - 1$ . An  
 800 exceptional curve must be 1-sided, since otherwise the curve would have a bracket of length  
 801 1. Figure 5 shows the lift of an exceptional curve; it is contained in an infinite straight strip  
 802 of quadrilaterals that covers a Möbius strip infinitely many times.  
 803



804  
 805  
 806  
 807  
 808 Fig. 5. The lift of an exceptional curve of length 5 has brackets of length 4.  
 809

810 **COROLLARY 14.** *Let  $c$  be a geodesic that is not exceptional. Then  $c$  has no nontrivial*  
 811 *index path whose image path is contractible.*  
 812

813 **PROOF.** If  $c$  has length at least two it follows from the characterization of geodesics that  
 814 the image path of any index path of  $c$  has no spur or brackets, hence is also a geodesic. If  $c$   
 815 has length one, then the image path of a nontrivial index path is a power of  $c$ , hence is  
 816 non-contractible since we are considering surfaces with negative Euler characteristic.  $\square$   
 817  
 818

819 The next two remarks follow directly from the characterization of geodesics and canonical  
 820 forms in terms of spurs, brackets and turns.  
 821

822 *Remark 1.* The image path of any index path of a combinatorial geodesic that is not  
 823 exceptional is geodesic. If the combinatorial geodesic is in canonical form, so is the image  
 824 path.  
 825

826 *Remark 2.* Likewise, any power  $c^k$  of a combinatorial closed geodesic  $c$  that is not exceptional  
 827 is also a combinatorial geodesic. Moreover, if  $c$  is in canonical form, so is  $c^k$ .  
 828

## 829 5 COUNTING INTERSECTIONS COMBINATORIALLY

830  
 831 Let  $c, d$  be primitive combinatorial closed geodesics on a system of quads  $\Sigma$ . We allow  
 832 the case where  $c$  and  $d$  are homotopic but assume that neither of them is a exceptional.  
 833 Referring to Section 3, we view the underlying surface of  $\Sigma$  as a quotient  $\mathbb{D}/\Gamma$  of the Poincaré  
 834 disk. The system of quads lifts to a quadrangulation of  $\mathbb{D}$  and the lifts of  $c, d$  in  $\Sigma$  are  
 835  
 836

837 combinatorial bi-infinite paths in this quadrangulation. We fix a lift  $\tilde{c}$  of  $c$  and consider  
 838 any lift  $\tilde{d}$  of  $d$  whose limit points alternate with the limit points of  $\tilde{c}$  along  $\partial\mathbb{D}$ . It follows  
 839 from Remark 2 and Corollary 13 that  $\tilde{c}$  and  $\tilde{d}$  are geodesics that each minimizes the length  
 840 between any two of its vertices. Let  $i$  be the smallest index along  $\tilde{c}$  such that  $\tilde{c}(i) \in \tilde{d}$  and  
 841 let  $\ell$  be maximal such that  $\tilde{c}(i + \ell) \in \tilde{d}$ . By the preceding discussion  $\tilde{c}(i)$  and  $\tilde{c}(i + \ell)$  also  
 842 delimitate a maximal subpath  $\tilde{d}[j, j + \varepsilon\ell]$  of  $\tilde{d}$  whose endpoints belong to  $\tilde{c}$ , with  $\varepsilon \in \{-1, 1\}$ .  
 843 We are thus in the situation depicted on Figure 2, right, where  $\tilde{c}[-\infty, i - 1]$  and  $\tilde{c}[i + 1, +\infty]$   
 844 are on either part of  $\tilde{d}$  in  $\mathbb{D}$ . In this case we say that the pair of index paths  $([i \xrightarrow{\ell}]_c, [j \xrightarrow{\varepsilon\ell}]_d)$   
 845 is **crossing**. This happens precisely when  $([i \xrightarrow{\ell}]_c, [j \xrightarrow{\varepsilon\ell}]_d)$  is a maximal pair of index paths  
 846 with homotopic image paths and when the circular ordering of the arcs  $\tilde{c}[i, i + 1]$ ,  $\tilde{c}[i, i - 1]$   
 847 and  $\tilde{d}[j, j - \varepsilon]$  is the same as the circular ordering of  $\tilde{c}[i + \ell, i + \ell - 1]$ ,  $\tilde{c}[i + \ell, i + \ell + 1]$  and  
 848  $\tilde{d}[j, j + \varepsilon(\ell + 1)]$ , where  $\varepsilon$  is the sign of  $k$ . This last condition can be checked by comparing  
 849 the direct circular orderings of the projection of those arcs on  $\Sigma$ , taking into account the  
 850 parity of the number of half-twisted arcs in  $c[i \xrightarrow{\ell}]$  (or equivalently in  $d[j \xrightarrow{\varepsilon\ell}]$ ). According to  
 851 Lemma 4 in the strategy section, we have

852  
 853  
 854  
 855  
 856 LEMMA 15.  *$i(c, d)$  is equal to the number of crossing pairs of index paths.*

857  
 858 The case where  $c$  or  $d$  is a exceptional can be dealt with separately. See the proof of  
 859 Lemma 18 and Section 5.3 for further details on the exceptional case.

## 860 5.1 Thick double-paths

861  
 862 Following the description of Theorem 12, the two sides  $c[i \xrightarrow{\ell}]$  and  $d[j \xrightarrow{\varepsilon\ell}]$  of a crossing pair  
 863 of index paths  $([i \xrightarrow{\ell}]_c, [j \xrightarrow{\varepsilon\ell}]_d)$  label a disk diagram composed of a sequence of paths and  
 864 staircases. In particular, the vertices of the two sides can be put in 1-1 correspondence  
 865 and corresponding vertices satisfy a local condition: they stay at distance zero or two and  
 866 bound a same quad in the disk diagram. Hence, when looking for crossing pairs of index  
 867 paths of  $(c, d)$ , we can start from any double point  $(i, j)$  and walk in parallel along the two  
 868 sides from  $i$  and  $j$ , checking the above local condition at each step. However, we do not  
 869 know a priori if the two sides will meet again to form a pair of homotopic paths and the  
 870 search may be unsuccessful. In order to analyze the complexity of the search we consider  
 871 pairs of paths that could potentially be part of a crossing pair of index paths, but are not  
 872 necessarily so. Formally, a pair  $([i \xrightarrow{\ell}]_c, [j \xrightarrow{\varepsilon\ell}]_d)$  of distinct index paths such that  $c[i \xrightarrow{\ell}]$  and  
 873  $d[j \xrightarrow{\varepsilon\ell}]$  are corresponding subpaths of homotopic geodesic paths is called a **thick double**  
 874 **path** of length  $\ell$ . In other words, a thick double path is such that its image paths can be  
 875 extended to form homotopic geodesic paths. A thick double path gives rise to a sequence  
 876  
 877  
 878  
 879  
 880

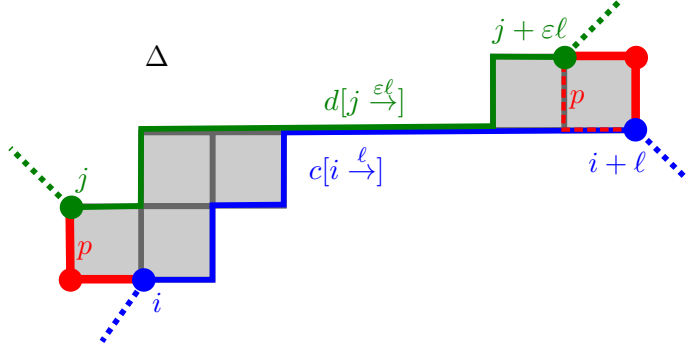


Fig. 6. A thick double path extends to a pair of homotopic geodesics and bound a partial diagram. When  $(i, j)$  and  $(i + l, j + \epsilon l)$  are in the same configuration, the corresponding pairs of vertices in  $\Delta$  are both joined by a path of length zero or two labelled by the same path  $p$ .

of  $\ell + 1$  index pairs  $(i + k, j + \epsilon k)$  for  $k \in [0, \ell]$ . Let  $\Delta$  be a disk diagram whose boundary is labelled by homotopic geodesic paths extending the thick double path as illustrated on Figure 6. The restriction of  $\Delta$  to the part delimited by the thick double path is called a **partial diagram**. In a partial diagram each index pair  $(i, j)$  may be in at most one of five **configurations**: either the corresponding vertices coincide in the partial diagram, or they appear diagonally opposite in a quad; in turn this quad may be labelled by one of the (at most) four quads incident to either  $c[i, i + 1]$  or  $d[j, j + \epsilon]$ . A partial diagram is **maximal** if it cannot be extended to form a partial diagram of a longer thick double path.

LEMMA 16. *If  $c$  and  $d$  are primitive geodesic curves, none of which is exceptional, then each configuration of an index pair may occur at most once in a partial diagram.*

PROOF. Suppose for a contradiction that the index pair  $(i, j)$  occurs twice in the same configuration in a partial diagram of a thick double path of  $(c, d)$ . The two occurrences of  $(i, j)$  are separated by a path whose length  $\ell$  is an integer multiple of  $|c|$ , say  $\ell = k|c|$ , and an integer multiple of  $|d|$ , say  $\epsilon \ell = t|d|$ . In the partial diagram,  $c(i)$  and  $d(j)$  label vertices that are either identical or opposite in a quad. They are thus connected by a path  $p$  of length zero or two. See Figure 6. We infer that

$$c[i \xrightarrow{k|c|}] \cdot p \cdot d[j \xrightarrow{t|d|}] \cdot p^{-1} \quad (1)$$

This implies  $c^k \sim d^t$ , considering free homotopy. Because  $c$  and  $d$  are primitive curves on a surface with negative Euler characteristic, this implies that  $c$  is homotopic to  $d$  or its inverse. Since the intersection number does not depend on the orientation of the curves, we can safely replace  $d$  by  $c$ . We first assume that the two index paths of the thick double

925 path are both forward (i.e.,  $\varepsilon = 1$ ). Exchanging the roles of  $i$  and  $j$  if necessary, we may  
 926 further assume that  $0 < j - i \leq |c|/2$ . Equation (1) now writes  
 927

$$928 \quad c[i \xrightarrow{k|c}] \stackrel{*}{\sim} p \cdot c[j \xrightarrow{k|c}] \cdot p^{-1} \stackrel{*}{\sim} p \cdot c[i, j]^{-1} \cdot c[i \xrightarrow{k|c}] \cdot c[i, j] \cdot p^{-1}$$

929  
 930 Equivalently,  $c'^k \cdot q \stackrel{*}{\sim} q \cdot c'^k$  where  $c' := c[i \xrightarrow{|c|}]$  is a cyclic permutation of  $c$  and  $q := p \cdot c[i, j]^{-1}$   
 931 is a (closed) path of length at most  $j - i + 2$ . Since they are commuting,  $c'^k$  and  $q$  must  
 932 admit a common primitive root [Reinhart 1962]. We thus have (i)  $c'^k \sim u^s$  and (ii)  $q \sim u^t$   
 933 for some primitive curve  $u$  and some  $s, t \in \mathbb{Z}$ . Relation (i) implies that  $c'$  and  $u^s$  are also  
 934 commuting so that  $c'$  is homotopic to a power of the primitive curve  $u$ . But  $c'$  being also  
 935 primitive we actually have  $c' \sim u^{\pm 1}$ . By Remark 2,  $c'^t$  is geodesic, hence has minimal length  
 936 in its homotopy class. From (ii) we obtain  $j - i + 2 \geq |t| \cdot |c|$ . This is only possible if  $t = 0$  or  
 937 if  $|t| = 1$  and  $j - i = |c| - 2$  (recall that the graph of the system of quads is bipartite so  
 938 that indices in a pair have the same parity).  
 939  
 940

- 941 • If  $t = 0$ , then  $q \sim 1$ , so that  $p \sim c[i, j]$ . Since  $c$  is geodesic, we must have  $j - i \leq |p| \leq 2$ ,  
 942 hence  $j = i + 2$  and  $(i, j)$  must correspond to diagonally opposite vertices in a  
 943 quad. Two homotopic paths each of length two bound a disk diagram composed of  
 944 either a length two path or a single quad. In other words,  $c[i, j]$  and  $p$  are either  
 945 equal or bound the first quad in the partial diagram. In either case we infer that  
 946  $c[i, j + 1] = c[i, j] \cdot c[j, j + 1]$  contains a spur or a bracket, leading to a contradiction.  
 947
- 948 • If  $|t| = 1$  and  $j - i = |c| - 2$ , then  $|c| = 4$  (recall that  $0 < j - i \leq |c|/2$ ). A simple  
 949 case study of the possible partial diagrams for such a  $c$  leads to a contradiction in  
 950 each case. See Appendix C for a proof.  
 951  
 952

953  
 954 We now assume that the thick double path is composed of a forward and a backward index  
 955 paths. Similarly to the previous case, we infer that  $c' \stackrel{*}{\sim} q \cdot (c')^{-1} \cdot q^{-1}$ , where  $c' := c[i \xrightarrow{|c|}]$   
 956 and  $q := p \cdot c[i, j]^{-1}$ . Equivalently,  $c$  and its inverse are freely homotopic. This is however  
 957 impossible unless  $c$  is contractible.  $\square$   
 958  
 959

960 **COROLLARY 17.** *Each configuration of an index pair may occur at most once in the set*  
 961 *of maximal partial diagrams.*  
 962  
 963

964 **PROOF.** By the preceding Lemma, we only need to check that a configuration of an index  
 965 pair cannot occur twice in distinct partial diagrams of maximal thick double paths. This is  
 966 essentially the unique lifting property of coverings.  $\square$   
 967

## 5.2 Proof of Theorem 1: the primitive case

LEMMA 18. *Let  $c, d$  be primitive curves of length at most  $\ell$  on a system of quads. The crossing number  $i(c, d)$  can be computed in  $O(\ell^2)$  time.*

PROOF. We may assume that  $c$  and  $d$  are geodesic by Theorem 10. We first consider the case where none of  $c$  or  $d$  is exceptional. According to Lemma 15, we can compute  $i(c, d)$  by enumerating the crossing pairs of index paths of  $(c, d)$ . Following the previous Section 5.1 we only need to list the maximal partial diagrams  $i(c, d)$  and to count those that correspond to crossing pairs of index paths. As described above Lemma 15, this last step can be performed in time proportional to the total length of the maximal partial diagrams, which is  $O(\ell^2)$  by Corollary 17. Since we are only interested in partial diagrams whose sides have coincident vertices, namely the endpoints of the crossing pairs of index paths, we can list the set of maximal partial diagrams as follows. Pick any index pair  $(i, j)$  such that  $c(i) = d(j)$  and form a trivial partial diagram with these vertices in coincident configuration. Extend the partial diagram maximally in both directions. By the unique lifting property of coverings, there is only one way to do so. Mark all the configurations of index pairs found in this diagram and pick a new index pair which is not marked in the coincident configuration. Repeat until all the coincident configurations of index pairs are marked. The total time spent by the procedure is proportional to the total length of the maximal partial diagrams, hence is  $O(\ell^2)$ .

We next consider the case where  $c$  is an exceptional 1-sided curve. Its square  $c^2$  is a 2-sided curve with a unique homotopic geodesic whose turn sequence is  $2^*$  or  $\bar{2}^*$ . In particular,  $c^2$  cannot form a staircase with any curve since both sides of a staircase must have a vertex whose corresponding turn is  $\pm 1$ . (Although it forms an infinite strip of width one with itself.) It follows that the crossing pairs of index paths of  $(c, d)$  are flat, i.e., the index paths have identical image paths. This makes the search for crossing pairs of index paths even easier than in the general case so that  $i(c^2, d)$  can be computed in  $O(\ell^2)$  time. Applying the formulas in Proposition 21 below we finally derive  $i(c, d) = i(c^2, d)/2$ . Similar arguments apply when both  $c$  and  $d$  are exceptional to compute  $i(c, d) = i(c^2, d^2)/4$ , including the case where  $c$  and  $d$  are homotopic.  $\square$

## 5.3 Non-primitive curves

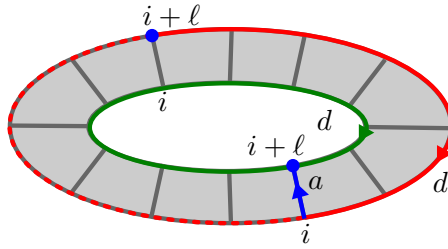
In order to finish the proof of Theorem 1 we need to handle the case of non-primitive curves. Thanks to canonical forms, computing the primitive root of a curve becomes extremely simple (see also Lustig [Lustig 1987, Rem. 5.2]) on oriented surfaces.

1013 LEMMA 19. *Let  $c$  be a combinatorial curve of length  $\ell > 0$  in canonical form on an*  
 1014 *oriented system of quads. A primitive curve  $d$  such that  $c$  is homotopic to  $d^k$  for some*  
 1015 *integer  $k$  can be computed in  $O(\ell)$  time.*  
 1016

1017 PROOF. By Theorem 9, we may assume that  $c$  and  $d$  are in canonical form. By Remark 2,  
 1018 the curve  $d^k$  is also in canonical form. The uniqueness of the canonical form implies that  
 1019  $c = d^k$ , possibly after some circular shift of  $d$ . It follows that  $d$  is the smallest prefix of  $c$   
 1020 such that  $c$  is a power of this prefix. It can be found in  $O(\ell)$  time using a variation of the  
 1021 Knuth-Morris-Pratt algorithm to find the smallest period of a word [Knuth et al. 1977].  $\square$   
 1022  
 1023

1024 We now consider the case of a curve  $c$  on a non-orientable system of quads. If  $c$  is 2-sided it  
 1025 can also be given one of two canonical forms by fixing one of the two consistent orientations  
 1026 along the curve before removing spurs, brackets and  $-1$ 's in its turn sequence. Alternately,  
 1027 we can build and orient the double cover of the system of quads and note that the 2-sided  
 1028 curves are precisely those that lift to closed curves in this cover. The projection of the  
 1029 canonical form of a lift provides one of two canonical forms corresponding to the two possible  
 1030 lifts. By Lemma 19 we can compute in linear time a primitive root of the lift in canonical  
 1031 form. Its projection  $d$  is thus a 2-sided geodesic. If  $d$  is itself primitive, then  $d$  is a primitive  
 1032 root of  $c$ . Otherwise,  $d \sim e^2$  for some 1-sided primitive curve  $e$ .  
 1033  
 1034

- 1035 • If  $e$  is exceptional then  $d$  has a constant turn sequence  $2^*$  or  $\bar{2}^*$  and bounds an  
 1036 immersed annulus wrapping twice around a Möbius strip. Consider any non-boundary  
 1037 arc  $a$  of this annulus. Let  $d(i)$  be the source point of  $a$ , and let  $\ell = |d|/2$ . Then  
 1038  $d \sim (d[i + \ell \xrightarrow{\ell}] \cdot a)^2$  so that  $e$  must be homotopic to  $d[i \xrightarrow{\ell}] \cdot a$ . See Figure 7.  
 1039



1040  
1041  
1042  
1043  
1044  
1045  
1046  
1047  
1048 Fig. 7. An annular diagram for  $d$  with itself.  
1049

- 1050 • If  $e$  is not exceptional, then  $|e| = \ell$  and  $e^2$  is geodesic. Consider an annular diagram  
 1051  $\Delta$  for  $d$  and  $e^2$ . As for a thick partial diagram, the boundary loops of  $\Delta$  can be put  
 1052 in 1-1 correspondence so that corresponding vertices appear in one of five possible  
 1053 configurations (in fact, only three are possible since  $d$  is canonical). Let  $p_0$  and  
 1054  $p_\ell$  be paths of length at most two connecting  $d(0)$  and  $d(\ell)$  to respectively  $e^2(0)$   
 1055  
 1056



1057 and  $e^2(\ell)$ . The possible configurations provide at most five candidates for  $p_0$  and  
 1058 similarly for  $p_\ell$ . For each pair of candidates, say  $(q_0, q_\ell)$ , we consider the curve  
 1059  $e' := q_0^{-1} \cdot d[0 \xrightarrow{\ell}] \cdot q_\ell$ . We can confirm that the path candidates are the right ones by  
 1060 checking whether  $e'^2$  is indeed homotopic to  $d$ . This takes  $O(\ell)$  time by Theorem 9.  
 1061

1062 Finally, if  $c$  is 1-sided we can reduce the computation of a primitive root to the 2-sided  
 1063 case by noting that  $c$  and  $c^2$  have the same primitive roots. To summarize the discussion,  
 1064

1065 PROPOSITION 20. *Given a curve  $c$  of length  $\ell$  on a system of quads, orientable or not, a*  
 1066 *primitive root of  $c$  can be computed in  $O(\ell)$  time.*  
 1067

#### 1068 5.4 End of proof of Theorem 1

1069 We know have all the ingredients to complete the proof of Theorem 1. We essentially need  
 1070 to extend Lemma 18 to non-primitive curves and to handle the case of curves on surfaces  
 1071 of non-negative Euler characteristic. The geometric intersection number of non-primitive  
 1072 curves is related to the geometric intersection number of their primitive roots by simple  
 1073 formulas. The next result is rather intuitive, see Figures 8 and 9, and is part of the folklore  
 1074 although we could only find references in some relatively recent papers.  
 1075  
 1076  
 1077

1078 PROPOSITION 21 ([DE GRAAF AND SCHRIJVER 1997; GONÇALVES ET AL. 2005]). *Let*  
 1079  *$c$  and  $d$  be primitive curves such that  $c$  is not homotopic to  $d$  or its inverse and let  $p, q$  be*  
 1080 *positive integers. Then,*  
 1081

$$1082 \quad i(c^p, d^q) = pq \times i(c, d)$$

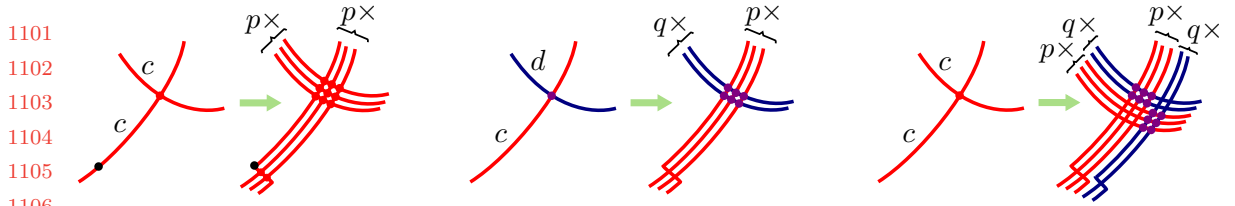
1083 and

$$1084 \quad i(c^p, c^q) = \begin{cases} 2pq \times i(c) + \min\{p, q\} & \text{if } c \text{ is 1-sided and } p \text{ and } q \text{ are odd,} \\ 2pq \times i(c) & \text{otherwise.} \end{cases}$$

1087 Moreover, the geometric self-intersection number of a curve is related to the geometric  
 1088 self-intersection number of its root thanks to the formulas  
 1089

$$1090 \quad i(c^p) = \begin{cases} p^2 \times i(c) + p - 1 & \text{if } c \text{ is 2-sided,} \\ p^2 \times i(c) + \lfloor \frac{p-1}{2} \rfloor & \text{otherwise.} \end{cases}$$

1094 PROOF OF THEOREM 1. Let  $c, d$  and  $\Sigma$  be the two combinatorial curves and the combina-  
 1095 torial surface as in the Theorem. By Lemma 6 we can assume after  $O(n)$  time preprocessing  
 1096 that  $\Sigma$  is a system of quads. We first consider the case where  $\Sigma$  has negative Euler character-  
 1097 istic. Thanks to Theorem 10 and Proposition 20 we can determine geodesic primitive curves  
 1098  $c'$  and  $d'$  and integers  $p, q$  such that  $c \sim c'^p$  and  $d \sim d'^q$  in  $O(\ell)$  time. We then compute  
 1099  
 1100



1107 Fig. 8. Left, each self-intersection of a 2-sided curve  $c$  gives rise to  $p^2$  self-intersections of its  $p$ th power  
 1108 obtained by wrapping  $p$  times around  $c$  in a small tubular neighborhood.  $p - 1$  additional self-intersections  
 1109 are needed to connect the end of the wrapping curve with the basepoint. Middle, each intersection of  $c$   
 1110 and  $d$  gives rise to  $pq$  intersections of (homotopic perturbations of)  $c^p$  and  $d^q$ . Right, when  $c$  and  $d$  are  
 1111 homotopic and  $c^p$  or  $c^q$  is 2-sided, one should count  $2pq$  intersections per self-intersection of  $c$ .



1122 Fig. 9. Left, the  $p$ th power of a 1-sided curve  $c$  is obtained from  $p$  copies of  $c$  running parallel to  $c$   
 1123 and arriving at the starting basepoint of  $c$  in reverse order. By ordering the copies conveniently we get  
 1124  $\lfloor \frac{p-1}{2} \rfloor$  self-intersections to reconnect the copies instead of  $p - 1$  for a 2-sided curve. Right, a minimal  
 1125 configuration for  $c^p$  and  $c^q$  with  $p = 3$  and  $q = 5$ .

1128  $i(c', d')$  and  $i(c', c')$  in  $O(\ell^2)$  time according to Corollary 18. We finally use the formulas in  
 1129 the previous proposition to deduce  $i(c, d)$  and  $i(c)$  from  $i(c', d')$  and  $i(c', c')$ .

1130 We next consider the case where  $\Sigma$  has non-negative Euler characteristic.

- 1132 • If  $\Sigma$  is a sphere or a disk, then every curve is contractible and  $i(c, d) = i(c) = 0$ .
- 1133 • If  $\Sigma$  is a cylinder, then every two curves can be made non crossing so that  $i(c, d) = 0$   
 1134 while  $i(c) = p - 1$ .
- 1135 • If  $\Sigma$  is a projective plane, there is only one non-trivial homotopy class, say  $c'$ , for  
 1136 which  $i(c', c') = 1$  and  $i(c') = 0$ .
- 1137 • If  $\Sigma$  is a torus, there is no need to build a system of quads and we may just  
 1138 compute the reduced surface which is composed of two loop edges. Those loop  
 1139 edges, say  $\alpha$  and  $\beta$ , represent generators of the fundamental group of the torus and  
 1140 we can write  $c \sim \alpha^x \cdot \beta^y$  and  $d \sim \alpha^{x'} \cdot \beta^{y'}$ . It results from classical formulas that:  
 1141  $i(c) = \gcd(x, y) - 1$  and  $i(c, d) = |\det((x, y), (x', y'))|$ .

- Finally, if  $\Sigma$  is a Klein bottle, similarly to the torus case the reduced surface is composed of two loops  $\alpha, \beta$  satisfying either the relation  $\alpha^2\beta^2 \sim 1$  or  $\alpha\beta\alpha\beta^{-1} \sim 1$ . We can transform the embedded graph in constant time so that the second relation holds. This relation can be written as a pseudo commutation relation  $\alpha\beta = \beta\alpha^{-1}$  that preserves the cumulative sum of the exponents of  $\beta$  and the parity of the cumulative sum of the exponents of  $\alpha$ . From this simple remark we easily derive that every conjugacy class in the fundamental group has a unique normal form  $\alpha^m\beta^{2n}, \beta^{2n+1}$  or  $\alpha\beta^{2n+1}$ , where  $m, n$  can take any integer value. Table 1 provides all the geometric intersection numbers for the primitive classes, which must have one of the forms  $\beta, \alpha\beta$ , or  $\alpha^n\beta^{2m}$  with  $m$  and  $n$  coprime. We can combine this table

	$\alpha^k\beta^{2\ell}$		$\beta$	$\alpha\beta$
$\alpha^m\beta^{2n}$	$\left\  \begin{smallmatrix} k & m \\ \ell & n \end{smallmatrix} \right\  + \left\  \begin{smallmatrix} k & -m \\ \ell & n \end{smallmatrix} \right\ $	$ m $	$ m $	
$\beta$	$ k $	1	0	
$\alpha\beta$	$ k $	0	1	

$c$	$\alpha^k\beta^{2\ell}$	$\beta$	$\alpha\beta$
$i(c)$	$ k\ell $	0	0

Table 1. Left table, the geometric intersection numbers for the pairs of distinct primitive homotopy classes. Here,  $k$  and  $\ell$  are coprime, as well as  $m$  and  $n$ , and  $(k, \ell) \neq \pm(m, n)$ . We use the notation  $\left\| \begin{smallmatrix} x & y \\ z & t \end{smallmatrix} \right\| := |xt - yz|$ . Right table, the geometric self-intersection numbers of primitive classes. Again,  $k$  and  $\ell$  are assumed to be coprime.

with the formulas of Propositions 21 to compute the geometric intersection number of any curves.

□

## 6 COMPUTING INTERSECTION NUMBERS ON ORIENTED SURFACES

For the rest of the paper we assume that **all considered system of quads are orientable** (and consistently oriented). In this case we can rely on canonical forms to obtain a simpler algorithm for the computation of the geometric intersection number. Since the resulting asymptotic complexity is the same as for the general case, the reader may skip this rather technical and independent section and proceed with Section 7.

The next technical Lemma will be used in Proposition 27 to analyze the intersection of canonical curves. Let  $c_R$  and  $c_L^{-1}$  be canonical paths such that  $c_R \sim c_L$ . In other words,  $c_L$  is the leftmost geodesic homotopic to  $c_R$ . By Theorem 12, there is a disk diagram  $\Delta$  composed of quad staircases and paths and whose left and right boundaries  $\Delta_L$  and  $\Delta_R$  are labelled by  $c_L$  and  $c_R$  respectively. A **spoke** is a non-boundary edge of  $\Delta$ .

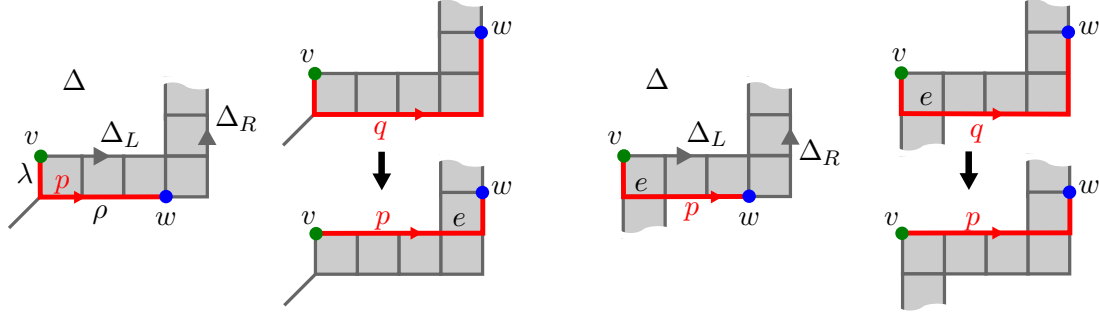


Fig. 10. The canonical path  $p$  from  $v$  to  $w$  when  $v$  is not incident to a spoke.

LEMMA 22. Let  $v, w$  be two vertices, one on each side of  $\Delta$ . Then  $\Delta$  contains a path  $p$  from  $v$  to  $w$  labelled by a canonical path. Moreover,  $p$  can be uniquely decomposed as either  $\lambda.\rho$ ,  $\rho.\lambda$ ,  $\lambda.e.p$  or  $p.e.\lambda$ , where

- (1)  $\lambda$  is a subpath (possibly reduced to a vertex) of  $\Delta_L$  or  $\Delta_L^{-1}$ ,
- (2)  $\rho$  is a subpath (possibly reduced to a vertex) of  $\Delta_R$  or  $\Delta_R^{-1}$ ,
- (3)  $e$  is a spoke,
- (4) if  $\lambda$  is a subpath of  $\Delta_L^{-1}$  of positive length then  $p \cap \Delta_L^{-1} = \lambda$ ,
- (5) if  $\rho$  is a subpath of  $\Delta_R$  of positive length then  $p \cap \Delta_R = \rho$ .
- (6) if  $\rho$  is a subpath of  $\Delta_R^{-1}$  and  $\lambda$  is a subpath of  $\Delta_L$  then either  $\rho$  is reduced to a vertex and  $p \cap \Delta_R = \rho$  or  $\lambda$  is reduced to a vertex and  $p \cap \Delta_L^{-1} = \lambda$ .

PROOF. We assume that  $v$  is on the left side and  $w$  on the right side of  $\Delta$ , the other case being symmetric. Let  $i, j$  be such that  $v = \Delta_L(i)$  and  $w = \Delta_R(j)$ . We first consider the case where  $j \geq i$ . If  $\Delta_L$  and  $\Delta_R$  coincide at  $v$ , then we trivially obtain the desired decomposition as  $p = \Delta_L[i \xrightarrow{0}] . \Delta_R[i \xrightarrow{j-i}]$ . Otherwise,  $v$  may be incident to 0, 1 or 2 spokes.

- If  $v$  is not incident to a spoke then  $\Delta_L(i-1)$  is either the initial tip of a staircase or is incident to a spoke  $e$ . We set  $q = \Delta_L[i \xrightarrow{-1}] . \Delta_R[i-1 \xrightarrow{j-i+1}]$  in the first case and  $q = \Delta_L[i \xrightarrow{-1}] . e . \Delta_R[i-1 \xrightarrow{j-i+1}]$  otherwise. The path  $q$  has no spurs or  $-1$  turns but may start with a bracket. If not, by the characterization of Theorem 11,  $q$  is already canonical and we can set  $p = q$ . Otherwise, we short cut the bracket in  $q$  to obtain a canonical path  $p$  satisfying the above points 1 to 5. See Figure 10.
- If  $v$  is incident to exactly one spoke  $e$ , then  $e$  connects  $v$  to either  $\Delta_R(i-1)$  or  $\Delta_R(i+1)$ . In the former case we set  $q = e . \Delta_R[i-1 \xrightarrow{j-i+1}]$ . As above,  $q$  may be canonical or starts with a bracket and we easily obtain the path  $p$  with the desired properties. See Figure 11. If  $e$  is incident to  $\Delta_R(i+1)$  and  $j > i$  the path

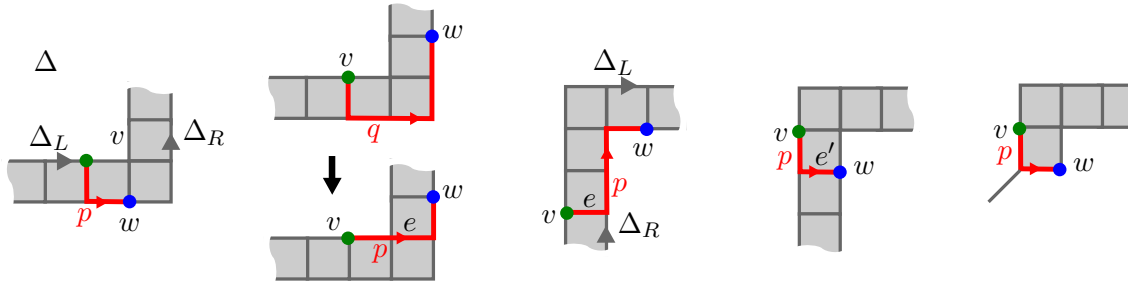


Fig. 11. The canonical path  $p$  from  $v$  to  $w$  when  $v$  is incident to exactly one spoke.

$p = \Delta_L[i \xrightarrow{0}].e.\Delta_R[i + 1 \xrightarrow{j-i-1}]$  has the required properties. When  $e$  is incident to  $\Delta_R(i + 1)$  and  $j = i$ , then either  $\Delta_L(i - 1)$  is incident to a spoke  $e'$  and we must have  $p = \Delta_L[i \xrightarrow{-1}].e'.\Delta_R[i \xrightarrow{0}]$ , or  $\Delta_L(i - 1)$  must be the initial tip of a staircase and we must have  $p = \Delta_L[i \xrightarrow{-1}].\Delta_R[i - 1 \xrightarrow{1}]$ .

- If  $v$  is incident to two spokes, then one of them,  $e_-$ , connects  $v$  to  $\Delta_R(i - 1)$  and the other  $e_+$  connects  $v$  to  $\Delta_R(i + 1)$ . We can directly set  $p = e_-.\Delta_R[i - 1 \xrightarrow{1}]$  if  $j = i$  and  $p = e_+.\Delta_R[i + 1 \xrightarrow{j-i-1}]$  if  $j > i$ .

For Point 6 in the Lemma, we note that we cannot have  $p = \lambda.\rho$  or  $p = \lambda.e.\rho$  with both  $\lambda$  and  $\rho$  being subpaths of positive length of  $\Delta_L$  and  $\Delta_R^{-1}$  respectively. Indeed,  $p$  would have a spur or a  $\bar{1}$  turn in the first case and a bracket in the other case. Moreover, if  $\rho$  is reduced to a vertex and  $\lambda$  is a subpath of  $\Delta_L$ , we may assume that the intersection  $p \cap \Delta_R$  is reduced to  $\rho$ . Otherwise, the canonical path between any other intersection point and  $\rho$  would have to follow  $\Delta_R$  and we could express  $p$  so that  $\rho$  is a subpath of positive length of  $\Delta_R$ . An analogous argument holds to show that we can assume  $p \cap \Delta_L^{-1} = \lambda$  if  $\lambda$  is reduced to a vertex.

We next consider the case  $i > j$ . When  $\Delta_L$  and  $\Delta_R$  coincide at  $w$ , we obtain the desired decomposition as  $p = \Delta_L[i \xrightarrow{j-i}].\Delta_R[i \xrightarrow{0}]$ . Otherwise,  $w$  may be incident to 0, 1 or 2 spokes. Similar arguments as in the case  $j \geq i$  allow to conclude the proof.  $\square$

## 6.1 Crossing double-paths

Let  $c, d$  be two combinatorial closed curves on a combinatorial surface. A **double-path** of  $(c, d)$  of length  $\ell$  is a pair of forward index paths  $([i \xrightarrow{\ell}]_c, [j \xrightarrow{\ell}]_d)$  with the same image path  $c[i \xrightarrow{\ell}] = d[j \xrightarrow{\ell}]$ . If  $\ell = 0$  then the double path is just a double point. A double path of  $c$  is defined similarly, taking  $c = d$  and assuming  $i \neq j$ . The next Lemma follows from Remark 1.

1277 LEMMA 23. Let  $[i \xrightarrow{\ell}]_c$  and  $[j \xrightarrow{k}]_d$  be forward index paths of two canonical curves  $c$  and  $d$   
 1278 such that the image paths  $c[i \xrightarrow{\ell}]$  and  $[j \xrightarrow{k}]$  are homotopic. Then  $k = \ell$  and  $([i \xrightarrow{\ell}]_c, [j \xrightarrow{\ell}]_d)$   
 1279 is a double path.  
 1280

1281 A double path  $([i \xrightarrow{\ell}]_c, [j \xrightarrow{\ell}]_d)$  gives rise to a sequence of  $\ell + 1$  double points  $(i + k, j + k)$   
 1282 for  $k \in [0, \ell]$ . A priori a double point could occur several times in this sequence. The next  
 1283 two lemmas claim that this is not possible when the curves are primitive.  
 1284

1285 LEMMA 24. A double path of a primitive combinatorial curve  $c$  cannot contain a double  
 1286 point more than once in its sequence. In particular, a double path of  $c$  must be strictly  
 1287 shorter than  $c$ .  
 1288

1289 PROOF. Suppose that a double path  $\mathbb{P}$  of  $c$  contains two occurrences of a double point  
 1290  $(i, j)$ . Because the couples  $(i, j)$  and  $(j, i)$  represent the same double point there are two  
 1291 cases to consider.  
 1292

- 1293 • If  $\mathbb{P}$  contains the couple  $(i, j)$  twice then it must contain a subsequence of length  $|c|$   
 1294 starting with  $(i, j)$ . We thus have  $c[i \xrightarrow{|c|}] = c[j \xrightarrow{|c|}]$ . This implies that  $c$  is equal to  
 1295 some nontrivial circular permutation of itself. It is a simple exercise to check that  $c$   
 1296 must then be a proper power of some other curve, contradicting that  $c$  is primitive.  
 1297
- 1298 • Otherwise  $\mathbb{P}$  contains  $(i, j)$  and  $(j, i)$ . Let  $\ell$  be the distance between these two  
 1299 occurrences in  $\mathbb{P}$ . We thus have  $c[i \xrightarrow{\ell}] = c[j \xrightarrow{|c|-\ell}]$  from which we deduce that  $c$  is a  
 1300 square (and  $\ell = |c|/2$ ), contradicting that  $c$  is primitive.  
 1301

□

1302  
 1303  
 1304 LEMMA 25. Let  $c$  and  $d$  be two non-homotopic primitive combinatorial curves. A double  
 1305 path of  $(c, d)$  cannot contain a double point more than once in its sequence. Moreover, the  
 1306 length of a double path of  $(c, d)$  must be less than  $|c| + |d| - 1$ .  
 1307

1308 PROOF. Suppose that a double path of  $(c, d)$  contains two occurrences of a double point.  
 1309 After shortening the double path if necessary, we may assume that these two occurrences  
 1310 are the first and the last double points of the double path. Its length must accordingly be a  
 1311 nonzero integer multiple  $p$  of  $|c|$  as well as a nonzero integer multiple  $q$  of  $|d|$ . It follows that  
 1312 for some circular permutations  $c'$  of  $c$  and  $d'$  of  $d$  we have  $c'^p = d'^q$ . By a classical result of  
 1313 combinatorics on words [Lothaire 1997, Prop. 1.3.1] this implies that  $c'$  and  $d'$  are powers of  
 1314 a same curve, in contradiction with the hypotheses in the lemma. In fact, by a refinement  
 1315 due to Fine and Wilf [Lothaire 1997, Prop. 1.3.5] it suffices that  $c'^p$  and  $d'^q$  have a common  
 1316 prefix of length  $|c| + |d| - 1$  to conclude that  $c'$  and  $d'$  are powers of a same curve. This  
 1317 proves the second part of the lemma.  
 1318  
 1319

□

1321 A double path whose index paths cannot be extended is said **maximal**. As an immediate  
 1322 consequence of Lemmas 24 and 25 we have:

1323  
 1324 **COROLLARY 26.** *The maximal double paths of a primitive curve or of two primitive*  
 1325 *curves in canonical form induce a partition of the double points of the curves.*

1326 Let  $(i, j)$  and  $(i + \ell, j + \ell)$  be the first and the last double points of a maximal double  
 1327 path of  $(c, d)$ , possibly with  $c = d$ . When  $\ell \geq 1$  the arcs  $c[i, i - 1]$ ,  $d[j, j - 1]$ ,  $c[i, i + 1]$  must  
 1328 be pairwise distinct because canonical curves have no spurs, and similarly for the three  
 1329 arcs  $c[i + \ell, i + \ell + 1]$ ,  $d[j + \ell, j + \ell + 1]$ ,  $c[i + \ell, i + \ell - 1]$ . We declare the maximal double  
 1330 path to be a **crossing double path** if the circular ordering of the first three arcs at  $c(i)$   
 1331 and the circular ordering of the last three arcs at  $c(i + \ell)$  are either both clockwise or both  
 1332 counterclockwise with respect to the rotation system of the system of quads. When  $\ell = 0$ ,  
 1333 that is when the maximal double path is reduced to the double point<sup>1</sup>  $(i, j)$ , we require  
 1334 that the arcs  $c[i, i - 1]$ ,  $d[j, j - 1]$ ,  $c[i, i + 1]$ ,  $d[j, j + 1]$  are *pairwise distinct* and appear in  
 1335 this circular order, or its opposite, around the vertex  $c(i) = d(j)$ .

## 1339 6.2 Proof of Theorem 1 in the orientable case

1340 Let  $c, d$  be primitive combinatorial curves such that  $d$  is canonical and let  $c_R$  and  $c_L^{-1}$  be the  
 1341 canonical curves homotopic to  $c$  and  $c^{-1}$  respectively. We denote by  $\Delta$  the annular diagram  
 1342 corresponding to  $c_R$  and  $c_L$ . When the two boundaries  $\Delta_R$  and  $\Delta_L$  of  $\Delta$  have a common  
 1343 vertex we implicitly assume that  $c_R$  and  $c_L$  are indexed so that this vertex corresponds to  
 1344 the same index along  $\Delta_R$  and  $\Delta_L$ . We consider the following set of double paths:

- 1347 •  $\mathcal{D}_+$  is the set of crossing double paths of positive length of  $c_R$  and  $d$ ,
- 1348 •  $\mathcal{D}_0$  is the set of crossing double paths  $(i, j)$  of zero length of  $c_R$  and  $d$  such that  
 1349 either  
 1350 – the two boundaries of  $\Delta$  coincide at  $\Delta_L(i) = \Delta_R(i)$  and  $d[j - 1, j] = c_L[i - 1, i]$   
 1351 or  $d[j, j + 1] = c_L[i, i + 1]$ , or  
 1352 – one of  $d[j, j - 1]$  or  $d[j, j + 1]$  is the label of a spoke  $(\Delta_R(i), \Delta_L(i'))$  of  $\Delta$  and  
 1353  $d[j - 2, j - 1] = c_L[i' - 1, i']$  in the first case or  $d[j + 1, j + 2] = c_L[i', i' + 1]$  in  
 1354 the other case.
- 1355 •  $\mathcal{D}_-$  is the set of crossing double paths  $([i \xrightarrow{\ell}]_{c_L^{-1}}, [j \xrightarrow{\ell}]_d)$  ( $\ell \geq 0$ ) of  $c_L^{-1}$  and  $d$  such  
 1356 that *none* of the following situations occurs:  
 1357 – the two boundaries of  $\Delta$  coincide at  $\Delta_L^{-1}(i) = \Delta_R(i')$  and  $d[j - 1, j] = c_R[i' -$   
 1358  $1, i']$ ,

1362 <sup>1</sup>Those crossing double points should not be confused with the combinatorial crossings of an immersion as  
 1363 defined in Section 4. Which notion of crossings is used should always be clear from the context.

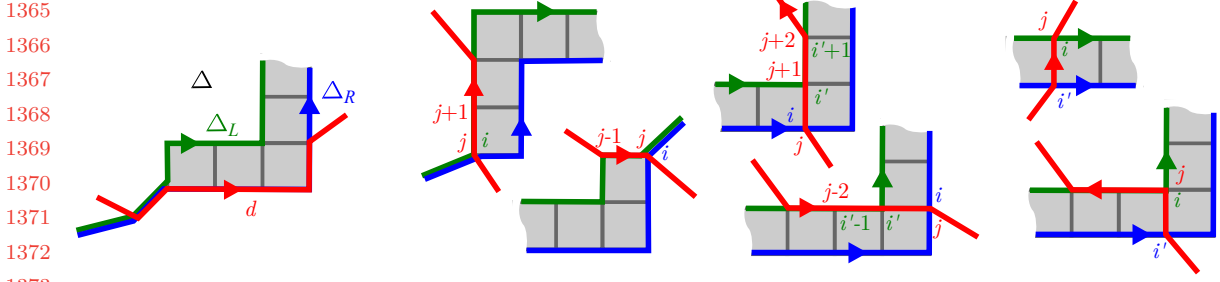


Fig. 12. Left, a typical crossing double path in  $\mathcal{D}_+$ . Middle, four configurations in  $\mathcal{D}_0$ . Right, two configurations in  $\mathcal{D}_-$ .

- the two boundaries of  $\Delta$  coincide at  $\Delta_L^{-1}(i+\ell) = \Delta_R(i')$  and  $d[j+\ell, j+\ell+1] = c_R[i', i'+1]$ ,
- $d[j-1, j]$  is the label of a spoke  $(\Delta_L^{-1}(i), \Delta_R(i'))$  of  $\Delta$  and  $d[j-2, j-1] = c_R[i'-1, i']$ ,
- $d[j+\ell, j+\ell+1]$  is the label of a spoke  $(\Delta_L^{-1}(i+\ell), \Delta_R(i'))$  of  $\Delta$  and  $d[j+\ell+1, j+\ell+2] = c_R[i', i'+1]$ .

Those definitions allow the case  $c \sim d$ , recalling that the index paths of a double path of  $c$  must be distinct by definition. Figure 12 depicts some configurations. Referring to Section 3, we view the underlying surface of the system of quads  $\Sigma$  as a quotient  $\mathbb{D}/\Gamma$  of the Poincaré disk. The system of quads lifts to a quadrangulation of  $\mathbb{D}$  and the lifts of a combinatorial curve in  $\Sigma$  are combinatorial bi-infinite paths in this quadrangulation. By Remark 2, if the combinatorial curve is geodesic (resp. canonical) so are its lifts. In this case, each lift is simple by Corollary 14. We fix a lift  $\tilde{c}_R$  of  $c_R$  and consider the set  $B/\tau$  of Lemma 4 corresponding to the classes of lifts of  $d$  whose limit points alternate with the limit points of  $\tilde{c}_R$  along  $\partial\mathbb{D}$ .

**PROPOSITION 27.**  *$B/\tau$  is in 1-1 correspondence with the disjoint union  $\mathcal{D}_+ \cup \mathcal{D}_0 \cup \mathcal{D}_-$ .*

**PROOF.** Let  $\tilde{c}_L$  be the lift of  $c_L$  with the same limit points as  $\tilde{c}_R$ . These two lifts project onto the boundaries of the annular diagram  $\Delta$  and thus form an infinite strip  $\tilde{\Delta}$  of width at most 1 in  $\mathbb{D}$  composed of paths and quad staircases (possibly a single infinite staircase). We shall define a correspondence between  $B/\tau$  and  $\mathcal{D}_+ \cup \mathcal{D}_0 \cup \mathcal{D}_-$ . To this end we consider a lift  $\tilde{d}$  of  $d$  whose limit points alternate with those of  $\tilde{c}_R$ . In other words,  $\tilde{d} \in B$ . The lift  $\tilde{d}$  must cross  $\tilde{\Delta}$ . Let  $i$  and  $j$  be respectively the smallest and largest index  $k$  such that  $\tilde{d}(k)$  is in  $\tilde{\Delta}$ . By Remark 1, the corresponding subpath  $\tilde{d}[i, j]$  of  $\tilde{d}$  is canonical. Since  $\mathbb{D}$  is simply connected,  $\tilde{d}[i, j]$  is homotopic to any path joining the same extremities and we can apply



1409 Lemma 22 to show that  $\tilde{d}[i, j]$  is actually contained in  $\tilde{\Delta}$  and that it can be decomposed  
 1410 as either  $\lambda.\rho$ ,  $\rho.\lambda$ ,  $\lambda.e.\rho$  or  $\rho.e.\lambda$  where  $e$  is a spoke of  $\tilde{\Delta}$ ,  $\rho = \tilde{c}_R[a \xrightarrow{r}]$  and  $\lambda = \tilde{c}_L[b \xrightarrow{\ell}]$  for  
 1411 some  $a, b, r, \ell \in \mathbb{Z}$ .  
 1412

- 1413 • If  $r > 0$  then by Point 5 of Lemma 22 we have  $\tilde{d} \cap \tilde{c}_R = \rho$  so that this intersection  
 1414 defines a maximal double path of  $\tilde{d}$  and  $\tilde{c}_R$ . It must be crossing since  $\tilde{d} \in B$ . Its  
 1415 projection on  $\Sigma$  is a crossing double path of length  $r > 0$  of  $d$  and  $c_R$ , hence in  $\mathcal{D}_+$ ,  
 1416 to which we map  $\tilde{d}$ .  
 1417
- 1418 • If  $r = 0$  and  $\ell > 0$ , then Point 6 of Lemma 22 implies  $\tilde{d} \cap \tilde{c}_R = \rho$ . As above,  $\rho$  must  
 1419 define a crossing double path of length zero of  $\tilde{d}$  and  $\tilde{c}_R$ . We map  $\tilde{d}$  to the projection  
 1420 of this crossing double point on  $\Sigma$  and remark that this projection is in  $\mathcal{D}_0$ .  
 1421
- 1422 • Otherwise, we must have  $r \leq 0$  and  $\ell \leq 0$  by Point 6 of Lemma 22. If  $\ell < 0$  then  
 1423 Point 4 of Lemma 22 implies  $\tilde{d} \cap \tilde{c}_L^{-1} = \lambda$ . This intersection defines a crossing  
 1424 double path of  $\tilde{d}$  and  $\tilde{c}_L^{-1}$  and we map  $\tilde{d}$  to its projection on  $\Sigma$ . If  $\ell = 0$  and  $r < 0$   
 1425 then Point 6 of Lemma 22 implies  $\tilde{d} \cap \tilde{c}_L^{-1} = \lambda$ , which also holds true if  $r = \ell = 0$ .  
 1426 In both cases  $\lambda$  corresponds to a crossing double path of length zero of  $\tilde{d}$  and  $\tilde{c}_L^{-1}$   
 1427 and we map  $\tilde{d}$  to its projection on  $\Sigma$ . We finally remark that this last projection or  
 1428 the above one belong to  $\mathcal{D}_-$ .  
 1429

1430 Because  $\tilde{\Delta}$  is left globally invariant by  $\tau$  (the hyperbolic motion that sends  $\tilde{c}_R(0)$  to  
 1431  $\tilde{c}_R(|c_R|)$ ), we have  $\tau(\tilde{d}) \cap \tilde{\Delta} = \tau(\tilde{d}) \cap \tau(\tilde{\Delta}) = \tau(\tilde{d} \cap \tilde{\Delta})$ . It follows that  $\tilde{d}$  and  $\tau(\tilde{d})$  are mapped  
 1432 to the same crossing double path by the above rules. We thus have a well defined map  
 1433  $B/\tau \rightarrow \mathcal{D}_+ \cup \mathcal{D}_0 \cup \mathcal{D}_-$ . The uniqueness of the decomposition in Lemma 22 implies that  
 1434 this map is 1-1. In order to check that the map is onto we consider a maximal crossing  
 1435 double path  $\mathbb{P} = ([i \bmod |c_R| \xrightarrow{\ell}]_{c_R}, [j \bmod |d| \xrightarrow{\ell}]_d)$  of  $c_R$  and  $d$  in  $\mathcal{D}_+$ . By the unique  
 1436 lifting property of coverings there is a unique lift  $\tilde{d}$  of  $d$  such that  $\tilde{d}(j) = \tilde{c}_R(i)$  and  $\mathbb{P}$  lifts to  
 1437 a crossing double path of  $\tilde{d}$  and  $\tilde{c}_R$ . By Lemma 23 this double path is the only intersection  
 1438 of  $\tilde{d}$  and  $\tilde{c}_R$  so these lifts must have alternating limit points. In other words  $\tilde{d}$  is in  $B$  and is  
 1439 mapped to  $\mathbb{P}$ . A similar argument applies to the crossing double paths of  $\mathcal{D}_0$  and  $\mathcal{D}_-$ .  $\square$   
 1440  
 1441  
 1442

1443 This leads to a simple algorithm for computing combinatorial crossing numbers.  
 1444

1445 **COROLLARY 28.** *Let  $c, d$  be primitive curves of length at most  $\ell$  on an orientable combi-*  
 1446 *natorial surface with complexity  $n$ . The crossing numbers  $i(c, d)$  and  $i(c)$  can be computed*  
 1447 *in  $O(n + \ell^2)$  time.*  
 1448

1449 **PROOF.** By Lemma 6 we may assume that the surface is a system of quads. By Theorem 9  
 1450 we may compute the canonical forms of  $c, c^{-1}$  and  $d$  in  $O(\ell)$  time. According to Proposition 27,  
 1451

1453 we have

$$1454 \quad i(c, d) = |\mathcal{D}_+| + |\mathcal{D}_0| + |\mathcal{D}_-|$$

1455 The set  $\mathcal{D}_+$  can be constructed in  $O(\ell^2)$  time. Indeed, since the maximal double paths of  $c$   
 1456 and  $d$  form disjoint sets of double points by Corollary 26, we just need to traverse the grid  
 1457  $\mathbb{Z}/|c|\mathbb{Z} \times \mathbb{Z}/|d|\mathbb{Z}$  and group the double points into maximal double paths. Those correspond  
 1458 to diagonal segments in the grid that can be computed in time proportional to the size of  
 1459 the grid. We can also determine which double paths are crossing in the same amount of  
 1460 time. Likewise, we can construct the sets  $\mathcal{D}_0$  and  $\mathcal{D}_-$  in  $O(\ell^2)$  time.  $\square$   
 1461  
 1462

1463 We may complete the proof of Theorem 1 in the orientable case exactly as in Section 5.4.  
 1464

## 1465 7 COMPUTING A MINIMAL IMMERSION

1466  
 1467 In the subsequent sections we only deal with the self-intersection number of a single curve  
 1468 on an oriented system of quads. We thus drop the subscript  $c$  to denote an index path  
 1469  $[i \xrightarrow{\ell}]$  or an arc occurrence  $[i, i + 1]$ . We also write intersections for self-intersections. By  
 1470 Theorem 1 we can compute the geometric intersection number of a curve efficiently. Here,  
 1471 we describe a way to compute a minimal immersion, that is an actual immersion with the  
 1472 minimal number of intersections. We refer to the combinatorial framework of Section 4  
 1473 to describe such an immersion combinatorially. Thanks to Lemma 5, we know that this  
 1474 framework faithfully encodes the topological configurations.  
 1475  
 1476

### 1477 7.1 Bigons and monogons

1478  
 1479 A **bigon** of an immersion  $\mathcal{I}$  of  $c$  is a pair of index paths  $([i \xrightarrow{\ell}], [j \xrightarrow{k}])$  whose **sides**  $c[i \xrightarrow{\ell}]$  and  
 1480  $c[j \xrightarrow{k}]$  have strictly positive lengths, are homotopic, and whose **tips**  $(i, j)$  and  $(i + \ell, j + k)$   
 1481 are combinatorial crossings for  $\mathcal{I}$ . A **monogon** of  $\mathcal{I}$  is an index path  $[i \xrightarrow{\ell}]$  of strictly  
 1482 positive length such that  $(i, i + \ell)$  is a combinatorial crossing and the image path  $c[i \xrightarrow{\ell}]$  is  
 1483 contractible.  
 1484  
 1485

1486 **PROPOSITION 29.** *A combinatorial immersion of a primitive curve has excess self-crossing*  
 1487 *if and only if it contains a bigon or a monogon.*  
 1488

1489 **PROOF.** We just need to prove the existence of a bigon or monogon for a continuous  
 1490 realization  $\gamma : \mathbb{R}/\mathbb{Z} \rightarrow S$  of the combinatorial immersion. This bigon or monogon corresponds  
 1491 to a combinatorial bigon or monogon as claimed in the Proposition. To prove the topological  
 1492 counterpart, we first note as in Section 3 that the minimal number of intersections is counted  
 1493 by the lifts of  $\gamma$  whose limit points alternate along  $\partial\mathbb{D}$ . It follows that  $\gamma$  is minimally crossing  
 1494 when its lifts are pairwise disjoint unless the corresponding limit points alternate in  $\partial\mathbb{D}$  and  
 1495  
 1496 Manuscript submitted to ACM

1497 they should intersect exactly once in that case. When  $\gamma$  is not minimally crossing there must  
 1498 exist two lifts intersecting more than necessary, thus forming a bigon in  $\mathbb{D}$ . The projection  
 1499 of such a bigon on  $S$  gives the desired result. Note that a statement similar to the one in  
 1500 the Proposition holds for an immersion of a pair of primitive curves  $c$  and  $d$  with excess  
 1501 crossing. In Appendix A, we provide a purely combinatorial proof of the direct implication  
 1502 of the Proposition in the case of two curves.  $\square$   
 1503

1504 Suppose that  $\mathcal{I}$  is a combinatorial immersion of a primitive geodesic  $c$ . It cannot have a  
 1505 monogon by Corollary 14. Hence, according to Proposition 29 the immersion  $\mathcal{I}$  is minimal  
 1506 unless it contains a bigon. One could eliminate such a bigon by swapping its sides. However,  
 1507 it may happen that the index paths of the bigon share some common part, which would  
 1508 make the swapping ambiguous. In agreement with the terminology of Hass and Scott [Hass  
 1509 and Scott 1985], a bigon  $([i \xrightarrow{\ell}], [j \xrightarrow{k}])$  is said **singular** if  
 1510

- 1512 (1) its two index paths have disjoint interiors, i.e. they do not share any arc occurrence;
- 1513 (2) when  $j = i + \ell$  the following arc occurrences  
 1514

$$1515 \quad [i, i - 1], [j, j - 1], [i, i + 1], [j + k, j + k + 1], [j, j + 1], [j + k, j + k - 1]$$

1516 do not appear in this order or its opposite in the circular ordering induced by  $\mathcal{I}$  at  
 1517  $c(j)$ ;

- 1519 (3) when  $i = j + k$  the following arc occurrences  
 1520

$$1521 \quad [i, i - 1], [j, j - 1], [i + \ell, i + \ell - 1], [i, i + 1], [i + \ell, i + \ell + 1], [j, j + 1]$$

1522 do not appear in this order or its opposite in the circular ordering induced by  $\mathcal{I}$  at  
 1523  $c(i)$ .  
 1524

1525 The reason for conditions 2 and 3 is explained below. Note that when  $c$  is geodesic and  
 1526  $k = -\ell$  there cannot be any identification between  $\{i, i + \ell\}$  and  $\{j, j - \ell\}$ . For instance,  
 1527  $i = j$  implies  $c[i \xrightarrow{\ell}] \sim c[j \xrightarrow{-\ell}] = c[i \xrightarrow{-\ell}]$  so that  $c[i - \ell \xrightarrow{2\ell}] \sim 1$ , while  $j = i + \ell$  implies  
 1528  $c[i \xrightarrow{\ell}] \sim c[j \xrightarrow{-\ell}] = c^{-1}[i \xrightarrow{\ell}]$  so that  $c^2[i \xrightarrow{\ell}] \sim 1$ . In both cases  $c$  would have a monogon  
 1529 which would contradict Corollary 14.  
 1530

1531 When  $c$  is primitive and geodesic, we cannot have  $j = i + \ell$  and  $i = j + \ell$  at the same  
 1532 time. Otherwise, we must have  $k = \ell$  by the preceding paragraph, and  $c$  would be a circular  
 1533 shift of  $c[i \xrightarrow{\ell}] \cdot c[j \xrightarrow{\ell}]$  and thus homotopic to a square. Also remark that when one of the  
 1534 last two conditions in the definition is not satisfied, the bigon maps to a non-singular bigon  
 1535 in the continuous realization of  $\mathcal{I}$  as in Lemma 5. See Figure 13.  
 1536

1537 When the bigon is singular we can swap its two sides by exchanging the two arc occurrences  
 1538  $[i + p, i + p + 1]$  and  $[j + \varepsilon p, i + \varepsilon(p + 1)]$ , for  $0 \leq p < \ell$  and  $k = \varepsilon\ell$ .  
 1539

1540

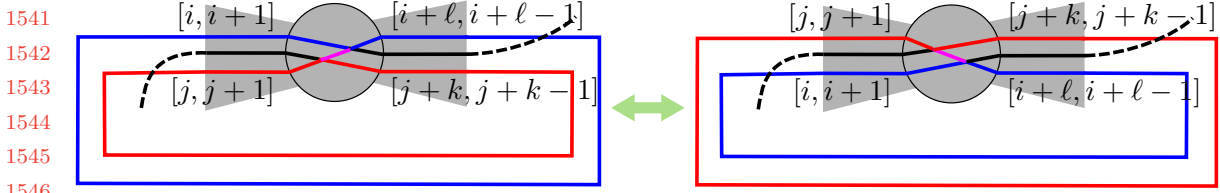


Fig. 13. Right, the realization of the bigon  $([i \xrightarrow{\ell}], [j \xrightarrow{k}])$  where  $j = i + \ell$  and  $[i, i - 1]$  is in-between  $[i + \ell, i + \ell - 1]$  and  $[j + k, j + k - 1]$ , and  $[j + k, j + k + 1]$  is in-between  $[i, i + 1]$  and  $[j, j + 1]$ . The small purple part is at the same time the beginning of the red side of the bigon and the end of the blue side. Swapping this bigon does not reduce the number of crossings.

LEMMA 30. *Swapping the two sides of a singular bigon of an immersion of a geodesic primitive curve decreases its number of crossings by at least two.*

This is relatively obvious if one considers a continuous realization of the immersion, performs the swapping and comes back to a combinatorial immersion as in the proof of Lemma 5. We nonetheless provide a purely combinatorial proof in Appendix B.

Hence, by swapping singular bigons we may decrease the number of crossings until there is no more singular bigons. It follows from the next theorem that the resulting immersion has no excess crossing.

THEOREM 31 (HASS AND SCOTT [HASS AND SCOTT 1985, TH. 4.2]). *An immersion of a primitive geodesic curve has excess crossing if and only if it contains a singular bigon.*

PROOF. We realize  $\mathcal{I}$  by a continuous curve  $\gamma$  with the same construction as in Lemma 5. By Theorem 4.2 in [Hass and Scott 1985] the curve  $\gamma$  has a singular bigon. In turn this bigon corresponds to a singular bigon in  $\mathcal{I}$ .  $\square$

In the next section we describe how to detect bigons in practice.

## 7.2 Proof of Theorem 2

If an immersion  $\mathcal{I}$  of a primitive geodesic  $c$  has a bigon then, by the same arguments as for a crossing pair of index paths in Section 5.1, the two sides label a disk diagram and their vertices can be put in 1-1 correspondence such that corresponding vertices stay at distance zero or two and bound a same quad in the disk diagram. Hence, we can look for bigons among the maximal partial diagrams of  $c$ . This leads to a quadratic algorithm for finding a bigon of  $\mathcal{I}$ , or deciding that  $\mathcal{I}$  has no bigon.

PROOF OF THEOREM 2. By Theorem 9 we can assume that  $c$  is geodesic. We first consider the case where  $c$  is primitive. Let  $\mathcal{I}$  be a randomly chosen immersion of  $c$ . We

1585 store the induced vertex orderings of the arc occurrences in arrays so that we can test if  
 1586 a double point is a crossing in constant time using pointer arithmetic. By Theorem 31, if  
 1587  $\mathcal{I}$  has excess crossing it has a singular bigon. This singular bigon defines a thick double  
 1588 path that must appear in some maximal partial diagram of  $\mathcal{I}$  as two boundary paths with  
 1589 common extremities. Hence, in order to find a singular bigon we just need to scan in each  
 1590 maximal partial diagram the index pairs that are combinatorial crossings and test whether  
 1591 the two sides between any two consecutive such index pairs define a singular bigon. By the  
 1592 very definition of a singular bigon, each test can be easily performed in constant time. The  
 1593 number of tests is itself bounded by the number of index pairs in all the maximal partial  
 1594 diagrams. This is  $O(\ell^2)$  by Corollary 17. Once a singular bigon is found we swap its sides in  
 1595  $O(\ell)$  time. This preserves the geodesic character and, by Lemma 30, the number of crossings  
 1596 is reduced by at least two. Since  $\mathcal{I}$  may have  $O(\ell^2)$  excess crossings, we need to repeat the  
 1597 above procedure  $O(\ell^2)$  times and we may conclude the theorem in the case of primitive  
 1598 curves. When  $c = d^p$ , with  $d$  primitive, we first find a minimally crossing immersion for  $d$  by  
 1599 the above procedure. We further traverse the immersion  $p$  times duplicating  $d$  as many times.  
 1600 As we start each traversal we connect the last arc occurrence of the previously traversed  
 1601 copy with the first occurrence of the next copy. We continue this copy by duplicating each  
 1602 traversed arc occurrence to its right. It is easily seen that the number of crossings of the  
 1603 final immersion of  $c$ , after connecting the last traversed arc with the first one, satisfies the  
 1604 formula in Proposition 21. □

1609

## 1610 8 DETECTING SIMPLE CURVES

1611

### 1612 8.1 Some preparatory lemmas for Theorem 3

1613

1614 Before studying the recognition of curves homotopic to simple curves, we state some  
 1615 refinements of Lemma 16 and its Corollary that will be useful for the proof of Theorem 3.  
 1616 We first highlight a simple property of the system of quads.

1617

1618 **LEMMA 32.** *The facial walk of a quad cannot contain an arc twice, either with the same*  
 1619 *or the opposite orientations.*

1620

1621 **PROOF.** If the facial walk of a quad contains two occurrences of an arc with the same  
 1622 orientation, then their identification creates a Möbius strip in the system of quads, in  
 1623 contradiction with its orientability. If the facial walk contains two consecutive occurrences  
 1624 of an arc with opposite orientations, then their common endpoint must have degree one in  
 1625 the system of quads. This contradicts the minimal degree (8 on a closed orientable surface)  
 1626 in our system of quads. Finally, if the facial walk contains non consecutive occurrences of  
 1627

1628

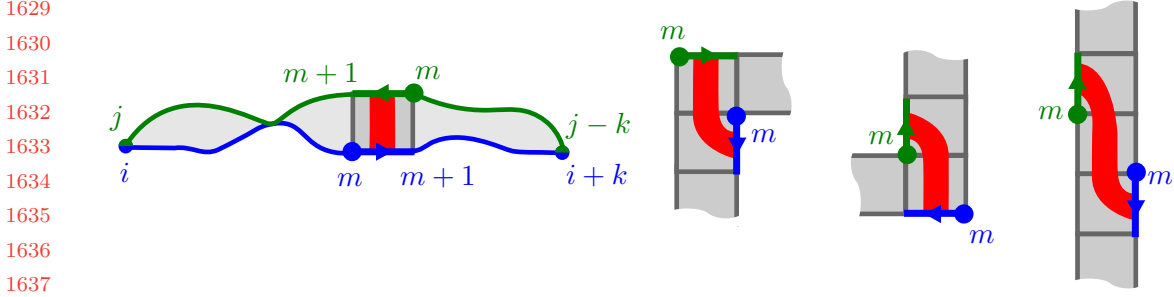


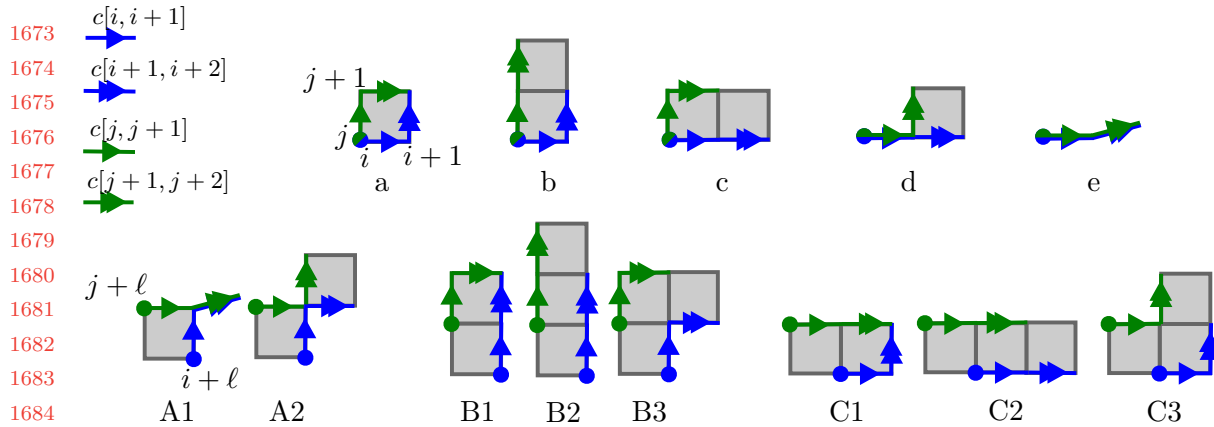
Fig. 14. When the index pair  $(m, m)$  corresponds to distinct vertices (the thick  $m$  dots) in the diagram, the arc  $c[m, m + 1]$  labels two arcs that may be in one of four possible configurations. In each case the red strip projects to a Möbius strip in the system of quads. Note that the whole diagram is only represented in the left case, and is actually forbidden by Lemma 32.

an arc with opposite orientations, then their identification creates a cylinder bounded by loop edges. However, the radial graph being bipartite, this cannot occur.  $\square$

LEMMA 33. *Let  $c$  be a primitive geodesic curve. If a forward index path  $[i \xrightarrow{k}]$  and a backward index path  $[j \xrightarrow{-k}]$  have homotopic image paths  $c[i \xrightarrow{k}] \sim c[j \xrightarrow{-k}]$ , then they cannot share any index.*

PROOF. Remark that we cannot have  $i = j$  for otherwise  $c[j - k \xrightarrow{2k}] = (c[j \xrightarrow{-k}])^{-1} \cdot c[i \xrightarrow{k}] = 1$  in contradiction with Corollary 14. Likewise, we cannot have  $i + k = j - k$ . By way of contradiction, suppose that the index paths  $[i \xrightarrow{k}]$  and  $[j \xrightarrow{-k}]$  have a common index  $i + r = j - t$  for some integers  $0 \leq r, t \leq k$ . By the previous remark we have  $0 < \frac{r+t}{2} < k$ . It follows that  $(m, m)$  is an interior index pair of  $([i \xrightarrow{k}], [j \xrightarrow{-k}])$ , where  $m = i + \frac{r+t}{2} = j - \frac{r+t}{2}$  (recall that  $i$  and  $j$  have the same parity). Consider a disk diagram for  $c[i \xrightarrow{k}] \sim c[j \xrightarrow{-k}]$ . The index pair  $(m, m)$  cannot correspond to the same vertex in the diagram since the path  $c[i, j] = c[i, m] \cdot c[m, j]$  would then label a closed path in the diagram, hence be contractible. This would again contradict Corollary 14. It ensues that  $(m, m)$  corresponds to opposite vertices in a quad of the diagram. This quad is part of a staircase where the arc  $c[m, m + 1]$  labels two arcs on either sides of the partial diagram. Figure 14 depicts the four possible configurations. In each case we infer that the system of quads would contain a Möbius strip, in contradiction with its orientability.  $\square$

LEMMA 34. *Two distinct index paths of a nontrivial primitive geodesic curve  $c$  having homotopic image paths have length distinct from  $|c|$  and at most  $|c| + 1$ .*



1686 Fig. 15. Upper row, the five possible configurations at the beginning of the disk diagram for  $c[i \xrightarrow{k}] \sim$   
 1687  $c[j \xrightarrow{k}]$ . Lower row, the eight possible configurations in the neighborhood of the index pair  $(i, j)$  in this  
 1688 diagram.

1689  
 1690  
 1691 PROOF. When the index paths have opposite orientations, the previous lemma directly  
 1692 implies the result. Put  $\ell = |c|$  and let  $[i \xrightarrow{k}], [j \xrightarrow{k}]$  be two index paths such that  $c[i \xrightarrow{k}]$   
 1693  $\sim c[j \xrightarrow{k}]$ . Clearly,  $k \neq \ell$  since otherwise  $c$  would be homotopic to a conjugate of itself  
 1694 by the shorter curve  $c[i, j]$ , in contradiction with the primitivity of  $c$ . For the sake of a  
 1695 contradiction, suppose that  $k > \ell + 1$ . Consider a diagram  $\Delta$  with sides  $\Delta_R$  and  $\Delta_L$  for  
 1696 the homotopic paths  $c[i \xrightarrow{k}] \sim c[j \xrightarrow{k}]$ . By Lemma 16 the vertices  $\Delta_R(i + \ell)$  and  $\Delta_L(j + \ell)$   
 1697 must be diagonally opposite in a quad of  $\Delta$ . Using that  $\Delta_R[i \xrightarrow{2}]$  and  $\Delta_R[i + \ell \xrightarrow{2}]$  are  
 1698 labelled by the same edges and similarly for  $\Delta_L[j \xrightarrow{2}]$  and  $\Delta_L[j + \ell \xrightarrow{2}]$  we easily deduce  
 1699 that the system of quads has a quad with two occurrences of a same arc in its facial walk,  
 1700 or has a vertex of degree at most 5, or is non-orientable. This would contradict Lemma 32  
 1701 or the hypotheses on the system of quads. In details, Figure 15 depicts the five possible  
 1702 configurations (a,b,c,d,e) for  $\Delta_R[i \xrightarrow{2}]$  and  $\Delta_L[j \xrightarrow{2}]$  in the diagram  $\Delta$  and the eight possible  
 1703 configurations (A1-2, B1-3, C1-3) for  $\Delta_R[i + \ell \xrightarrow{2}]$  and  $\Delta_L[j + \ell \xrightarrow{2}]$ . Remark that cases C1-3  
 1704 are symmetric to cases B1-3, so that we only need to consider the five configurations A1-2,  
 1705 B1-3. We denote by  $(x, Y) \in \{a, b, c, d, e\} \times \{A1-2, B1-3\}$  the conjunction of configurations  $x$   
 1706 and  $Y$  in  $\Delta$ . The quads in configurations a,b,c,d are part of a staircase  $\sigma_0$  in  $\Delta$ . Similarly,  
 1707 the vertices  $\Delta_R(i + \ell)$  and  $\Delta_L(j + \ell)$  are contained in a staircase  $\sigma_\ell$  in  $\Delta$  (possibly the  
 1708 same). Being drawn in the plane the staircases of  $\Delta$  inherit an orientation from the plane.  
 1709 This orientation is said positive or negative according to whether or not it is consistent  
 1710 with some default orientation of the quad system.  
 1711  
 1712  
 1713  
 1714  
 1715  
 1716

- 1717 • If the orientations of the two staircases  $\sigma_0$  and  $\sigma_\ell$  have the same sign, then the  
1718 face to the right of  $\Delta_L[j, j+1]$  has the same facial walk as the face to the right of  
1719  $\Delta_L(j+\ell, j+\ell+1)$ . The induced identifications imply that for  $(x, Y) \in \{a, b, c, d\} \times$   
1720  $\{A1-2, B1-3\} \cup \{e\} \times \{A1-2, B1\}$  one quad is bounded twice by the same arc (with  
1721 or without the same orientation) in contradiction with Lemma 32. If  $(x, Y) \in$   
1722  $\{e\} \times \{B2-3\}$ , we easily deduce that  $c(i+1) = c(j+1)$  has degree four in the system  
1723 of quads, again a contradiction.  
1724
- 1725 • When the orientations of  $\sigma_0$  and  $\sigma_\ell$  have opposite signs the faces to the right of  
1726  $\Delta_L[j, j+1]$  and to the right of  $\Delta_L(j+\ell, j+\ell+1)$  (resp. to the left of  $\Delta_R[i, i+1]$   
1727 and to the left  $\Delta_R[i+\ell, i+\ell+1]$ ) correspond to the two faces incident to  $c[j, j+1]$   
1728 (resp.  $c[i, i+1]$ ). We further split case A2 into two variants A2' and A2'' according  
1729 to whether the two quads (see Figure 15) have orientations with the same sign or  
1730 not, respectively. By the induced identifications we derive the following forbidden  
1731 situations: two occurrences of a same arc in a quad for  $(x, Y) \in \{(a, A1), (e, B1)\} \cup$   
1732  $\{d, e\} \times \{A1, A2'\} \cup \{a-e\} \times \{A2''\}$ , a degree two vertex (namely  $c(j+1)$ ) for  $(x, Y) \in$   
1733  $\{a, c\} \times \{B1, B3\}$ , a degree three vertex for  $(x, Y) \in \{b\} \times \{B1-3\} \cup \{a-c\} \times \{B2\}$ , a  
1734 degree four vertex for  $(x, Y) \in \{b, c\} \times \{A1\} \cup \{e\} \times \{B2-3\} \cup \{(a, A2'), (d, B1)\}$  and  
1735 a degree five vertex for  $(x, Y) \in \{b, c\} \times \{A2'\} \cup \{d\} \times \{B2-3\}$ .  
1736  
1737  
1738

□

1739  
1740 When the orientations of the staircases  $\sigma_0$  and  $\sigma_\ell$  in the above proof have the same sign  
1741 it is sufficient to use that  $\Delta_R[i \xrightarrow{1}]$  and  $\Delta_R[i+\ell \xrightarrow{1}]$  are labelled by the same edge, and  
1742 similarly for  $\Delta_L[j \xrightarrow{1}]$  and  $\Delta_L[j+\ell \xrightarrow{1}]$ , in order to reach a contradiction for cases A1 and  
1743 A2. In other words, the two homotopic paths  $c[i \xrightarrow{k}] \sim c[j \xrightarrow{k}]$  cannot have length  $\ell+1$ .  
1744 This leads to the following refinement.  
1745  
1746

1747 LEMMA 35. *A bigon  $([i \xrightarrow{k}], [j \xrightarrow{k}])$  of an immersion of a primitive geodesic curve  $c$  without*  
1748 *intermediate crossings (i.e., no index pair  $(i+r, j+r)$ ,  $1 < r < k$ , is a combinatorial*  
1749 *crossing) has length  $k < |c|$ .*  
1750

1751 LEMMA 36. *If two forward index paths of a canonical curve have homotopic image paths*  
1752 *then they actually have the same image paths, i.e. they form a double path. In particular,*  
1753 *bigons composed of two forward paths must be flat.*<sup>2</sup>  
1754  
1755

1756 PROOF. By Theorem 12 the image paths bound a disk diagram composed of paths and  
1757 staircase. Remark that a staircase with both sides directed forward must have a  $\bar{1}$  turn

1758 <sup>2</sup>In a preliminary version of this work posted on arXiv the authors erroneously claimed an analogous property  
1759 for the case of a bigon composed of a forward and a backward index paths.



1761 on its left side. Since the curve is canonical we infer that the diagram cannot have any  
 1762 staircase, implying that the two sides coincide.  $\square$   
 1763

## 1764 8.2 The unzip algorithm

1766 We now turn to the original problem of Poincaré [Poincaré 1904, §4], deciding whether a  
 1767 given curve  $c$  is homotopic to a simple curve. In the affirmative we know by Lemma 30 and  
 1768 Theorem 31 that some geodesic homotopic to  $c$  must have a (combinatorial) **embedding**,  
 1769 i.e. an immersion without crossings. Rather than swapping the sides of a singular bigon as  
 1770 in Lemma 30 we choose to switch one side along the other side. This will also decrease the  
 1771 number of crossings if the bigon contains no other interior bigons. This time, however, one  
 1772 side of the bigon is left unchanged and this allow us to enforce a given edge of  $c$  to stay fix  
 1773 as we remove crossings: each time the edge is involved in a bigon switch, we switch the side  
 1774 that does not contain the edge. This suggests an incremental computation of an embedding  
 1775 in which a larger and larger part of the curve is fixed as we switch bigons: we assume that  
 1776  $c$  is canonical and consider the trivial embedding of its first arc occurrence  $[0, 1]$ . We next  
 1777 insert the successive arc occurrences incrementally to obtain an embedding of the path  
 1778 formed by the already inserted arcs. When inserting the occurrence  $[i, i + 1]$  we need to  
 1779 compare its left-to-right order with each already inserted arc occurrence  $\beta$  of its supporting  
 1780 arc. If  $\beta \neq [0, 1]$  we can use the comparison of the occurrence  $[i - 1, i]$  with the occurrence  
 1781  $\gamma$  preceding  $\beta$  (or succeeding  $\beta$  if it is a backward occurrence). If  $[i - 1, i]$  and  $\gamma$  have the  
 1782 same supporting arc, we just propagate their relative order to  $[i, i + 1]$  and  $\beta$ . Otherwise,  
 1783 we use the circular ordering of the supporting arcs of  $[i - 1, i]$ ,  $\gamma$  and  $[i, i + 1]$  in order to  
 1784 conclude. When  $\beta = [0, 1]$ , we cannot use the occurrence preceding  $[0, 1]$  as it is not yet  
 1785 inserted. We rather compare  $[i, i + 1]$  and  $[0, 1]$  as follows. In the Poincaré disk, we consider  
 1786 two lifts  $\tilde{d}_i$  and  $\tilde{d}_0$  of  $c$  such that  $\tilde{d}_i[i, i + 1] = \tilde{d}_0[0, 1]$ . We decide to insert  $[i, i + 1]$  to the left  
 1787 (right) of  $[0, 1]$  if one of the limit points of  $\tilde{d}_i$  lies to the left (right) of  $\tilde{d}_0$ . Note that when  $c$   
 1788 is homotopic to a simple curve the two limit points of  $\tilde{d}_i$  should lie on the same side of  $\tilde{d}_0$ .

1794 After comparing  $[i, i + 1]$  with all the occurrences of its supporting arc, we can insert it  
 1795 in the correct place. If no crossings were introduced this way, we proceed with the next  
 1796 occurrence  $[i + 1, i + 2]$ . It may happen, however, that no matter how we insert  $[i, i + 1]$  in  
 1797 the left-to-right order of its supporting arc, the resulting immersion of  $[0 \xrightarrow{i+1}]$  will have a  
 1798 combinatorial crossing. In order to handle this case, we first check if  $[i, i + 1]$  is **switchable**,  
 1799 i.e. if for some  $k \geq 0$  and some turns  $t, u$  the subpath  $p := c[i \xrightarrow{k+2}]$  has turn sequence  $t2^k1u$   
 1800 and the index path  $[i \xrightarrow{k+2}]$  does not contain the arc occurrence  $[0, 1]$ . When  $[i, i + 1]$  is  
 1801 switchable we can switch  $p$  to a new subpath  $p'$  with turn sequence  $(t - 1)\bar{1}2^k(u - 1)$  such  
 1802  
 1803  
 1804

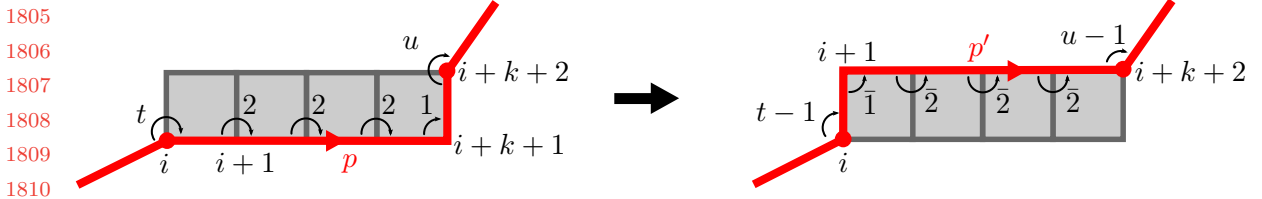
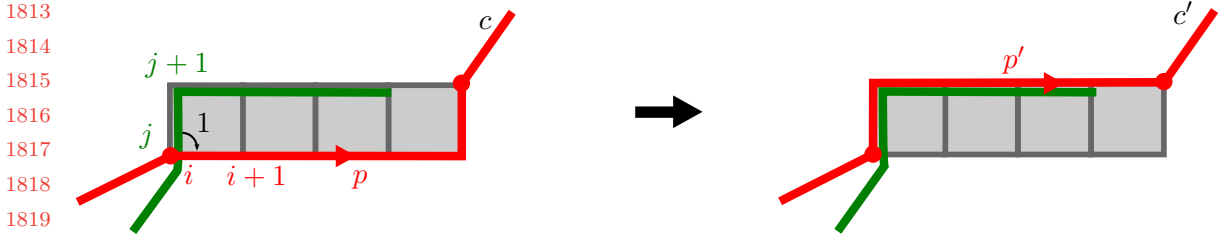
Fig. 16. The arc  $[i, i + 1]$  is switchable.

Fig. 17. A switch may avoid a crossing.

that  $p$  and  $p'$  bound a diagram composed of a single horizontal staircase. See Figure 16. We indeed perform the switch if some intersection is actually avoided this way. More formally, this happens when there is a crossing  $(i, j)$  such that the turn of  $(c[j, j + 1], c[i, i + 1])$  or of  $(c[j, j - 1], c[i, i + 1])$  is one as illustrated on Figure 17. Note that replacing  $p$  by  $p'$  leads to a curve  $c'$  that is still geodesic and homotopic to  $c$ . Moreover, *the part of  $c'$  that remains to be embedded is in canonical form* as it contains no  $\bar{1}$  turns. We then insert the arc occurrence  $[i, i + 1]$  and proceed with the algorithm using  $c'$  in place of  $c$ . The successive switches in the course of the computation untangle  $c$  incrementally and we call our embedding procedure the **unzip algorithm**. For further reference we make some observations that easily follows from the above switch procedure and the fact that  $c$  is initially canonical.

*Remark 3.* If  $[i, i + 1]$  is switchable but not switched at the time of being processed it remains true until the end of the algorithm, meaning that the vertex of index  $i$  is directly followed by a subpath  $p$  with a turn sequence of the form  $2^k 1$  ( $k$  may get smaller if some other arc of  $p$  is switched). Similarly, if  $[i, i + 1]$  is not switchable because of an inappropriate turn sequence, it remains true until the end of the algorithm.

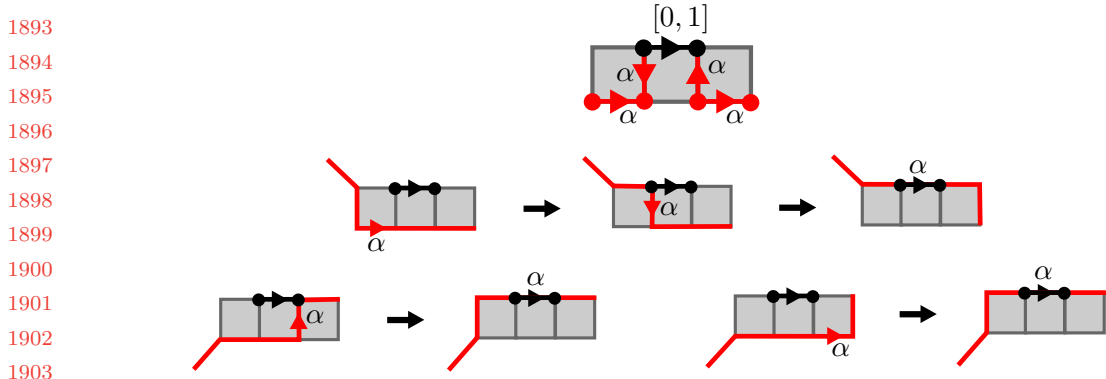
*Remark 4.* Let  $c'$  be a curve homotopic to  $c$  obtained after a certain number of switches during the execution of the unzip algorithm. Then  $c'$  cannot contain a subpath with turn sequence  $\bar{1}2^*$  that ends at index 0, nor can it contain a subpath with turn sequence  $\bar{2}^* \bar{1}$  that starts at index 0.

1849 LEMMA 37. *The unzip algorithm applied to a canonical primitive curve  $c$  of length  $\ell$  can*  
 1850 *be implemented to run in  $O(\ell \log^2 \ell)$  time.*  
 1851

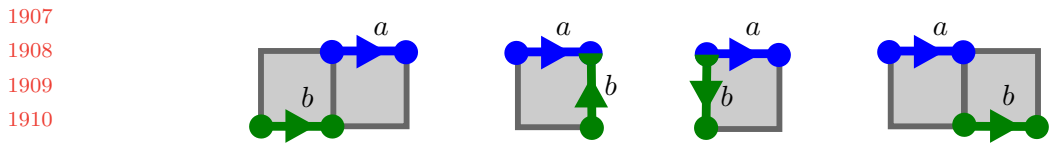
1852 PROOF. We first traverse  $c$  in reverse direction to mark all the switchable arcs. In the  
 1853 course of the algorithm, each time a switchable arc triggers the switch of a subpath  $p$  we  
 1854 unmark all the arcs in  $p$  except the last one that may become switchable (depending on the  
 1855 last turn of  $p$  and on the status of the arc following  $p$ ). It easily follows that an arc can be  
 1856 switched at most twice and that the amortized cost for the switches is linear. Alternatively,  
 1857 we could use the run-length encoded turn sequence of  $c$  (as defined in [Erickson and  
 1858 Whittelsey 2013]) to detect each switchable arc and update the turn sequence in constant  
 1859 time per switches. In a preprocessing phase we also compute the relative order of  $[0, 1]$   
 1860 with all the other occurrences of the same arc in  $c$  as follows. If  $c[i, i + 1] = c[0, 1]$ , the  
 1861 corresponding arc occurrences form a double path of length one and we compute their  
 1862 relative order by extending maximally this double path in the backward direction. Looking  
 1863 at the tip of this double path, say  $(j, k)$ , we can decide which side is to the left of the other.  
 1864 Indeed, the three arcs  $c[j, j - 1]$ ,  $c[k, k - 1]$  and  $c[j, j + 1] = c[k, k + 1]$  must be pairwise  
 1865 distinct and their circular order about their common origin vertex in the system of quads  
 1866 provides the necessary information as follows from Lemma 36.  
 1867  
 1868  
 1869

1870 The computation of the maximal extensions in the backward direction amounts to evaluate  
 1871 the longest common prefix of  $c^{-1}$  with all its circular shifts. Overall, this can be done  
 1872 in  $O(\ell)$  time thanks to a simple variation of the Knuth-Morris-Pratt algorithm. We next  
 1873 initialize an empty (balanced) binary search tree for every edge of the system of quads.  
 1874 Assuming a default orientation of each edge, its search tree should eventually contain the  
 1875 set of occurrences of the corresponding arc using the left-to-right order induced by the  
 1876 embedding.  
 1877  
 1878

1879 We now traverse  $c$  in the forward direction starting with  $[0, 1]$  and insert each traversed  
 1880 arc occurrence  $\alpha = [i, i + 1]$  in its tree. If the search tree is empty, we just insert  $\alpha$  at  
 1881 the root. Otherwise, either  $\alpha$  is switchable and needs to be switched to a new arc  $a$ , or it  
 1882 should be inserted into a non-empty search tree. The former case can be easily detected  
 1883 in  $O(\log \ell)$  time using a dichotomy over the occurrences of  $a$ :  *$\alpha$  needs to be switched when*  
 1884 *one of these occurrences defines a crossing with  $\alpha$  at their common endpoint.* In the latter  
 1885 case, we perform the usual tree insertion: each time  $\alpha$  must be compared with some already  
 1886 inserted arc occurrence  $\beta \neq [0, 1]$  we can use the comparison of the occurrence preceding  
 1887  $\alpha$  with the occurrence preceding  $\beta$  (or succeeding  $\beta$  if it is a backward occurrence). This  
 1888 takes  $O(\log \ell)$  time. When  $\beta = [0, 1]$  we can use our precomputed comparisons unless  $\alpha$  was  
 1889 previously switched, thus not compared with  $[0, 1]$  during the preprocessing phase. Since  $c$   
 1890  
 1891  
 1892



1893 Fig. 18. Top: the arc  $c(\alpha)$  may be in one of four possible configurations with respect to the first arc  
 1894  $c[0, 1]$ . Middle and bottom row: from its initial canonical position,  $\alpha$  is switched to the same arc as  $[0, 1]$ .  
 1895  
 1896  
 1897  
 1898  
 1899  
 1900  
 1901  
 1902  
 1903



1904 Fig. 19. The relative positions of  $a$  and  $b$ .  
 1905  
 1906  
 1907  
 1908  
 1909  
 1910  
 1911  
 1912  
 1913

1914 is canonical, arcs may only be switched to their left in one of four possible configurations as  
 1915 on Figure 18 and we infer that  $\alpha$  must lie to the right of  $[0, 1]$  as justified by Lemma 38  
 1916 below. In conclusion, each comparison costs  $O(\log \ell)$  time so that  $\alpha$  can be inserted in its  
 1917 search tree in  $O(\log^2 \ell)$  time.  
 1918

1919 Note that after  $\alpha$  is inserted we do not try to determine if the current immersion has  
 1920 a crossing or not. This will be checked in a second step after the unzip algorithm is  
 1921 completed.  $\square$   
 1922

1923 LEMMA 38. Let  $\tilde{c}$  and  $\tilde{d}$  be two lifts of a primitive canonical geodesic in the Poincaré  
 1924 disk  $\mathbb{D}$ . The limit points of  $\tilde{c}$  cut the boundary circle  $\partial\mathbb{D}$  into two pieces. By the right piece,  
 1925 we mean the piece of  $\partial\mathbb{D}$  that bounds the part of  $\mathbb{D} \setminus \tilde{c}$  to the right of  $c$ . Suppose that  $\tilde{c}$   
 1926 contains an arc  $a$  and that  $\tilde{d}$  contains an arc  $b$  such that  $a$  and  $b$  are in one of the four  
 1927 relative positions depicted on Figure 19. Then one of the limit points of  $\tilde{d}$  is in the right  
 1928 piece of  $\partial\mathbb{D}$ .  
 1929  
 1930  
 1931

1932 PROOF. We first note that  $b$  itself lies to the right of  $\tilde{c}$ . Indeed,  $\tilde{c}$  would have to use a  $\bar{1}$   
 1933 turn to see  $b$  on its left or to pass along  $b$ , in contradiction with its canonicity. If both limit  
 1934 points of  $\tilde{d}$  were to the left of  $\tilde{c}$ , then  $\tilde{c}$  and  $\tilde{d}$  would form a bigon with one staircase part  
 1935  
 1936 Manuscript submitted to ACM

1937 containing  $b$ . The  $\tilde{c}$  side of this staircase would thus see  $b$  on its right, which is impossible  
 1938 since  $\tilde{c}$  is canonical (here, we have not used that  $\tilde{d}$  is canonical but only geodesic).  $\square$   
 1939

1940 PROPOSITION 39. *If  $i(c) = 0$  the unzip algorithm returns an embedding of a geodesic*  
 1941 *homotopic to  $c$ .*

1942 PROOF. Let  $\mathcal{I}$  be the immersion computed by the unzip algorithm. We denote by  $c_k$  the  
 1943 geodesic homotopic to  $c$  resulting from the first switches in the algorithm up to and including  
 1944 the insertion of the arc occurrence  $[k, k + 1]$ . Note that  $k > r$  implies  $c_k[0 \xrightarrow{r+1}] = c_r[0 \xrightarrow{r+1}]$ .  
 1945 Suppose that  $\mathcal{I}$  has a crossing. For the rest of this proof, we denote by  $i$  the smallest index  
 1946 such that the insertion of  $[i, i + 1]$  creates a crossing, i.e. the restriction of  $\mathcal{I}$  to  $[0 \xrightarrow{i+1}]$  has a  
 1947 crossing double point while its restriction to  $[0 \xrightarrow{i}]$  is an embedding. By convention we set  
 1948  $i = \ell$  if the crossing appeared after the last arc insertion. We shall show that  $c_{\ell-1}$  has two  
 1949 lifts whose limit points are alternating on the boundary of the Poincaré disk. It will follow  
 1950 from Section 3 that  $i(c) = i(c_{\ell-1}) > 0$  thus proving the Proposition. We first establish some  
 1951 preparatory claims.  
 1952  
 1953  
 1954

1955 CLAIM 1. *If  $(i, j)$  is a crossing of  $\mathcal{I}$  with  $0 < j < i$ , then the backward arc  $c_i[j, j - 1]$*   
 1956 *and the forward arc  $c_i[j, j + 1]$  are distinct from the supporting arc  $c_i[i, i + 1]$  of  $[i, i + 1]$ .*  
 1957 *Moreover, if  $[i, i + 1]$  was switched just before its insertion, then  $c_i[j, j - 1]$  and  $c_i[j, j + 1]$*   
 1958 *are also distinct from the supporting arc  $c_{i-1}[i, i + 1]$  of  $[i, i + 1]$  just before its switch.*  
 1959  
 1960

1961 PROOF. The first part of the claim follows directly from our insertion procedure and the  
 1962 fact that the restriction of  $\mathcal{I}$  to  $[0 \xrightarrow{i}]$  is an embedding. Moreover, assume that  $[i, i + 1]$   
 1963 was switched just before its insertion. By the insertion procedure, this means that the  
 1964 insertion of  $[i, i + 1]$  before the switch would have induced a crossing  $(i, k)$  where  $0 < k < i$   
 1965 and  $c_{i-1}[k, k + 1], c_{i-1}[k, k - 1] \neq c_{i-1}[i, i + 1]$  by the first part of the claim. By the same  
 1966 first part we have  $c_i[j, j - 1], c_i[j, j + 1] \neq c_i[i, i + 1]$ . Since the restriction of  $\mathcal{I}$  to  $c_i[0 \xrightarrow{i}]$   
 1967 has no crossing, the length 2 path  $c_{i-1}[k - 1 \xrightarrow{2}] = c_i[k - 1 \xrightarrow{2}]$  separates  $c_i[j - 1 \xrightarrow{2}]$  from  
 1968  $c_{i-1}[i, i + 1]$ , implying  $c_i[j, j - 1], c_i[j, j + 1] \neq c_{i-1}[i, i + 1]$  as desired.  $\square$   
 1969  
 1970

1971 CLAIM 2. *If  $c_i$  has a  $\bar{1}$  turn at index  $k + 1$ , with  $0 < k < i - 1$ , then there is an index  $r$*   
 1972 *with  $0 < r < k$  such that*

- 1973  $\bullet c_k[k, k + 1] = c_k[r, r - 1],$
- 1974  $\bullet$  *the arc  $c_i[r, r - 1]$  lies to the right of  $c_i[k, k + 1],$*
- 1975  $\bullet c_k[r, r - 1] \neq c_{k-1}[k, k + 1].$

1976  
 1977 PROOF. A  $\bar{1}$  turn can only occur at the destination of an arc that has been switched and  
 1978 such that the next arc was not switched (otherwise, we would get a  $\bar{2}$  turn). If  $c_i$  has a  $\bar{1}$   
 1979  
 1980

1981 turn at  $k + 1$  then so has  $c_k$  since the algorithm never backtracks. It follows that the arc  
 1982  $c_k[k, k + 1]$  must have been switched just before its insertion, thus witnessing the existence  
 1983 of an arc  $a$  of the form  $c_k[u, u - 1]$  or  $c_k[u, u + 1]$ , with  $0 < u < k$ , that lies parallel to and  
 1984 to the right of  $c_k[k, k + 1]$  (with respect to  $\mathcal{I}$ ). Moreover, according to Claim 1 we can also  
 1985 assume  $c_k[u, u - 1]$  and  $c_k[u, u + 1]$  to be distinct from the supporting arc of  $[k, k + 1]$  just  
 1986 before it was switched, namely  $c_{k-1}[k, k + 1]$ . In the case  $a = c_k[u, u - 1]$ , we may set  $r = u$   
 1987 and conclude. Otherwise,  $a = c_k[u, u + 1]$  and recalling that the restriction of  $\mathcal{I}$  to  $[0 \xrightarrow{i}]$ ,  
 1988 hence to  $[0 \xrightarrow{k+2}]$ , has no crossing, it must be that  $c_k[u \xrightarrow{2}]$  also lies parallel to and to the  
 1989 right of  $c_k[k \xrightarrow{2}]$ . So  $c_i$  has a  $\bar{1}$  turn at index  $u + 1$ , and we are back to the hypothesis of the  
 1990 claim, decreasing the value of  $k$  to  $u$ . We can repeat the same arguments inductively, each  
 1991 time decreasing the value of  $k$  in the claim. Since  $k > 1$ , the process must stop, implying  
 1992 that we have reached the former case.  $\square$

1996 Recall that  $i$  is the smallest index such that the restriction of  $\mathcal{I}$  to  $[0 \xrightarrow{i+1}]$  has a crossing.  
 1997 We denote by  $c' = c_{\ell-1}$  the geodesic homotopic to  $c$  resulting from all the switches in the  
 1998 course of the algorithm execution. Let  $(i, j)$  be a crossing of  $\mathcal{I}$  with  $0 < j < i$ . We consider  
 1999 two lifts  $\tilde{d}_i$  and  $\tilde{d}_j$  of  $c'$  in the Poincaré disk such that  $\tilde{d}_i(i) = \tilde{d}_j(j)$ . We first suppose  $i < \ell$ .  
 2000

2001 CLAIM 3. *We can choose  $j$  so that  $\tilde{d}_i[i \xrightarrow{+\infty}]$  has no crossing with  $\tilde{d}_j$ . (Crossings are*  
 2002 *defined with respect to the lift of  $\mathcal{I}$  in the Poincaré disk.)*

2004 PROOF. Fix any  $j$  such that  $(i, j)$  is a crossing of  $\mathcal{I}$  ( $0 < j < i$ ) and suppose that  $\tilde{d}_i[i \xrightarrow{+\infty}]$   
 2005 and  $\tilde{d}_j$  cross. Let  $s$  be the smallest positive integer such that  $\tilde{d}_i$  and  $\tilde{d}_j$  crosses at  $\tilde{d}_i(i + s)$ .  
 2006 We thus have a bigon of the form  $([i \xrightarrow{s}], [j \xrightarrow{\varepsilon s}])$  for some  $\varepsilon \in \{-1, 1\}$ . Moreover, this bigon  
 2007 has no intermediate crossings by the choice of  $s$ . Let  $\Delta$  be a disk diagram for this bigon,  
 2008 oriented consistently with the system of quads.  $\Delta$  must start with a staircase part by  
 2009 Claim 1. In particular, the turn  $t$  between  $c'[j, j + \varepsilon]$  and  $c'[i, i + 1]$  should be  $\pm 1$ . The unzip  
 2010 algorithm may have run across four possible situations at step  $i$ .  
 2011

- 2013 (1) Either  $[i, i + 1]$  was switchable just before its insertion but was not switched,
- 2014 (2) or it was switchable and switched,
- 2015 (3) or it was not switchable because of an inappropriate turn sequence,
- 2016 (4) or it was not switchable because the part to be switched contains  $[0, 1]$ .

2018 In the first situation, we know by Remark 3 that  $c'(i)$  is followed by a turn sequence of the  
 2019 form  $2^*1$ . Hence,  $t$  is exactly 1; but this contradicts the fact that  $[i, i + 1]$  was not switched  
 2020 though switchable. The third situation together with Remark 3 also lead to a contradiction  
 2021 as the inappropriate turn sequence prevents  $c[i \xrightarrow{s}]$  from being part of any staircase. Thanks  
 2022 to Claim 1, the second situation equally prevents  $c[i \xrightarrow{s}]$  from being part of any staircase. It  
 2023

2025 remains to consider the fourth situation. We first suppose  $\varepsilon = -1$ , i.e. that the diagram  
 2026  $\Delta$  corresponds to the bigon  $([i \xrightarrow{s}], [j \xrightarrow{-s}])$ . By Lemma 35, we have  $s < \ell$  and the fourth  
 2027 situation implies that the  $[i \xrightarrow{s}]$  side of the bigon contains  $[0, 1]$ . These two properties imply  
 2028 that  $0 < i + s - \ell < i$ . It ensues that the  $[j \xrightarrow{-s}]$  side contains index  $i$ , for otherwise  $(i + s, j - s)$   
 2029 would be a crossing occurring before step  $i$ . However, the occurrence of  $i$  on both sides  
 2030 of the bigon contradicts Lemma 33. Hence, it must be that  $\varepsilon = 1$ , i.e. that  $\Delta$  is bounded  
 2031 by two forward paths. Since the  $[i \xrightarrow{s}]$  side of  $\Delta$  contains  $[0, 1]$  and since  $i \neq \ell$ , it ensues  
 2032 from Remark 4 and the hypothesis in the fourth situation that  $\Delta$  starts with a horizontal  
 2033 staircase. It follows that  $\mathcal{I}$  has a  $\bar{1}$  turn at index  $j + 1$ . Claim 2 ensures the existence of  
 2034 a smaller index  $r$  such that  $c_j[j, j + 1] = c_j[r, r - 1]$  and  $c_j[r, r - 1] \neq c_{j-1}[j, j + 1]$ . Since  
 2035  $c_j[j, j + 1]$  makes a one turn with both  $c_{j-1}[j, j + 1]$  and  $c'[i, i + 1]$ , these last arcs are equal  
 2036 and, since  $(j, r)$  is not a crossing,  $(i, r)$  must be a crossing of  $\mathcal{I}$ . We replace  $j$  by  $r$  to obtain  
 2037 another lift  $\tilde{d}_r$  that crosses  $\tilde{d}_i$  at the same point  $\tilde{d}_i(i) = \tilde{d}_r(r)$  with the additional property  
 2038 that  $\tilde{d}_r[r, r - 1]$  and  $\tilde{d}_i[i, i + 1]$  make a one turn. We finally observe that  $\tilde{d}_r$  satisfies the  
 2039 claimed property. Indeed, applying the same arguments as above, if  $\tilde{d}_r$  crossed  $\tilde{d}_i[i \xrightarrow{+\infty}]$  then  
 2040 we would have a bigon starting at  $(i, r)$  with a staircase. This staircase must lie to the left  
 2041 of its  $[i \xrightarrow{s}]$  side by Remark 4, hence the other side of the staircase must start with  $[r, r - 1]$ .  
 2042 This is however impossible by the preceding argument for  $\varepsilon = -1$ . It follows that  $\tilde{d}_i[i \xrightarrow{+\infty}]$   
 2043 and  $\tilde{d}_r$  have no crossing.  $\square$

2044 We next consider the smallest positive integer  $r$  such that  $\tilde{d}_i$  and  $\tilde{d}_j$  crosses at  $\tilde{d}_i(i - r)$ .  
 2045 If no such  $r$  exists, then by the above Claim 3,  $\tilde{d}_j$  and  $\tilde{d}_i$  have a unique intersection point  
 2046 and we may conclude that their limit points alternate. We can thus assume the existence  
 2047 of a bigon  $([i - r \xrightarrow{r}], [j - \varepsilon r \xrightarrow{-\varepsilon r}])$  with  $r > 0$  and  $\varepsilon \in \{-1, 1\}$ , and without intermediate  
 2048 crossings. We first examine the case  $\varepsilon = -1$  where the bigon  $([i - r \xrightarrow{r}], [j + r \xrightarrow{-r}])$  has  
 2049 oppositely oriented index paths. We must have  $r \geq i - j$  for otherwise the tip  $(i - r, j + r)$   
 2050 of the bigon would define a crossing occurring before step  $i$ , contradicting the choice of  
 2051  $i$ . Hence,  $[i - r \xrightarrow{r}]$  contains  $j$ . This is however impossible by Lemma 33. We now look at  
 2052 the case of two forwards index paths ( $\varepsilon = 1$ ). We must have  $r \geq j$  for otherwise the tip  
 2053  $(i - r, j - r)$  of the bigon would define a crossing occurring before step  $i$ , again contradicting  
 2054 the choice of  $i$ . It follows that  $[j - r \xrightarrow{r}]$  contains  $[0, 1]$  and that the forward branches  
 2055  $\tilde{d}_i[i - j \xrightarrow{+\infty}]$  and  $\tilde{d}_j[0 \xrightarrow{+\infty}]$  have a unique intersection point. The bigon labels a disk diagram  
 2056  $\Delta$  composed of paths and staircases as described in Theorem 12.

- 2057 • If  $[0, 1]$  and  $\alpha := [i - j, i - j + 1]$  label the same arc of a path part in  $\Delta$  there are  
 2058 two possibilities: either it holds initially that  $c[0, 1] = c(\alpha)$  or  $\alpha$  was switched in the  
 2059 course of the algorithm. In the former case, we know by the preprocessing phase and

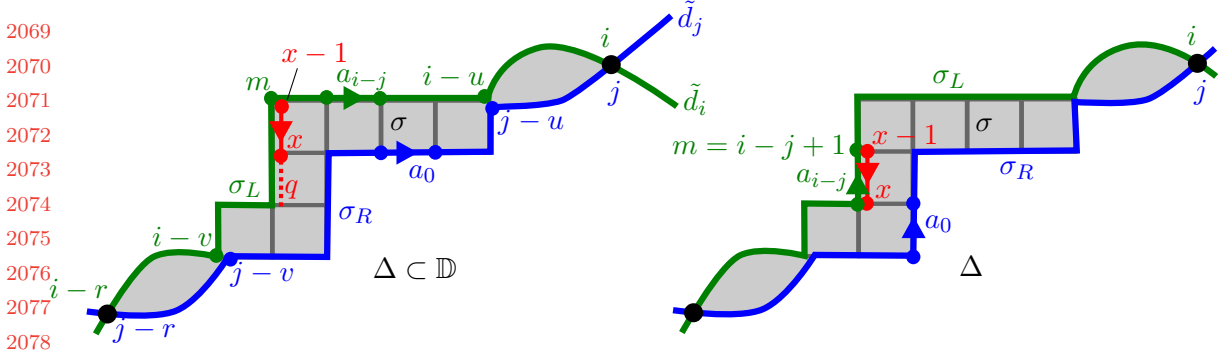


Fig. 20.  $a_{i-j}$  may belong to a horizontal (left figure) or vertical (right figure) part of  $\sigma_L$ .

Lemma 36 that the left-to-right order of  $[0, 1]$  and  $\alpha$  is coherent with its extension in the backward direction. This implies that ultimately in the backward direction  $\tilde{d}_i$  lies on the same side of  $\tilde{d}_j$  as does  $\alpha$ . In the latter case, as described in the end of the proof of Lemma 37, we know by the insertion procedure that at least one of the limit points of  $\tilde{d}_i$  lies on the same side of  $\tilde{d}_j$  as does  $\alpha$ . Since  $(i, j)$  is the only crossing in the forward direction, we conclude in both cases that  $\tilde{d}_j$  and  $\tilde{d}_i$  have alternating limit points.

- Otherwise,  $[0, 1]$  and  $\alpha$  label two distinct arcs, say  $a_0$  and  $a_{i-j}$ , of a staircase part  $\sigma$  of  $\Delta$ . Let  $[i - v \xrightarrow{v-u}]$  and  $[j - v \xrightarrow{v-u}]$ ,  $0 \leq u < v \leq r$ , be the index paths corresponding to the sides  $\sigma_L$  and  $\sigma_R$  of  $\sigma$ . By Remark 4,  $[j - v \xrightarrow{v-u}]$  must label the right side  $\sigma_R$  while  $[i - v \xrightarrow{v-u}]$  cannot contain  $[0, 1]$ . It follows that  $v < i$ , whence  $[i - v \xrightarrow{v-u}] \subset [1 \xrightarrow{i-1}]$ . If  $a_{i-j}$  belongs to a horizontal part of  $\sigma_L$ , the first vertex in this part has a  $\bar{1}$  turn and we let  $m$  be the index of this vertex. Otherwise,  $a_{i-j}$  belongs to a vertical part whose last vertex has a  $\bar{1}$  turn. It follows that the vertex of index  $i - j + 1$  had a  $\bar{1}$  turn at step  $i - j$  of the algorithm and we set  $m = i - j + 1$ . See Figure 20. By Claim 2, there is an arc occurrence  $[x, x - 1]$ , with  $x < m - 2$ , that lies to the right of  $a_{i-j}$  and such that the turn at  $x - 1$  is not one. We view  $\Delta$  as a subset of the Poincaré disk so that  $\Delta_L$  and  $\Delta_R$  can be seen as portions of  $\tilde{d}_i$  and  $\tilde{d}_j$  respectively. Let  $\tilde{q}$  be the lift of  $c'$  that extends the above occurrence  $[x, x - 1]$  in  $\mathbb{D}$ . We denote by  $q_+ := \tilde{q}[x \xrightarrow{+\infty}]$  and  $q_- := \tilde{q}[x \xrightarrow{-\infty}]$  the portion of  $\tilde{q}$  respectively after and before its vertex with index  $x$ . See Figure 21.

We claim that  $q_+$  cannot cross  $\tilde{d}_i$ . Otherwise, we would get a pair of homotopic paths, one piece of  $q_+$  starting at index  $x$  and one piece of  $\tilde{d}_i$  ending at index  $m$ , with opposite orientations. By Lemma 33, the  $q_+$  piece would not contain index  $m$  and would thus have length at most  $m - x < m$ . In turn, this would imply that the



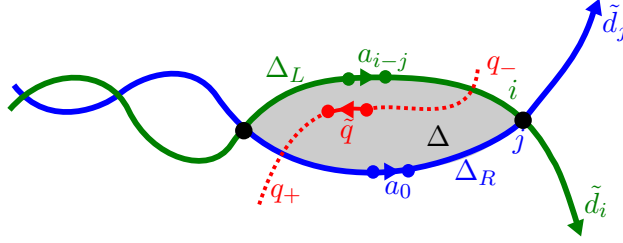


Fig. 21.  $q_+$  cannot cross  $\tilde{d}_i$ ,  $q_-$  cannot cross  $\tilde{d}_j$ , and  $\tilde{d}_j$  cannot cross  $\tilde{d}_i[i \xrightarrow{+\infty}]$ .

$\tilde{d}_i$  piece would only contain vertices with indices in  $[1, m]$ . The crossing of  $q_+$  and  $\tilde{d}_i$  would thus occur before step  $i$ , a contradiction.

We next claim that  $q_-$  cannot cross  $\tilde{d}_j$ . To see this, first note that  $q_+$  crosses  $\tilde{d}_j$  before  $a_0$  by the previous claim. If  $q_-$  crossed  $\tilde{d}_j$ , say at  $q_-(u) = \tilde{d}_j(v)$ , then we would have a bigon between  $\tilde{q}$  and  $\tilde{d}_j$  whose  $\tilde{d}_j$  side contains  $a_0$ . Since no crossing occurs before step  $i$ , we would have either  $u \geq i$  or  $v \geq i$ . We infer in both cases that the index path of the  $\tilde{q}$  side of the bigon contains index 0. This would contradict Lemma 33.

It follows from the above claims that the two lifts  $\tilde{q}$  and  $\tilde{d}_i$  of  $c'$  have alternating limit points.

It remains to consider the case  $i = \ell$  where the first crossing appears after the last arc insertion. Since all the arcs have been inserted without introducing crossings it means that the crossings of the computed immersion  $\mathcal{I}$  have the form  $(0, j)$ . We first claim that each bigon of  $\mathcal{I}$  must have its two sides oriented the same way. Otherwise, the tips of the bigon have the form  $(0, j)$  and  $(j, 0)$  for some index  $j \neq 0$ , implying that  $c_\ell[0 \xrightarrow{j}]$  or  $c_\ell[j \xrightarrow{\ell-j}]$  is contractible. This would contradict Corollary 14. Let  $\tilde{d}_\ell$  and  $\tilde{d}_j$  be two intersecting lifts of  $c'$  in the Poincaré disk. If  $\tilde{d}_\ell$  and  $\tilde{d}_j$  intersect only once, then we are done as they must have alternating limit points. We now suppose that  $\tilde{d}_\ell$  and  $\tilde{d}_j$  intersect at least twice and we consider the bigon  $\Delta$  between their *last two* intersections in the forward direction. By Lemma 35, the length of  $\Delta$  is smaller than  $\ell$ . Let  $(\ell - j, 0)$  and  $(0, j)$  be the tips of  $\Delta$ , so that  $\tilde{d}_j[0 \xrightarrow{j}] \sim \tilde{d}_\ell[\ell - j \xrightarrow{j}]$ .

- If  $[0, 1]$  and  $\alpha = [\ell - j, \ell - j + 1]$  label the same arc  $\tilde{d}_j[0, 1] = \tilde{d}_\ell(\alpha)$  then, by the insertion procedure, one of the limit points of  $\tilde{d}_\ell$  is on the same side of  $\tilde{d}_j$  as  $\alpha$ . The same argument as in the general case  $i < \ell$  allows to conclude that  $\tilde{d}_\ell$  and  $\tilde{d}_j$  have alternating limit points.

- We finally suppose that  $[0, 1]$  and  $\alpha$  label distinct arcs, say  $a_0$  and  $a_{\ell-j}$ , of a staircase part  $\sigma$  of  $\Delta$ . As in the general case  $i < \ell$ ,  $a_0$  must see  $\sigma$  on its left, while  $a_{\ell-j}$  must see  $\sigma$  on its right. Hence, the  $\tilde{d}_j$  side of  $\sigma$  is canonical while the side along  $\tilde{d}_\ell$  is not and must have been switched. By Claim 2, there is an arc occurrence  $\beta$  to the right of  $\tilde{d}_\ell[\ell - j, \ell - j + 1]$  with the opposite orientation. Let  $\tilde{q}$  be the lift of  $c'$  that extends  $\beta$ . As in the general case  $i < \ell$ , we can show that the part of  $\tilde{q}$  after  $\beta$  cannot cross  $\tilde{d}_\ell$ , while the part before  $\beta$  cannot cross  $\tilde{d}_j$ . Using that  $(0, j)$  is the last crossing along  $\tilde{d}_\ell$  and  $\tilde{d}_j$ , we equally conclude that  $\tilde{d}_\ell$  and  $\tilde{q}$  have alternating limit points. See Figure 21 with  $i = \ell$ .

□

PROOF OF THEOREM 3. Let  $c$  be a combinatorial curve of length  $\ell$  on a combinatorial surface of size  $n$ . We compute its canonical form in  $O(n + \ell)$  time and check in linear time that  $c$  is primitive. In the negative, we conclude that either  $c$  is contractible, hence reduced to a vertex, or that  $c$  has no embedding by Proposition 21. In the affirmative, we apply the unzip algorithm to compute an immersion  $\mathcal{I}$  of some geodesic  $c'$  homotopic to  $c$ . According to Proposition 39, we have  $i(c) = 0$  if and only if  $\mathcal{I}$  has no crossings. This is easily verified in  $O(n + \ell)$  time by checking for each vertex  $v$  of the system of quads that the set of paired arc occurrences with  $v$  as middle vertex form a well-parenthesized sequence with respect to the local ordering  $\prec_v$  induced by  $\mathcal{I}$ . We conclude the proof thanks to Lemma 37. □

A related problem was tackled by Chang *et al.* [Chang et al. 2015, Th. 8.2] who try to find an embedding of a given closed path on a combinatorial surface. In their formulation, though, the path is not authorized to be modified. In our terminology, they only look for the existence of a combinatorial immersion without crossings. They suggest a linear time complexity for this problem and it seems likely that we could also eliminate the  $\log^2 \ell$  factor in our complexity.

## 9 CONCLUDING REMARKS

The existence of a singular bigon claimed in Theorem 31 relies on Theorem 4.2 of Hass and Scott [Hass and Scott 1985]. As noted by the authors themselves this result is “surprisingly difficult to prove”. Except for this result and the recourse to some hyperbolic geometry in the general strategy of Section 3 our combinatorial framework allows to provide simple algorithms and to give simple proofs of results whose known demonstrations are rather involved. Concerning Proposition 29, the existence of an immersion without bigon could be achieved in our combinatorial viewpoint by showing that if an immersion has bigons, then

2201 one of them can be swapped to reduce the number of crossings. (The example in Figure 1  
2202 shows that such a bigon need not be singular.) What is more, if those swappable bigons  
2203 could be found easily this would provide an algorithm to compute a minimally crossing  
2204 immersion of two curves by iteratively swapping bigons as in Section 7 for the case of a single  
2205 curve. However, we were unable to show the existence or even an appropriate definition of a  
2206 swappable bigon. Note that in the analogous approaches using Reidemeister-like moves by de  
2207 Graaf and Schrijver [de Graaf and Schrijver 1997] or by Paterson [Paterson 2002], the number  
2208 of moves required to reach a minimal configuration is unknown. Comparatively, the number  
2209 of bigon swapping would be just half the excess crossing of a given immersion. We would thus  
2210 obtain a polynomial time algorithm for computing a minimally crossing immersion of two  
2211 curves (there is an exponential time algorithm by a result of Neumann-Coto [Neumann-Coto  
2212 2001, Prop. 2.2]).

2215 Although the geometric intersection number of a combinatorial curve of length  $\ell$  may be  
2216  $\Omega(\ell^2)$ , it is not clear that the complexity in Theorem 1 is optimal. In particular, it would be  
2217 interesting to see if the unzip algorithm of Section 8.2 yields minimally crossing curves even  
2218 with curves that are not homotopic to simple curves, thus improving Theorem 2. This would  
2219 yield a quasi-linear algorithm for computing the geometric intersection number based on  
2220 the counting of inversions in a permutation [Bentley et al. 1984]. It is also tempting to check  
2221 whether the unzip algorithm applies to compute the geometric intersection number of two  
2222 curves rather than a single curve. Another intriguing question related to the computation  
2223 of minimally crossing immersions comes from the fact that they are not unique. Given  
2224 a combinatorial immersion we can construct a continuous realization as described in the  
2225 proof of Lemma 5. Say that two realizations are in the **same configuration** if there is an  
2226 ambient isotopy of the surface where they live that brings one realization to the other. It was  
2227 shown by Neumann-Coto [Neumann-Coto 2001] that every minimally crossing immersion  
2228 is in the configuration of shortest geodesics for some Riemannian metric  $\mu$ , but Hass and  
2229 Scott [Hass and Scott 1999] gave counterexamples to the fact that we could always choose  
2230  $\mu$  to be hyperbolic.

2231 *Is there an algorithm to construct or detect combinatorial immersions that have a realization*  
2232 *in the configuration of geodesics for some hyperbolic metric?*  
2233

2234

2235

2236

2237

2238

2239

2240

## 2240 REFERENCES

2241

2242

2243

2244

Chris Arettines. 2015. A combinatorial algorithm for visualizing representatives with minimal self-intersection.  
*Journal of Knot Theory and Its Ramifications* 24, 11 (2015), 1–17.

- 2245 Jon Bentley, Charles Leiserson, Ronald Rivest, and Christopher van Wyk. 1984. Problem 84-2 (Leo Guibas  
2246 Editor). *Journal of Algorithms* 5, 4 (1984), 592–594.
- 2247 Joan S. Birman and Caroline Series. 1984. An algorithm for simple curves on surfaces. *J. London Math.*  
2248 *Soc.* 29, 2 (1984), 331–342.
- 2249 Hsien-Chih Chang, Jeff Erickson, and Chao Xu. 2015. Detecting weakly simple polygons. In *Proc. 26th Ann.*  
2250 *ACM-SIAM Symp. Discrete Algorithms*. 1655–1670.
- 2251 Moira Chas. 2014. Self-intersection numbers of length-equivalent curves on surfaces. *Experimental Mathe-*  
2252 *matics* 23, 3 (2014), 271–276.
- 2253 Moira Chas and Steven P Lalley. 2012. Self-intersections in combinatorial topology: statistical structure.  
2254 *Inventiones mathematicae* 188, 2 (2012), 429–463.
- 2255 David R.J. Chillingworth. 1969. Simple Closed Curves on Surfaces. *Bulletin of the London Mathematical*  
2256 *Society* 1, 3 (1969), 310–314.
- 2257 David R.J. Chillingworth. 1971. An algorithm for families of disjoint simple closed curves on surfaces.  
2258 *Bulletin of the London Mathematical Society* 3, 1 (1971), 23–26.
- 2259 David R.J. Chillingworth. 1972. Winding numbers on surfaces. II. *Math. Ann.* 199, 3 (1972), 131–153.
- 2260 Marshall Cohen and Martin Lustig. 1987. Paths of geodesics and geometric intersection numbers: I. In  
2261 *Combinatorial group theory and topology*. Ann. of Math. Stud., Vol. 111. Princeton Univ. Press, 479–500.
- 2262 Éric Colin de Verdière and Francis Lazarus. 2005. Optimal System of Loops on an Orientable Surface.  
2263 *Discrete & Computational Geometry* 33, 3 (March 2005), 507 – 534.
- 2264 Maurits de Graaf and Alexander Schrijver. 1997. Making curves minimally crossing by Reidemeister moves.  
2265 *Journal of Combinatorial Theory, Series B* 70, 1 (1997), 134–156.
- 2266 Pierre De La Harpe. 2010. Topologie, théorie des groupes et problèmes de décision: célébration d’un article  
2267 de Max Dehn de 1910. *Gazette des mathématiciens* 125 (2010), 41–75.
- 2268 Tamal K. Dey and Sumanta Guha. 1999. Transforming Curves on Surfaces. *Journal of Computer and*  
2269 *System Sciences* 58, 2 (1999), 297–325.
- 2270 Jeff Erickson and Kim Whittelsey. 2013. Transforming curves on surfaces redux. In *Proc. 24th Ann.*  
2271 *ACM-SIAM Symp. Discrete Algorithms*.
- 2272 Benson Farb and Dan Margalit. 2012. *A primer on mapping class groups*. Princeton university Press.
- 2273 Steve M. Gersten and Hamish B. Short. 1990. Small cancellation theory and automatic groups. *Inventiones*  
2274 *mathematicae* 102 (1990), 305–334.
- 2275 Daciberg L. Gonçalves, Elena Kudryavtseva, and Heiner Zieschang. 2005. An algorithm for minimal number  
2276 of (self-)intersection points of curves on surfaces. In *Proceedings of the Seminar on Vector and Tensor*  
2277 *Analysis*, Vol. 26. 139–167.
- 2278 Joel Hass and Peter Scott. 1985. Intersections of curves on surfaces. *Israel Journal of Mathematics* 51, 1-2  
2279 (1985), 90–120.
- 2280 Joel Hass and Peter Scott. 1994. Shortening curves on surfaces. *Topology* 33, 1 (1994), 25–43.
- 2281 Joel Hass and Peter Scott. 1999. Configurations of curves and geodesics on surfaces. *Geometry and Topology*  
2282 *Monographs* 2 (1999), 201–213.
- 2283 Donald E. Knuth, James H. Morris, Jr, and Vaughan R. Pratt. 1977. Fast pattern matching in strings.  
2284 *SIAM journal on computing* 6, 2 (1977), 323–350.
- 2285  
2286  
2287  
2288 Manuscript submitted to ACM

- 2289 Francis Lazarus and Julien Rivaud. 2012. On the homotopy test on surfaces. In *Proc. 53rd Ann. IEEE*  
2290 *Symp. Foundations of Computer Science*. 440–449.
- 2291 M. Lothaire. 1997. *Combinatorics on words*. Cambridge University Press.
- 2292 Martin Lustig. 1987. Paths of geodesics and geometric intersection numbers: II. In *Combinatorial group*  
2293 *theory and topology*. Ann. of Math. Stud., Vol. 111. Princeton Univ. Press, 501–543.
- 2294 Maryam Mirzakhani. 2008. Growth of the number of simple closed geodesics on hyperbolic surfaces. *Annals*  
2295 *of Mathematics* (2008), 97–125.
- 2296 Maryam Mirzakhani. 2016. Counting Mapping Class group orbits on hyperbolic surfaces. (January 2016).  
2297 <http://arxiv.org/pdf/1601.03342> Preprint [arxiv:1601.03342](http://arxiv.org/abs/1601.03342).
- 2298 Bojan Mohar and Carsten Thomassen. 2001. *Graphs on Surfaces*. Johns Hopkins University Press.
- 2299 Max Neumann-Coto. 2001. A characterization of shortest geodesics on surfaces. *Algebraic and Geometric*  
2300 *Topology* 1 (2001), 349–368.
- 2301 J.M. Paterson. 2002. A combinatorial algorithm for immersed loops in surfaces. *Topology and its Applications*  
2302 123, 2 (2002), 205–234.
- 2303 Henri Poincaré. 1904. Cinquième complément à l’analysis situs. *Rendiconti del Circolo Matematico di*  
2304 *Palermo* 18, 1 (1904), 45–110.
- 2305 Bruce L. Reinhart. 1962. Algorithms for Jordan curves on compact surfaces. *Annals of Mathematics* (1962),  
2306 209–222.
- 2307 Jenya Sapir. 2015. Bounds on the number of non-simple closed geodesics on a surface. Preprint  
2308 [arxiv:1505.07171](http://arxiv.org/abs/1505.07171). (May 2015). <http://arxiv.org/abs/1505.07171>
- 2309 Marcus Schaefer, Eric Sedgwick, and Daniel Stefankovic. 2008. Computing Dehn Twists and Geometric  
2310 Intersection Numbers in Polynomial Time. In *CCCG*. 111–114.
- 2311 Vladimir G. Turaev. 1979. Intersections of loops in two-dimensional manifolds. *Mathematics of the*  
2312 *USSR-Sbornik* 35, 2 (1979), 229.
- 2313 Heiner Zieschang. 1965. Algorithmen für einfache Kurven auf Flächen. *Math. Scand.* 17 (1965), 17–40.
- 2314 Heiner Zieschang. 1969. Algorithmen für einfache Kurven auf Flächen II. *Mathematica scandinavica* 25  
2315 (1969), 49–58.
- 2316
- 2317
- 2318
- 2319
- 2320
- 2321
- 2322
- 2323
- 2324
- 2325
- 2326
- 2327
- 2328
- 2329
- 2330
- 2331
- 2332

# Appendix

## A PROOF OF THE DIRECT IMPLICATION OF PROPOSITION 29

PROPOSITION. *If a combinatorial immersion of one or primitive curves has excess (self-)crossing then it contains a bigon or a monogon.*

We first introduce some terminology. An **elementary homotopy** on a combinatorial curve  $c$  consists in adding or removing a spur, or replacing in  $c$  a possibly empty part of a facial walk by its complementary part. For a free elementary homotopy we can also apply a circular shift to the indices of the closed curve  $c$ . The equivalence relation generated by (free) homotopies is called combinatorial (free) homotopy.

Let  $\rho : G \rightarrow S$  be a cellular embedding of  $G$  in a topological surface  $S$  corresponding to the combinatorial surface we are working with. Every combinatorial curve  $c$  can be realized by a continuous curve on  $S$  by replacing each arc in  $c$  with a continuous arc deduced from the restriction of  $\rho$  to the corresponding arc. We denote this continuous realization by  $\rho(c)$ . It is part of the folklore that (free) combinatorial homotopy coincides with continuous (free) homotopy, meaning that  $c$  is (freely) homotopic to  $d$  if and only if  $\rho(c)$  is (freely) homotopic to  $\rho(d)$ .

An **elementary move** of a combinatorial immersion consists either in an elementary homotopy or in an **adjacent transposition**, i.e. in exchanging the left-to-right order of two occurrences in a same arc where one occurrence is next to the right of the other. We further require before performing an elementary homotopy that the immersion is in **good position**. This means, if the elementary homotopy applies to a nonempty part  $u$  of a facial walk of some face, that each arc occurrence in  $u$  should be the rightmost element of its arc, i.e. the most interior to the face. When removing a spur, we just require that the two arc occurrences to be removed are adjacent in left-to-right order. See Figure 22. The elementary homotopy does not modify the order of the remaining arc occurrences. When inserting a spur we make the inserted arc occurrences adjacent and when inserting part of a facial walk we insert each arc occurrence after the rightmost element of its arc. Remark that by a sequence of adjacent transpositions we can always enforce an immersion to be in good position.

PROOF OF THE PROPOSITION. We consider the case of an immersion  $\mathcal{I}$  of two curves  $c$  and  $d$ . Suppose that  $\mathcal{I}$  has  $p$  excess crossings. We shall prove the stronger claim that  $\mathcal{I}$  has at least  $\lceil p/2 \rceil$  bigons whose tips are pairwise distinct. Let  $\mathcal{J}$  be an immersion of two curves  $c'$  and  $d'$  respectively homotopic to  $c$  and  $d$  such that  $\mathcal{J}$  has no excess crossings.

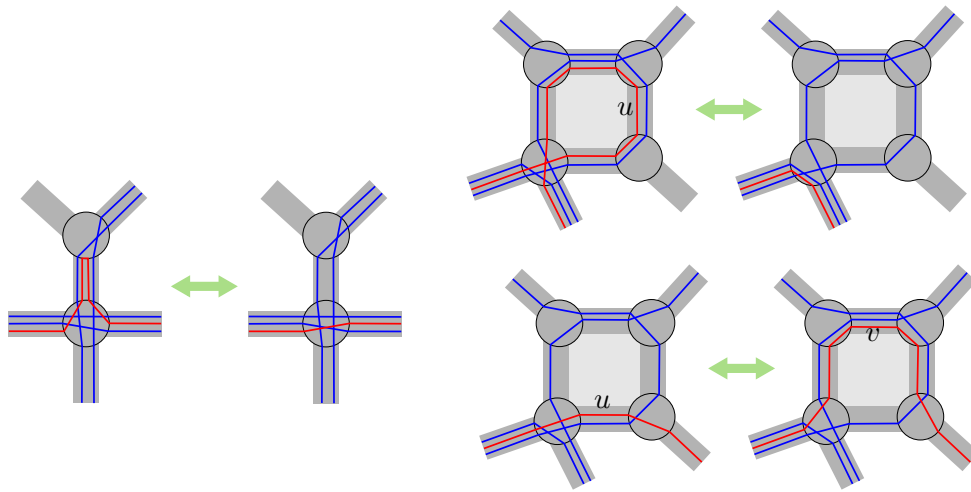


Fig. 22. Left, the removal of a spur in good position. Right, two elementary homotopies replacing a subpath  $u$  of a facial walk by the complementary subpath  $v$ . In the upper right,  $v$  is empty. The immersions being in good positions, crossings may only appear or disappear by pairs.

Consider a sequence of elementary homotopies from  $(c', d')$  to  $(c, d)$ . Following the above remark, we can insert adjacent transpositions between each elementary homotopy in order to obtain a sequence of elementary moves from  $\mathcal{J}$  to  $\mathcal{I}$ . See the above remark. The claim is trivially verified by  $\mathcal{J}$ . We now check that the claim remains true after each elementary move. If the move is an adjacent transposition we may assume that we exchange an arc occurrence of  $c$  with an arc occurrence of  $d$  since we only consider intersections between  $c$  and  $d$ . Without loss of generality we also assume exchanging the forward occurrences  $[i, i + 1]_c$  and  $[j, j + 1]_d$ . There are three cases to consider.

- (1) If none of  $(i, j)$  and  $(i + 1, j + 1)$  is a crossing then the transposition adds two crossings that we may pair as the tips of a new bigon. We now have  $p + 2$  excess crossings with at least  $\lceil (p + 2)/2 \rceil$  bigons as required.
- (2) If  $(i, j)$  is a crossing but  $(i + 1, j + 1)$  is not and if  $(i, j)$  is paired to form the tips of a bigon, say  $([i \xrightarrow{\ell}]_c, [j \xrightarrow{k}]_d)$ , we may just replace this bigon by  $([i + 1 \xrightarrow{\ell-1}]_c, [j + 1 \xrightarrow{k-1}]_d)$  sliding its tip  $(i, j)$  to  $(i + 1, j + 1)$ . A similar procedure applies when  $(i + 1, j + 1)$  is a crossing but  $(i, j)$  is not. In each case the number of excess crossings and bigons is left unchanged.
- (3) It remains the case where both  $(i, j)$  and  $(i + 1, j + 1)$  are crossings. If none of the two is paired to form the tips of a bigon, then the transposition removes two crossings and no pairing, so that the claim remains trivially true. If exactly one

2421 of the two is paired or if the two are paired together, we loose one bigon and two  
 2422 crossings after the transposition so that the claim remains true. Otherwise, there  
 2423 are two bigons of the form  $([i \xrightarrow{\ell}]_c, [j \xrightarrow{k}]_d)$  and  $([i + 1 \xrightarrow{\ell'}]_c, [j + 1 \xrightarrow{k'}]_d)$  that we can  
 2424 recombine to form the bigon  $([i + \ell \xrightarrow{1+\ell'-\ell}]_c, [j + k \xrightarrow{1+k'-k}]_d)$ . We again have one less  
 2425 bigon and two less crossings.  
 2426

2427 We now consider the application of an elementary homotopy as described before the proof.  
 2428 There are again three possibilities.  
 2429

- 2430 (1) If the homotopy replaces a nonempty subpath  $u$  of a facial walk  $uv^{-1}$  by the  
 2431 nonempty complementary part  $v$  then no crossing may appear or disappear as  
 2432 we assume the immersion in good position. In particular, no crossing may use an  
 2433 internal vertex of  $u$  and  $u$  is either entirely included in or excluded from any side of  
 2434 any bigon. We can replace  $u$  by  $v$  in any bigon side where  $u$  occurs to obtain valid  
 2435 bigons in the new immersion after the elementary homotopy is applied. The number  
 2436 of excess crossings and bigons is left unchanged.  
 2437  
 2438 (2) When  $u$  is empty in the above replacement, or when inserting a spur, we may only  
 2439 add crossings by pairs forming bigons with one zero-length side and the complement  
 2440 of  $u$  or the spur as the other side. A similar analysis as in case (2) of a transposition  
 2441 applies to take care of each pair.  
 2442  
 2443 (3) When  $v$  is empty in the above replacement, or when removing a spur, we may only  
 2444 remove crossings by pairs and a similar analysis as in case (3) of a transposition  
 2445 applies to take care of each pair.  
 2446  
 2447

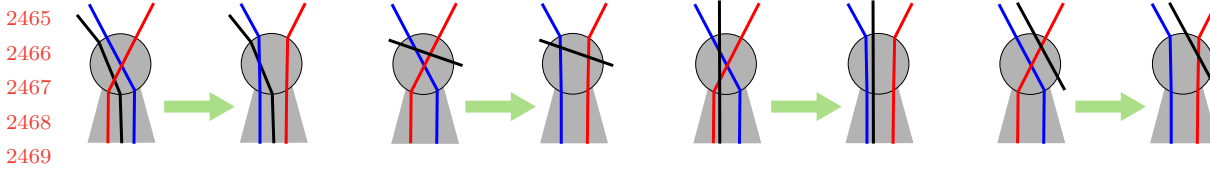
2448 This ends the proof for the case of two curves. A similar proof holds for the existence of  
 2449 a bigon or a monogon in an immersion with excess self-intersection. This time the excess  
 2450 crossings are either paired to form bigons or left alone as the tips of monogons.  $\square$   
 2451

## 2452 B PROOF OF LEMMA 30

2453 LEMMA. *Swapping the two sides of a singular bigon of an immersion of a geodesic*  
 2454 *primitive curve decreases its number of crossings by at least two.*  
 2455

2456 PROOF. Consider a singular bigon  $([i \xrightarrow{\ell}]_c, [j \xrightarrow{\ell}]_d)$  of an immersion  $\mathcal{I}$  of a closed primitive  
 2457 canonical curve  $c$ . Let  $\mathcal{J}$  be the immersion after the bigon has been swapped. We shall  
 2458 partition the set of potential double points and show that the net change of the number of  
 2459 crossings with respect to  $\mathcal{I}$  and  $\mathcal{J}$  is non positive in each part. As the tips of the bigon are  
 2460 not crossings in  $\mathcal{J}$ , this will prove the lemma. We set for  $x \in \mathbb{Z}/|c|\mathbb{Z} \setminus ([i \xrightarrow{\ell}]_c \cup [j \xrightarrow{\ell}]_d)$  and  
 2461  
 2462  
 2463  
 2464





2470 Fig. 23. Up to some obvious symmetries the case  $\mathbb{D}_{x,0}$ ,  $\mathbb{D}_{x,\ell}$ ,  $\mathbb{D}_{p,0}$  or  $\mathbb{D}_{p,\ell}$  has four distinct possible  
 2471 configurations. The blue and red strands represent the crossing  $(i, j)$  (resp.  $(i + \ell, j + \ell)$ ) and each arrow  
 2472 links the left configuration before the bigon swap (in  $\mathcal{I}$ ) with the right configuration after the swap is  
 2473 applied (in  $\mathcal{J}$ ).

2474

2475

2476

2477

2478

0 < p, q < ℓ:

2479

$$\mathbb{D}_{p,q} = \{(i + p, j + q), \{(i + q, j + p)\},$$

$$\mathbb{D}_{x,p} = \{(x, i + p), (x, j + p)\},$$

2480

$$\mathbb{D}_{p,0} = \{(i, i + p), (i, j + p), (j, i + p), (j, j + p)\},$$

$$\mathbb{D}_{x,0} = \{(x, i), (x, j)\},$$

2481

$$\mathbb{D}_{p,\ell} = \{(i + \ell, i + p), (i + \ell, j + p), (j + \ell, i + p), (j + \ell, j + p)\},$$

$$\mathbb{D}_{x,\ell} = \{(x, i + \ell), (x, j + \ell)\},$$

2482

$$\mathbb{D}'_{p,q} = \{(i + p, i + q), \{(j + q, j + p)\},$$

$$\mathbb{D}_1 = \{(y, z) \mid y, z \notin ([i \xrightarrow{\ell}] \cup [j \xrightarrow{\ell}])\},$$

2483

$$\mathbb{D}_2 = \{(i, i + \ell), (i, j + \ell), (j, j + \ell), (j, i + \ell)\},$$

$$\mathbb{D}_3 = \{(i, j), (i + \ell, j + \ell)\}$$

2484

2485

2486

2487

2488

2489

2490

2491

2492

2493

2494

2495

2496

2497

2498

2499

2500

2501

2502

2503

2504

2505

2506

2507

2508

When  $i = j + \ell$  or  $j = i + \ell$ , the set  $\mathbb{D}_2$  consists of three double points only (or zero if  $c(i) \neq c(i + \ell)$ ). Note that we cannot have both equalities as this would imply  $j = j + 2\ell$ , whence  $\ell = |c|/2$  and  $c$  would be a square, in contradiction with the hypothesis that  $c$  is primitive. For each double point in  $\mathbb{D}_1$  the four incident arc occurrences are left in place in  $\mathcal{I}$  and  $\mathcal{J}$ . It ensues that  $\mathbb{D}_1$  has the same crossings in  $\mathcal{I}$  and  $\mathcal{J}$ . The double points in  $\mathbb{D}_3$  are the tips of the bigon. They are crossings in  $\mathcal{I}$  and not in  $\mathcal{J}$ , whence a net change of  $-2$  crossings. For each of  $\mathbb{D}_{x,p}$ ,  $\mathbb{D}_{p,q}$  or  $\mathbb{D}'_{p,q}$ , the first double point in their above definition is a crossing in  $\mathcal{I}$  (resp.  $\mathcal{J}$ ) if and only if the second one is a crossing in  $\mathcal{J}$  (resp.  $\mathcal{I}$ ). Their net change of crossings is thus null. For  $\mathbb{D}_{x,0}$ ,  $\mathbb{D}_{x,\ell}$ ,  $\mathbb{D}_{p,0}$  and  $\mathbb{D}_{p,\ell}$  there are a few case analysis depending on the relative ordering of the two arc occurrences incident to  $x$  (resp.  $i + p$ ,  $j + p$ ) with respect to the crossing  $(i, j)$  (resp.  $(i + \ell, j + \ell)$ ). In each case (see Figure 23) the number of crossings cannot increase from  $\mathcal{I}$  to  $\mathcal{J}$ . For  $\mathbb{D}_2$  there are three cases according to whether  $i + \ell = j$ ,  $j + \ell = i$ , or none of the two identifications occurs. Recall from the paragraph before the lemma that we cannot have both identifications. The first two cases can be treated the same way. See Figure 24. The number of possible configurations is much larger in the last case, i.e. when  $i + \ell \neq j$  and  $j + \ell \neq i$ . We essentially have to shuffle two circular orderings of length four corresponding to the two crossing tips. Without loss of generality we can assume that the path from  $i$  to  $i + \ell$  is the right side of the bigon. We

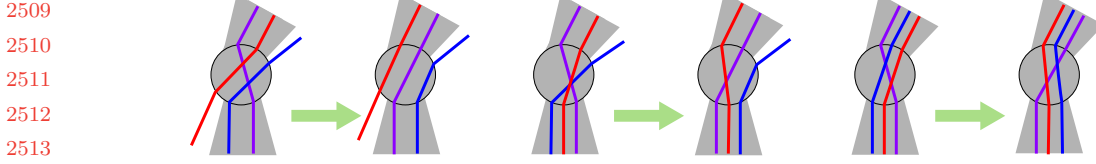


Fig. 24. When  $i + \ell = j$ , the end of  $[i \xrightarrow{\ell}]$  overlaps with the beginning of  $[j \xrightarrow{\ell}]$  (in the purple strand). The third configuration on the right is actually forbidden by the definition of a singular bigon! It corresponds to the non-singular bigon on Figure 13.

consider the following arc occurrences:

$$\begin{aligned} \alpha &= [i, i + 1], & \alpha' &= [i, i - 1], & \beta &= [j, j + 1], & \beta' &= [j, j - 1] \\ \gamma &= [i + \ell, i + \ell + 1], & \gamma' &= [i + \ell, i + \ell - 1], & \delta &= [j + \ell, j + \ell + 1], & \delta' &= [j + \ell, j + \ell - 1] \end{aligned}$$

Since  $(i, j)$  and  $(i + \ell, j + \ell)$  are crossings we must see  $(\alpha, \beta, \alpha', \beta')$  in this counterclockwise order around the vertex  $c(i) = c(i + \ell)$  and similarly for  $(\gamma, \delta, \gamma', \delta')$ . We denote by  $S_1$  and  $S_2$ , respectively, these two circular sequences. We need to consider the effect of the bigon swapping on all the possible shuffles of  $S_1$  and  $S_2$ . The restriction of these shuffles to  $\alpha, \beta$  and  $\delta$  gives the 6 possible shuffles of  $(\alpha, \beta)$  and  $(\gamma, \delta)$ . Among them the order  $(\alpha, \delta, \gamma, \beta)$  cannot occur. Indeed, since the bigon is a thick double path the arcs  $c(\alpha)$  and  $c(\beta)$  either coincide or form a corner of a quad. This would force  $c(\delta)$  and  $c(\gamma)$  to lie in a similar configuration. In turn, the constrained order  $S_2$  would also enforce  $c(\delta')$  and  $c(\delta)$  to coincide or form a corner of a quad in contradiction with the hypothesis that  $c$  has no spurs or brackets. Similar arguments show that the orders  $(\alpha, \gamma, \beta, \delta)$ ,  $(\alpha, \delta, \beta, \gamma)$ ,  $(\alpha, \gamma, \delta, \beta)$  and  $(\alpha, \beta, \delta, \gamma)$  can only occur as factors in the possible shuffles of  $S_1$  and  $S_2$ . These 4 orders thus leads to 24 distinct shuffles of  $S_1$  and  $S_2$  by factoring with the 6 shuffles of  $(\alpha', \beta')$  with  $(\gamma', \delta')$ . By exchanging the roles of  $(\alpha, \beta)$  and  $(\gamma, \delta)$  and by turning clockwise instead of counterclockwise we see that  $(\alpha, \delta, \beta, \gamma)$  leads to the same orders as  $(\alpha, \gamma, \beta, \delta)$  and a similar correspondence holds for  $(\alpha, \gamma, \delta, \beta)$  and  $(\alpha, \beta, \delta, \gamma)$ . We thus only need to check the 12 configurations depicted on Figure 25. It remains to consider the order  $(\alpha, \beta, \gamma, \delta)$ . Because of the constrained order  $S_2$ ,  $\gamma'$  and  $\delta'$  cannot lie between  $\gamma$  and  $\delta$ . This leaves out  $\binom{4}{2} = 6$  possible shuffles of  $(\gamma', \delta')$  and  $(\alpha, \beta, \gamma, \delta)$ :

$$\begin{aligned} S'_1 &: (\alpha, \beta, \gamma, \delta, \gamma', \delta') & S'_2 &: (\alpha, \beta, \delta', \gamma, \delta, \gamma') & S'_3 &: (\alpha, \beta, \gamma', \delta', \gamma, \delta) \\ S'_4 &: (\alpha, \delta', \beta, \gamma, \delta, \gamma') & S'_5 &: (\alpha, \gamma', \beta, \delta', \gamma, \delta) & S'_6 &: (\alpha, \gamma', \delta', \beta, \gamma, \delta) \end{aligned}$$

We finally shuffle each of these orders with  $(\alpha', \beta')$ . Since  $\alpha'$  and  $\beta'$  cannot lie between  $\alpha$  and  $\beta$ , we obtain  $\binom{6}{2} = 15$  possible shuffles when considering either  $S'_1, S'_2$  or  $S'_3$ ,  $\binom{5}{2} = 10$  possible shuffles with  $S'_4$  or  $S'_5$ , and  $\binom{4}{2} = 6$  possible shuffles with  $S'_6$ . By swapping left and

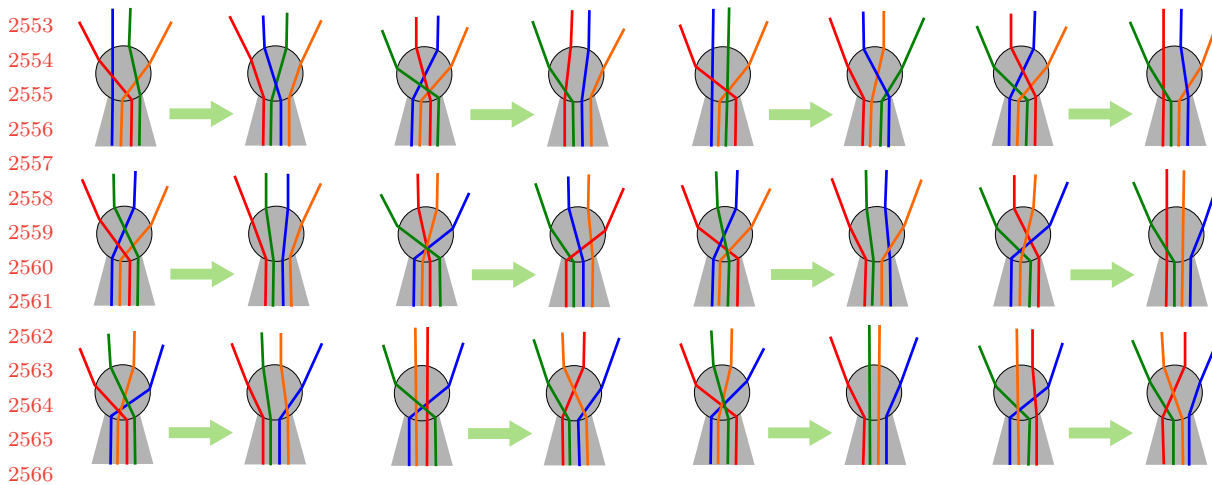


Fig. 25. Effect of swapping the singular bigon  $([i \xrightarrow{\ell}], [j \xrightarrow{\ell}])$  on  $\mathbb{D}_2$  for all the orders including the factor  $(\alpha, \gamma, \beta, \delta)$  or  $(\alpha, \gamma, \delta, \beta)$ . The blue strand represents  $(\alpha, \alpha')$ , the red one  $(\beta, \beta')$ , the orange one  $(\gamma, \gamma')$  and the green one  $(\delta, \delta')$ .

right and turning clockwise instead of counterclockwise, we remark that  $S'_1$  and  $S'_3$  lead to the same orders and similarly for  $S'_4$  and  $S'_5$ . We thus only need to consider the shuffles of  $(\alpha', \beta')$  and  $S'_1, S'_2, S'_4$  or  $S'_6$  to complete the inspection of all the cases. Those shuffles are represented on Figures 26, 27, 28, 29 respectively.

In each of the configurations, we trivially check that the number of crossings is not increasing. This allows to conclude the lemma when the two index paths of a singular bigon are directed the same way. A similar analysis can be made when their directions are opposite, that is when the considered bigon has the form  $([i \xrightarrow{\ell}], [j \xrightarrow{-\ell}])$ .  $\square$

## C END OF PROOF OF LEMMA 16

*Claim: Let  $c$  be a primitive geodesic of length four and let  $k$  be a positive integer. Then  $c[0 \xrightarrow{4k}]$  and  $c[2 \xrightarrow{4k}]$  cannot bound a partial diagram where the index pairs  $(0, 2)$  and  $(4k, 4k + 2)$  are in the same configuration.*

**PROOF.** Consider a partial diagram  $\Delta$  for the thick double path  $\mathbb{P} = ([0 \xrightarrow{4k}], [2 \xrightarrow{4k}])$  and suppose that the index pairs  $(0, 2)$  and  $(4k, 4k + 2)$  are in the same configuration. In order to reach a contradiction we will use the fact that  $c[0 \xrightarrow{2}] = c[4k \xrightarrow{2}]$  label the first arcs of the  $[0 \xrightarrow{4k}]$  side of  $\mathbb{P}$  as well as the last arcs of the  $[2 \xrightarrow{4k}]$  side, and similarly for  $c[2 \xrightarrow{2}] = c[4k - 2 \xrightarrow{2}]$ .

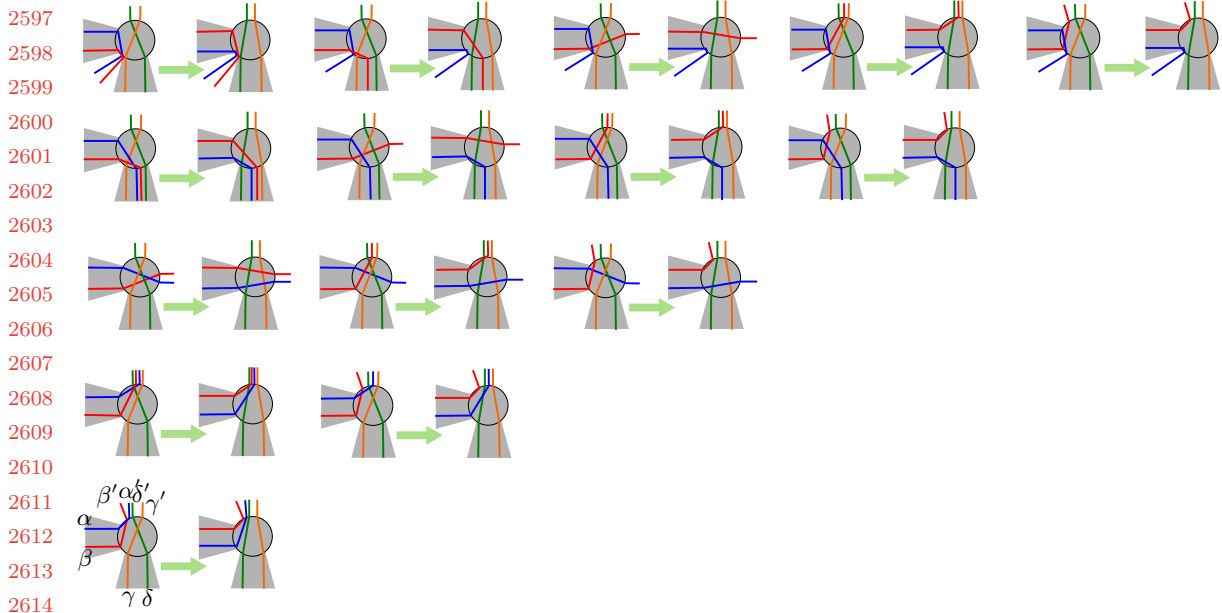


Fig. 26. Effect of the bigon swapping on the 15 shuffles of  $S'_1$  and  $(\alpha', \beta')$ .

If the first and last index pairs of  $\mathbb{P}$  correspond to the same vertex in  $\Delta$ , then there are five possible configurations for the first two arcs on each side of  $\mathbb{P}$  (depicted on Figure 30, b1-5) and five possible configurations for the last two arcs on each side of  $\mathbb{P}$  (depicted on Figure 30, e1-5). Clearly,  $\Delta$  cannot start with a path part of length two (case b1), as this would imply  $c[0 \xrightarrow{2}] = c[2 \xrightarrow{2}]$  and in turn  $c = c[0 \xrightarrow{2}].c[2 \xrightarrow{2}]$  would be a square; this would contradict the fact that  $c$  is primitive. Case b2 leads to the same contradiction noting that  $c[0 \xrightarrow{2}] \sim c[2 \xrightarrow{2}]$ . Cases e1 and e2 can be dealt with analogously. As in Lemma 34, we denote by  $(x, y)$  the conjunction of configurations  $x$  and  $y$ .

- If the orientations of the first and last staircases in  $\Delta$  coincide, we easily obtain that  $c(1)$  has degree 2 for the conjunctions  $(b3, e3)$ ,  $c(3)$  has degree 2 for  $(b4, e4)$ ,  $c(1)$  has degree 3 for  $(b3, e4)$  and  $(b4, e3)$  and  $c(1)$  has degree 4 for  $(b3, e5)$ ,  $(b4, e5)$ ,  $(b5, e3)$  and  $(b5, e4)$ . In case  $(b5, e5)$  a quad has two sides labelled by the same arc, which is forbidden by Lemma 32.
- If the orientations of the first and last staircases in  $\Delta$  are opposite then each conjunction of  $b3, 4, 5$  with  $e3, 4, 5$  implies that a quad has two sides labelled by the same arc, which is again forbidden.

When the first and last index pairs of  $\mathbb{P}$  correspond to diagonally opposite vertices in a quad, we get eight possible configurations for the first two arcs on each side of  $\mathbb{P}$  (depicted

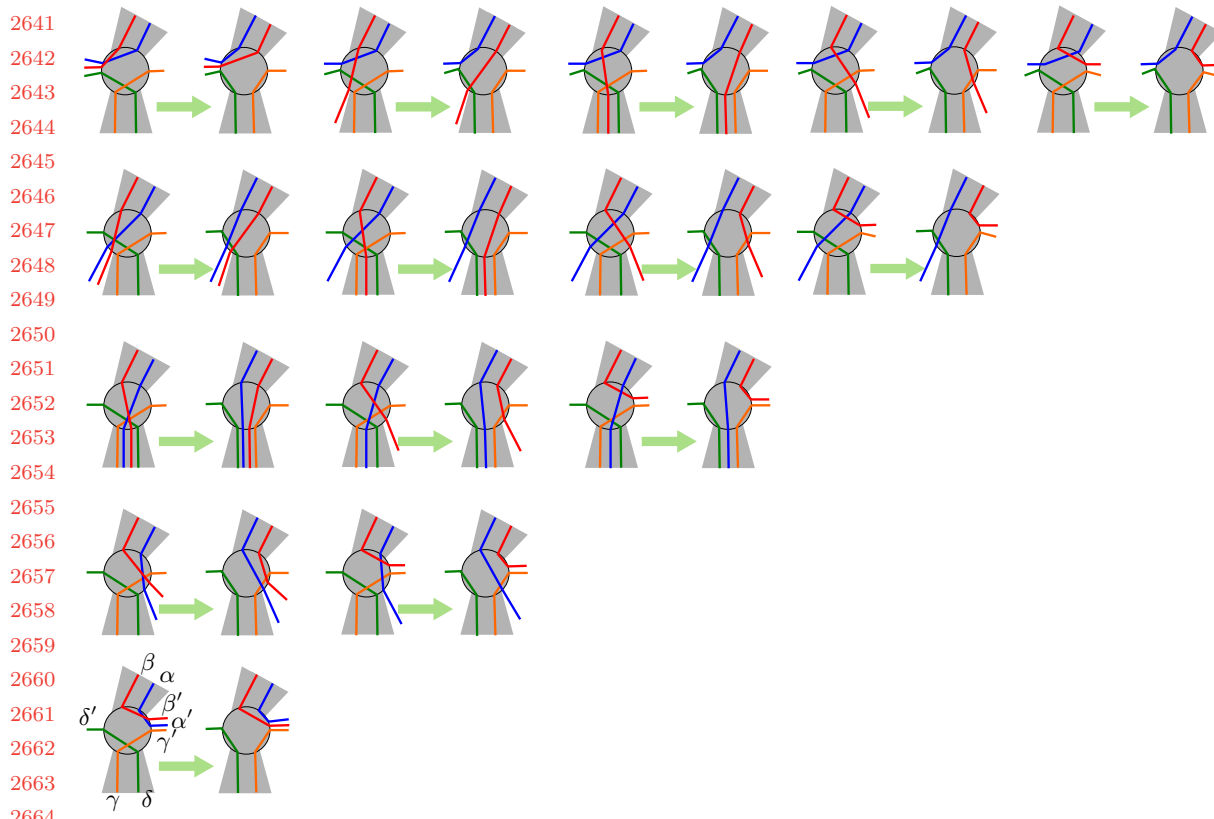


Fig. 27. Effect of the bigon swapping on the 15 shuffles of  $S'_2$  and  $(\alpha', \beta')$ .

on Figure 30, B1-8) and eight possible configurations for the last two arcs on each side of  $\mathbb{P}$  (depicted on Figure 30, E1-8). All the pink quads in the figure denote the same quad with the same orientation, recalling that the configuration for the first and last index pairs of  $\mathbb{P}$  is the same. We easily get in each case that a vertex has degree at most 5, or that a quad has two sides labelled by the same arc, or that  $c$  is a square (case  $(B2, E2)$ ). In each case, we have thus reached a contradiction.  $\square$

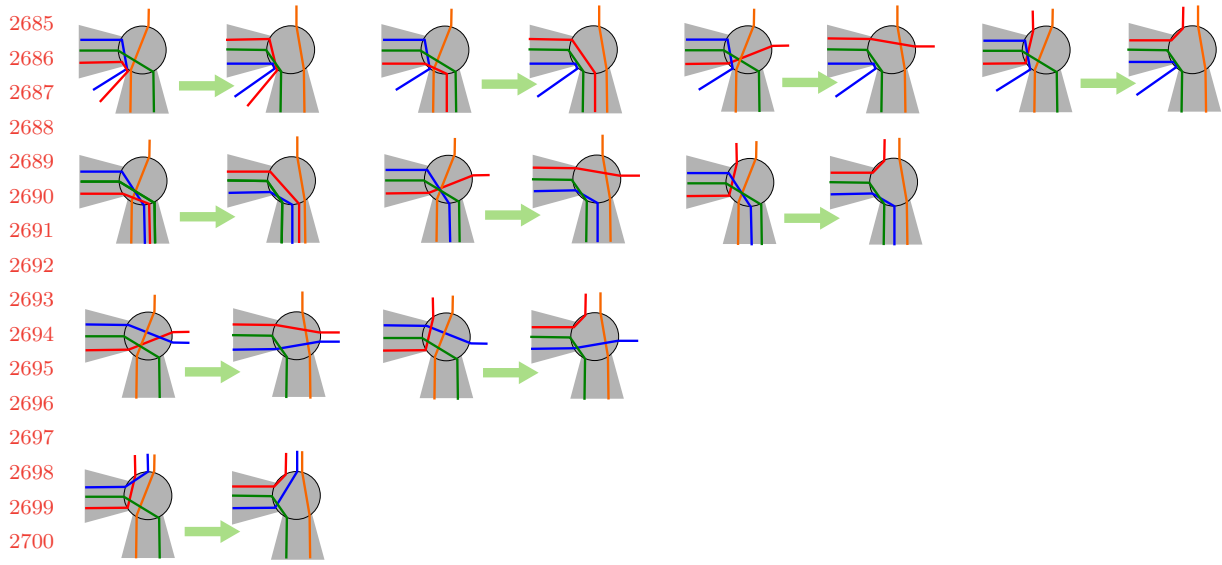


Fig. 28. Effect of the bigon swapping on the 10 shuffles of  $S'_4$  and  $(\alpha', \beta')$ .

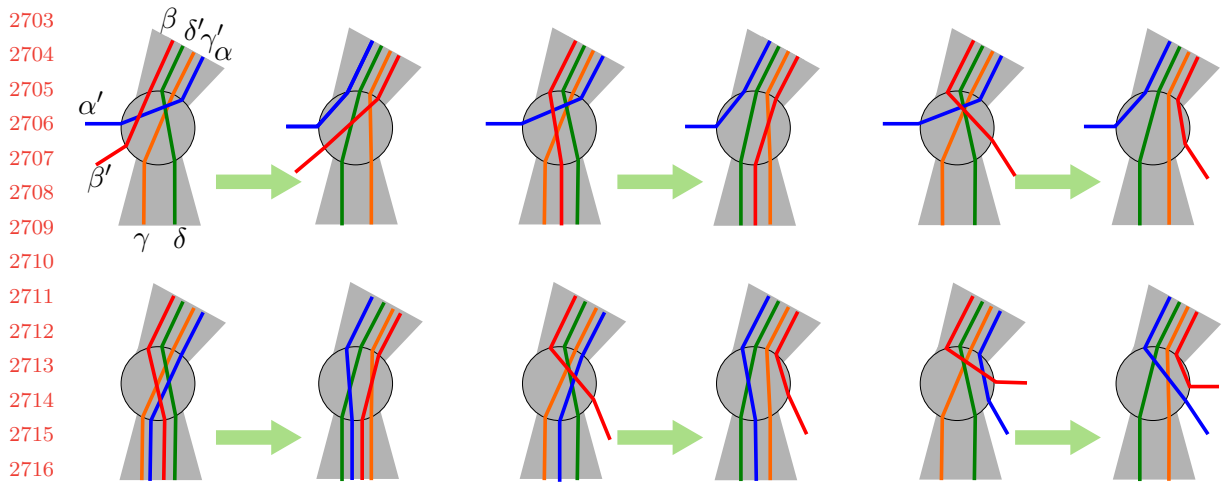


Fig. 29. Effect of the bigon swapping on the 6 shuffles of  $S'_6$  and  $(\alpha', \beta')$ .

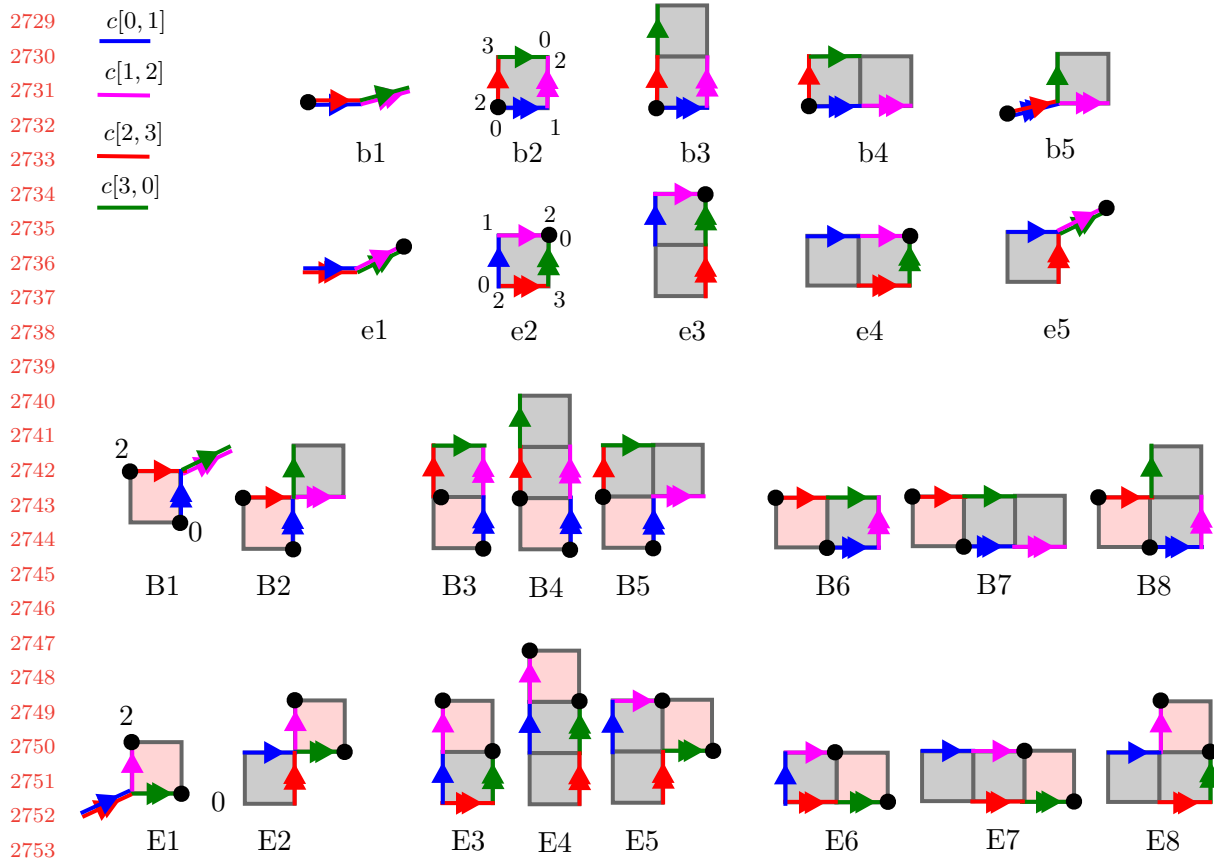


Fig. 30. The possible configurations for the first two arcs and the last two arcs on each side of  $\mathbb{P}$  in the corresponding partial diagram.